Evaluation of forecast models for Sclerotinia stem rot (Sclerotinia sclerotiorum)	of soybean in
Ouébec	

Césarée Morier-Gxoyiya

Department of Plant Science
Faculty of Agricultural and Environmental Sciences
Macdonald Campus of McGill University, Montréal
21111 Lakeshore Road, Sainte-Anne-de-Bellevue, Québec, H9X 3V9

December 2021

A thesis submitted to McGill University in partial fulfillment of the requirements of the degree of Master of Science

Table of Contents

Table of Contents	2
Acknowledgements	4
Abstract	5
Résumé	6
Contribution of authors	7
List of Tables	8
List of Figures	9
Chapter 1: Introduction	11
1.1 Objectives	13
1.2 Hypotheses	13
Chapter 2: Literature Review	14
2.1 Québec soybean industry	14
2.2 Soybean development	14
2.3 Diseases of soybean	15
2.4 Sclerotinia stem rot (SSR) 2.4.1 Life cycle and dispersal 2.4.2 Management strategies	16
2.5 SSR prediction modelling	30
2.6 Model validation	34
Connecting text between Chapter 2 and Chapter 3	37
Chapter 3: Effect of agro-environmental variables on <i>Sclerotinia sclerotiorum</i> cargermination and evaluation of SSR bioclimatic prediction models in soybean (<i>Gly</i> in Québec	ycine max)
3.1 Introduction	38
3.2 Materials and Methods	39
3.3 Results	51
3.3.1 Association between apothecia at selected soybean growth stages and DSI	51
3.3.2 Association between apothecia and selected weather variables	54
3.3.3 Association between SSR severity and selected weather variables	56
3.3.4 Effect row spacing and location on timing and abundance of apothecia formation	n57
3.3.5 Disease severity index at the research centres from 2019 to 2021	62
3.3.6 Validation of Sclerotinia-related prediction models	63
3.4 Discussion	69

3.5 Conclusion	75
Connecting text between Chapter 3 and Chapter 4	77
Chapter 4: Validation and modification of Sclerotinia sclerotiorum carpogen	ic germination
prediction models in soybean (Glycine max) in Québec	
4.1 Introduction	78
4.2 Materials and methods	80
4.2.1 Experimental sites and data collection	
4.2.1.1 Original model validation and model modifications 4.2.1.2 External validation of modified models	
4.2.2 Statistical Analysis	
4.2.2.1 Validation of original Willbur apothecia formation models	
4.2.2.3 Calibration performance	
4.2.3 Modification of Willbur models for Québec conditions	82
4.2.4 Validation of modified Willbur models	85
4.3 Results	88
4.3.1 Proportion of cases and controls	88
4.3.2 Validation of original Willbur apothecia formation models	89
4.3.2.1 AUC pairwise comparisons from 2019 to 2021	89
4.3.2.2 Youden index from 2019 to 2021	
4.3.2.4 AUC pairwise comparisons during the flowering period	91
4.3.3 Calibration plots of original Willbur models	93
4.3.4 Modified model fit (70% 2019-2021)	
4.3.4.1 Calibration plots of modified Willbur apothecia formation models	
4.3.5 Modified apothecia formation models	
4.3.5.2 Youden index for internal validation (30% 2019-2021)	
4.3.5.3 External validation 2017-2018	
4.3.5.4 Youden index for external validation in 2017-2018	
-	
4.4 Discussion	
4.5 Conclusion	
Chapter 5: General discussion	
Chapter 6: General conclusion	
References	121
Appendix 1 - Tables	130
Annendix 2 - Figures	147

Acknowledgements

This project was a collaborative effort, and I am very thankful to all who were involved for their contributions, help, guidance, and support along the way. To my supervisors Dr. Tanya Copley, CÉROM, and Dr. Valérie Gravel, McGill University, I cannot thank you enough for sharing your expertise with me. I have learned so much from your insights. I am also immensely grateful for the quality of your mentorship, thoughtful advice, and wealth of support and encouragements throughout my studies. I would like to thank my committee members Dr. Gaétan Bourgeois, AAFC, and Dr. Philippe Séguin, McGill University, for so generously taking the time to provide suggestions and feedback that were crucial in improving my work. I am also grateful for the project's partners including Yves Dion, MAPAQ, Yvan Faucher, MAPAQ, Francis Allard, IRDA, Dr. Anne Vanasse, Laval University, and Dr. Mamadou Fall, AAFC. Your perspectives and ideas during our discussions have greatly enriched my experience.

Marc Samoisette, Parghat Gopal and Anais Pierre-Estimé, I thank you for your time and assistance in the field at McGill. It was a joy to work with you during what have been incredibly hot and dry summers. Also, I would like to acknowledge the help from the team at CÉROM including Maxime Carrier and Naila Hafid for coordinating field and laboratory visits, and to Dominique Plouffe, AAFC, for helping with CIPRA. I am also very grateful to producers involved in the project and to the MAPAQ agronomists for the data collection in commercial sites.

I would also like to extend my thanks to the Gravel lab members and the community in the Plant Science department, despite seeing less of you, I felt your continuous support. I am also grateful to have received financial support from the Schulich Graduate Fellowship, the Natural Sciences and Engineering Research Council of Canada (NSERC) and the Fonds de recherche du Québec (FRQNT) to undertake this project. I would like to thank the MAPAQ for funding this project under the sub-component 3.2 of the 2013-2018 Prime-Vert program.

To my family and friends, thank you for listening to my rambles and always hyping me up.

Abstract

In Québec's soybean (Glycine max (L.) Merr.) farms, Sclerotinia stem rot (SSR), a disease caused by the fungal pathogen Sclerotinia sclerotiorum (Lib.) de Bary, is commonly controlled by chemical fungicides sprayed during the crop's flowering growth stages. However, fungicide use efficiency varies largely based on the risk of disease outbreak, which is strongly influenced by agro-environmental conditions. Unnecessary or improperly timed fungicide applications are costly not only economically, but also environmentally. Prediction models can guide disease management decisions by informing of the necessity and timing of fungicide applications. In this project, S. sclerotiorum sclerotia were placed in commercial and research fields across soybeanproducing regions of Québec. The goal was to assess the relationship between environmental and agronomic conditions and carpogenic germination of S. sclerotiorum. The predictive ability of Sclerotinia-related logistic regression models was evaluated under Québec's climatic conditions using data collected over three growing seasons. Based on the nature of the models selected, the predictive performance was assessed for two disease indicators: disease severity and apothecia presence. Upon validation and improvement, the models with the highest accuracy and predictive ability could be implemented in an integrated decision-support system for soybean producers in Québec.

Résumé

La sclérotiniose (Sclerotinia sclerotiorum (Lib.) de Bary) est une maladie qui s'attaque à plusieurs cultures, y compris le soya (Glycine max (L.) Merr.). Au Québec, la sclérotiniose est généralement contrôlée par l'application de fongicides chimiques pendant les stades de floraison de la culture. Cependant, l'efficacité des fongicides varie en fonction du risque d'épidémie, qui est largement influencé par les conditions agro-environnementales. Les applications de fongicides de façon préventive sont donc parfois superflues, ce qui engendre des coûts non seulement sur le plan économique, mais aussi sur le plan environnemental. Les modèles de prévision peuvent guider les décisions des producteurs quant à la gestion de la sclérotiniose en les informant de la nécessité et du moment le plus propice aux applications de fongicides. Dans ce projet, des sclérotes préconditionnés de S. sclerotiorum ont été enfouis dans des sites expérimentaux établis dans des champs commerciaux et de recherche situés dans des régions productrices de soya au Québec. Le but du projet était d'évaluer la relation entre les conditions agronomiques et environnementales sur la germination carpogène des sclérotes. En utilisant des données recueillies de 2019 à 2021 au Québec, la performance de différents modèles prédisant le risque de sévérité de la sclérotiniose et la formation d'apothécies dans le soya a été évaluée. Une fois validés et modifiés sous le climat du Québec, les modèles les plus précis pourraient être utilisés dans un système intégré d'aide à la décision pour les producteurs de soya du Québec.

Contribution of authors

Chapter 2 – Césarée Morier-Gxoyiya wrote the first draft, which was reviewed by Dr. Tanya Copley, CÉROM and Dr. Valérie Gravel, McGill University.

Chapter 3 – The project's experimental design and data collection from 2019 to 2021 was conducted by a team of collaborators from CÉROM, Quebec Ministry of Agriculture, Fisheries and Food (MAPAQ), Institut de Recherche et de Développement en Agroenvironnement (IRDA), Laval University and McGill University, led by Dr. Tanya Copley. Césarée Morier-Gxoyiya performed the statistical analyses under the supervision of Dr. Tanya Copley and Dr. Valérie Gravel. Césarée Morier-Gxoyiya wrote the first draft, which was reviewed by Dr. Tanya Copley and Dr. Valérie Gravel.

Chapter 4 - The project's experimental design and data collection from 2019 to 2021 was conducted by a team of collaborators from CÉROM, MAPAQ, IRDA, Laval University and McGill University, led by Dr. Tanya Copley. The data collection from 2017 and 2018 was performed by MAPAQ agronomists, led by Yvan Faucher and Yves Dion. Césarée Morier-Gxoyiya performed the statistical analyses under the supervision of Dr. Tanya Copley and Dr. Valérie Gravel. Césarée Morier-Gxoyiya wrote the first draft, which was reviewed by Dr. Tanya Copley and Dr. Valérie Gravel.

List of Tables

Table 2. 1. Environmental conditions for the formation of <i>S. sclerotiorum</i> sclerotia
Table 2. 2. Sclerotinia stem rot disease severity class and associated symptoms on soybean
(Grau, 1984)24
Table 2. 3. Effect of tillage practices on Sclerotinia stem rot
Table 2. 4. Forecast models developed for <i>Sclerotinia</i> spp. diseases internationally
Table 3. 1. Number and type of site for data collection in Québec from 2019 to 2021
Table 3. 3. Type III tests of fixed effects for the effect of row spacing on the area under the inoculum progress curve at research centres in Québec from 2019 to 2021
threshold of 10
Table 3. 7. Model performance indicators at their Youden index and at a probability threshold of 40% in Québec from 2019 to 2021 for different Sclerotinia models
 Table 4. 1. Regions and number of sites for data collection in Québec in 2017 and 2018
Table 4. 6. Comparisons between the AUCs and the line of no-discrimination of apothecia
prediction models in Québec from 2019 to 2021
 Table 4. 8. Performance parameters of modified apothecia formation models at their Youden index using 70% of the data collected from 2019 to 2021 in Québec
Table 4. 11 Performance parameters of apothecia formation of original and modified Willbur

rable 4. 12. Comparisons between the AUCs and the line of no-discrimination of original and modified apothecia prediction models in Québec using the data from the flowering period in 2017 and 2018				
Table 4. 13. Performance parameters of apothecia formation Willbur models original and modified versions at their Youden index from 2017 to 2018				
List of Figures				
Figure 2. 1. Carpogenic germination and infection cycle of <i>S. sclerotiorum</i> (Harvey, 1999) 17				
Figure 3. 1. Apothecia observations in the deposits at each experimental site at soybean growth stages in Québec from 2019 to 2021				
Figure 3. 4. Correlation matrices showing the correlation coefficients for Kendall correlations between A) 10-day, B) 20-day C) 30-day and D) 40-day moving averages of weather variables and the apothecia binary variable created based on a threshold of 0.25 mean apothecia/deposit in Québec from 2019 to 2021				
Figure 3. 5. Pearson correlations between A) June, B) July, C) August, and D) September weather variables and the DSI for soybean fields from 2019 to 2021				
Figure 4. 1. Workflow of model modifications, fit evaluation, and validations				

Figure 4. 5. Calibration plots for the A) Willbur 1r, B) Willbur 2r and C) Willbur 3r (Re	evised
models), D) Willbur 1x.1, E) Willbur 1x.2, F) Willbur 1x.3, G) Willbur 2x.1, H) V	Villbur
2x.2, I) Willbur 3x.1, and J) Willbur 3x.2 (Extended models) in Québec using 70%	6 2019-
2021 dataset	101
Figure 4. 6 McFadden index (r2.m) showing general dominance for variables in the Wi	llbur 3x.1
model based on 30-day moving averages of maximum temperature (Tmax30), max	ximum
wind speed (Wsmax30), AWDR (awdr_30) and maximum relative humidity (Rhm	nax30) in
A) 2019, B) 2020, C) 2021 and D) 2019-2021	110
Figure 4. 7. McFadden index (r2.m) showing general dominance for variables in the W.	illbur 3x.
model based on 30-day moving averages of maximum temperature (Tmax30), max	ximum
wind speed (Wsmax30), AWDR (awdr_30) and mean relative humidity (Rhmean3	30) in A)
2019, B) 2020, C) 2021 and D) 2019-2021	111

Chapter 1: Introduction

The pathogenic fungus *Sclerotinia sclerotiorum* (Lib.) de Bary causes diseases on a wide range of plant hosts comprising all dicotyledonous and some monocotyledonous plants (Boland and Hall, 1994). Several of these hosts are economically important oilseed and pulse crops grown throughout the world. In Canada, Sclerotinia stem rot (SSR) is a major disease of soybean (*Glycine max* (L.) Merr.), canola (*Brassica napus* L.), potato (*Solanum tuberosum* L.), and sunflower (*Helianthus annuus* L.). The fungus produces abundant white mycelium on infected plant tissues. Subsequently, sclerotia are produced on plant tissues and are deposited on the soil after harvest. In the following years, carpogenic germination of soilborne sclerotia produces apothecia. Ascospores are then expulsed from the asci of the apothecia and represent the most critical source of pathogenic inoculum for soybean (Boland and Hall, 1994). The long-term survival of sclerotia in soils, some report soilborne sclerotium viability of 10 years, makes the control of Sclerotinia diseases challenging (Rothman and McLaren, 2018).

In Québec, among the top three soybean-producing provinces in Canada, SSR sporadically occurs in soybean fields. Prevailing temperature and humidity during the soybean growing season can cause variations in how SSR reduces yields, which has been reported to reach 20% in Québec. However, environmental conditions suitable for soybean infections by *S. sclerotiorum* inoculum can exacerbate the problem and affect production even more severely (Breault et al., 2017). Crop losses due to SSR result in reductions in soybean grain quantity and quality. In turn, the repercussions from the incidence and severity of SSR on the producers' revenues and the economy are substantially affected (Bailey et al., 2004).

To date, there is no silver bullet when it comes to dealing with SSR. Instead, disease control relies on the use of multiple management strategies. These include modifying cultural and agronomic practices by incorporating non-host crops in rotations, using appropriate tillage and planting density, and selecting partially resistant soybean cultivars. Current SSR management in Québec also relies on preventative chemical fungicides sprayed according to the crop's growth stage. In soybean, programs generally include fungicide applications at the R1, R3, or both R1 and R3 growth stages depending on the chemistry used and the historical disease pressure in the field (Table A. 1) (Tremblay et al., 2016). Such practice may lead to superfluous applications when the

risk of SSR infection is low or inexistent. This prophylactic measure represents a health risk for the environment and humans, an unnecessary financial cost to producers, and may lead to resistance in the pathogenic fungus (Duan et al., 2013).

Forecasting the presence of *S. sclerotiorum* inoculum or potential SSR disease severity is a management strategy gaining popularity among farmers. Recent advances in modelling technologies, and the resolution and availability of weather data allow the development of precise and efficient tools to inform producers of whether fungicide use is justified. Moreover, if the risk of disease development is high, models can provide indications for adequate timing of applications. Forecasting models for SSR of soybean and canola have been developed in Canada (Turkington, 1993) and in the United States (Willbur et al., 2018b). However, no model has been developed or validated for soybean SSR under Québec's weather conditions. Evaluating and comparing the effectiveness of models developed outside of Québec under the province's growing conditions and agronomic practices is the first step in developing a tool that producers can use to effectively manage SSR in soybean.

1.1 Objectives

The general objective of this project is to evaluate environmental and agronomic conditions that affect *S. sclerotiorum* apothecia formation and SSR disease severity in research and commercial fields. This project also aims to test, compare, and improve SSR risk and apothecia development forecast models in soybean under Québec growing conditions. More specifically, the objectives are the following:

- 1. Describe the association between in-season *S. sclerotiorum* apothecia development, endof-season disease severity level and agro-environmental factors in soybean fields at research centres and commercial farms in Québec.
- 2. Evaluate the performance of SSR severity and apothecial formation forecast models under Québec weather and agronomic conditions in commercial and research soybean fields.
- a. Test models for 17.8-, 38.1-, and 76.2-cm row spacing of soybean in Québec.
- b. Identify the most promising model for use in Québec soybean production.
- c. Evaluate action thresholds to use with selected reliable models in Québec to further integrate them into a decision-support system for soybean producers.
- 3. Adapt previously developed SSR severity and apothecial development forecast models to improve their performance under Québec conditions.

1.2 Hypotheses

- 1. Environmental variables most strongly associated with *S. sclerotiorum* apothecia presence are relative humidity and temperature.
- 2. Narrow row spacing width results in earlier apothecia development by *S. sclerotiorum*.
- 3. Presence of *S. sclerotiorum* apothecia during the soybean flowering stage explains end-of-season SSR disease severity levels and soybean yield losses.
- 4. End-of-season SSR severity level is best predicted by apothecia formation, or inoculum-based, models rather than non-inoculum-based prediction models in both commercial and research soybean fields in Québec.
- 5. Apothecia formation prediction models updated using data collected in soybean-producing regions of Québec from 2019 to 2021 have a higher predictive ability compared to the original model equations developed outside of Québec.

Chapter 2: Literature Review

2.1 Québec soybean industry

Soybeans were introduced in Canada in 1893 as part of forage crop experiments at the Ontario Agricultural College. However, soybeans did not gain economic importance until the 1940s. At that time, the World Wars increased the oil demand, partly met by a rise in soybean production and processing. Even then, soybeans were grown only in Southern Ontario (Hartman et al., 2015). In the mid-1970s, the development of new high-yielding soybean cultivars suited for short growing seasons and cool weather allowed the expansion of soybean production in Québec and Manitoba. Currently, the soybean industry in Canada is mainly concentrated in Ontario, Québec, and Manitoba. Ontario is the leading producing province with a share of the national production estimated at 64.55% in 2021. Manitoba and Québec are the next highest producing regions accounting for 18.34% and 15.37% of Canadian soybean production, respectively (Statistics Canada, 2021).

2.2 Soybean development

The development of the soybean plant is divided into two growth phases; organs responsible for photosynthesis and nutrient absorption develop during the vegetative phase, and flowers, pods, and seeds form during the reproductive phase. In 1977, Fehr and Caviness designed a convention to describe soybean development still in use today (Table A. 1). The vegetative development stages (V) start with the emergence of the cotyledons above ground (VE). It continues with developing the primary unifoliate leaves until there is no longer contact between the leaf edges (VC). Both the cotyledons and primary leaves are arranged oppositely on the main stem. The secondary leaves are trifoliate, meaning three leaflets form one leaf, and are positioned alternately on the main stem. The subsequent vegetative stages are named after the number of unrolled trifoliate leaves (V1, V2, V3, ..., Vn). The reproductive development stage (R) begins with the flowering stage (R1-R2), continues with the pod growth (R3-R4), seed development (R5-R6), and finally, the plant maturation and senescence (R7-R8) (Fehr and Caviness, 1977).

Temperature and photoperiod are key factors that vary with geographical latitude and influence the soybean plant development (Singh, 2010). Soybean cultivars are classified in 13 maturity groups (MG) based on their time to reach maturity, from earliest (MG 000) to latest (MG X). There

are differences in the plant's response to changes in environmental conditions based on the soybean maturity group. In early-maturing soybean varieties, temperature plays a more prominent role in plant development compared to day length, whereas the opposite is true for varieties that mature later in the growing season (OMAFRA, 2017).

There are also genetic variations in soybean development. Therefore, it is helpful to categorize plants based on their growth habits, also referred to as stem types. Determinate soybeans are characterized by the interruption of the main stem growth once the plant enters the reproductive stage. The terminal bud halts vegetative growth and stem elongation at flowering. Most latematuring soybean cultivars (maturity groups of MG V and higher) are determinates and used in southern regions of the United States (Singh, 2010).

In indeterminate soybean varieties, the main stem elongation continues after the plant enters the flowering stage. Cultivars with maturity groups from MG 000 to MG IV are typically indeterminates and primarily grown in northern areas of the United States and Canada (Singh, 2010).

The third stem type is the semi-determinate, in which flowering does not stop the main stem elongation. However, at maturity, the main stem of the semi-determinate plant has fewer nodes and is shorter than the indeterminate plant. Currently, only one semi-determinate cultivar is commonly produced in the United States. However, identifying the *Dt2* gene that specifies semi-determinacy in soybean is promising for the breeding of semi-determinate commercial varieties (Ping et al., 2014).

2.3 Diseases of soybean

Soybean yields can be reduced by abiotic factors such as unfavorable temperature and rainfall, and biotic factors such as pests and diseases. In Canada, the latter is generally the most economically damaging (AAFC, 2006); however, the Soybean cyst nematode (*Heterodera glycines* Ichinohe) has been particularly damaging recently in Ontario (Bradley et al., 2021b). Soybeans are affected by over 200 known pathogens worldwide, and close to 40 of them occur in Canada (Hartman et al., 2015). These pathogens, even those of minor importance, are for the most part well

characterized. Diseases can be classified as bacterial (i.e. bacterial blight), viral (i.e. soybean mosaic virus), and fungal or oomycotic (i.e. Sclerotinia stem rot, stem canker, and Phytophthora rot) (Bailey et al., 2004). Not all diseases suppress yields in the same way or to the same extent. Diseases can be categorized by the plant part damaged: seedling, root, stem, and foliar diseases. They can also impact the grain or seed quantity and quality. The importance of yield loss ultimately varies based on the pathogen involved, the health status of the plant and its growth stage at the time of infection, the extent to which individual plants are infected and colonized by the pathogen, the level of plant resistance, and the total area of the field attained. Some pathogens, such as *Sclerotinia sclerotiorum* (Lib.) de Bary causing Sclerotinia stem rot (SSR) in soybean, have a known history of causing major yield reductions by affecting pod size and quality. From 2010 to 2014, an estimated 101 million bushels were lost in the United States and Ontario due to SSR and the estimate jumped to 201.6 million bushels for the period of 2015 to 2019 (Allen et al., 2017, Bradley et al., 2021a).

2.4 Sclerotinia stem rot (SSR)

2.4.1 Life cycle and dispersal

In soybean, SSR is caused by the plant pathogenic fungus *Sclerotinia sclerotiorum* (Lib.) de Bary. The fungus inhabits all continents apart from Arctica and Antarctica. It is described as a plurivorous fungus because of its extensive host range, including many herbaceous plants from the subclass Dicotyledonae. The non-specificity of the pathogen makes it particularly important in agriculture, as many crops are susceptible to infections, including canola, sunflower, soybean, dry bean, peanut, potato, and lettuce (Boland and Hall, 1994). An overview of the fungus life cycle through carpogenic germination is presented in Figure 2. 1.

Sclerotia constitute a significant component of the life cycle of *S. sclerotiorum*. They are the structures responsible for the long-term survival of the fungus in the soil and the production of inoculum. General sclerotia formation in *Sclerotinia* spp. has been described in detail and was initially divided into three phases of development, namely initiation, growth (or development), and maturation. Through the initiation phase, hyphal tissue aggregates to form sclerotial initials. In the growth phase, the hyphal tissue produces a large white mass and reaches its final size. During the maturation phase, the hyphal tissue consolidates and is surrounded by a dark-pigmented outer rind

composed of several layers of peripheral cells (Le Tourneau, 1979). Melanin is responsible for sclerotium pigmentation and is an essential protective element of the outer layer as it makes it resistant to microbial and environmental degradation (Henson et al., 1999). A fourth development phase of *S. sclerotiorum* sclerotium formation was added by recognizing rind rupture by the primordia as the final formation stage (Saharan and Mehta, 2008). Furthermore, Li and Rollins (2009) have described sclerotium formation as a six-step process comprising initiation, condensation, enlargement, consolidation, pigmentation, and maturation (Li and Rollins, 2009).

Sclerotium formation was studied under laboratory and field conditions and is influenced by numerous environmental factors, including temperature, light, pH, soil water potential, and nutrient availability (Abawi and Grogan, 1975, Bedi, 1962, Humpherson-Jones and Cooke, 1977, Marukawa et al., 2014, Le Tourneau, 1979, Vega and Le Tourneau, 1974, Wang and Le Tourneau, 1972) (Table 2. 1).

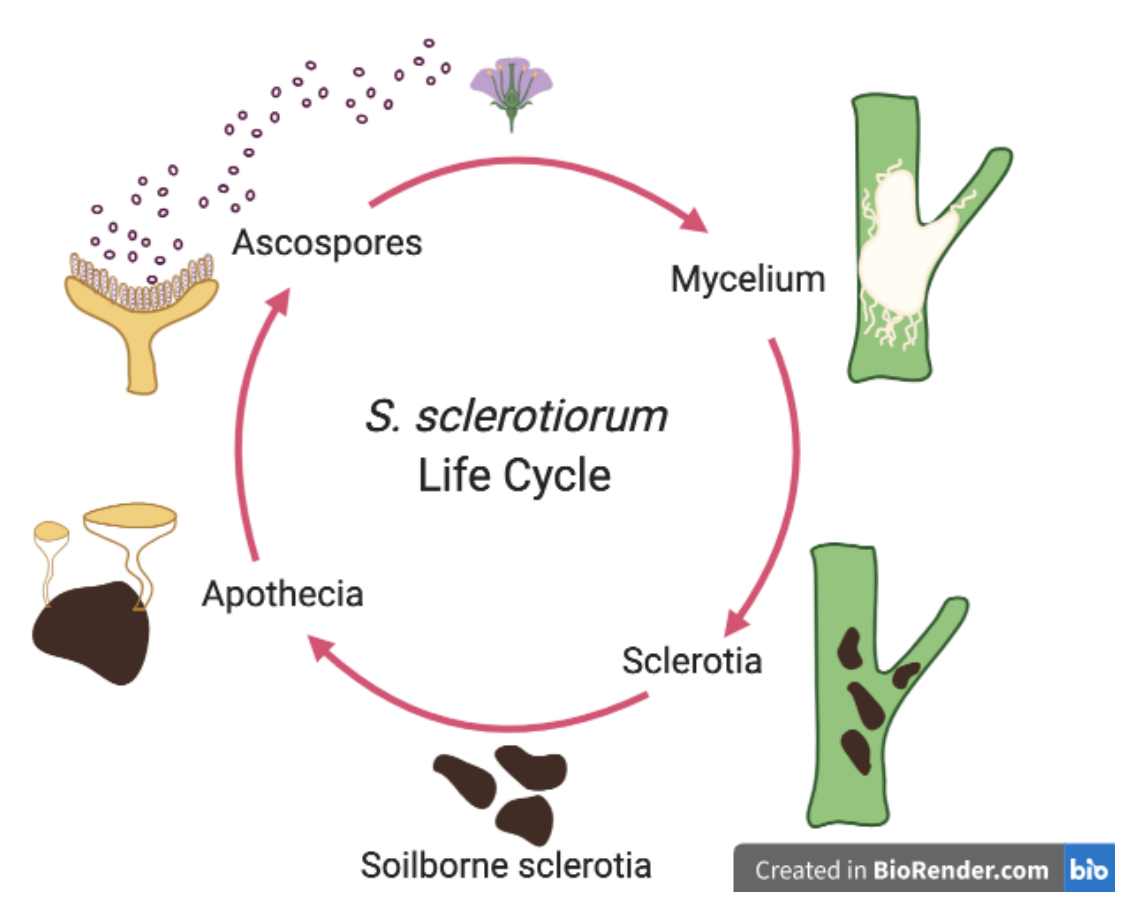


Figure 2. 1. Carpogenic germination and infection cycle of S. sclerotiorum (Harvey, 1999).

Table 2. 1. Environmental conditions for the formation of S. sclerotiorum sclerotia.

Environmental Factor	Formation of Sclerotia	References
Temperature effect	5°C to 30°C	Bedi, 1962
	Numerous, small sclerotia in high temperatures	Le Tourneau, 1979
	Fewer, large sclerotia in low temperatures	
Light effect	Numerous, small sclerotia in light	Humperson-Jones and Cooke,
	Fewer, large sclerotia in darkness	1977; Marukawa et al., 1975
Optimal pH	Between 4.0 and 6.0	Marakuwa et al., 1975
Optimal water potential	Between -1 and -56 bars	Abawi and Grogan, 1975
Important nutrients	K, Mg, P, S and Zn	Le Tourneau, 1979;
		Vega and Le Tourneau 1974;
		Wang and Le Tourneau, 1972

Sclerotia survival

Long-term survival of sclerotia in soils is a critical challenge for the control of diseases caused by *Sclerotinia* spp.. Reports of *S. sclerotiorum* sclerotia longevity in various locations indicate different survival times in soil: some observed sclerotia survival of at least two years in Great Britain, while others detected three-year-old viable sclerotia in Nebraska (Cook, 1975, Williams and Western, 1965). Other studies on different *Sclerotinia* spp. report sclerotia surviving up to 10 years in the soil (Rothman and McLaren, 2018). Such variability suggests that environmental and biological soil factors and their interaction influence the viability of sclerotia.

Higher rates of sclerotia survival were observed under dry field conditions compared to wet soils (Coley-Smith and Cooke, 1971, Imolehin, 1980, Wu and Subbarao, 2008). Field flooding over 26 to 31 days was found to destroy *S. sclerotiorum* sclerotia and was proposed as a potential disease eradication strategy (Moore, 1949). More recently, soil aeration has been suggested as an important factor in sclerotia longevity, partially explaining the rapid rates of degradation under flood conditions. *S. sclerotiorum* sclerotia viability was lower under high soil moisture and

temperature coupled with ultralow oxygen concentrations (0.1% O₂) compared to normal oxygen levels (21% O₂) (Wu and Subbarao, 2008).

Burial depth also influences the longevity of sclerotia in the soil. It was observed that sclerotia survived better at greater burial depths compared to shallow depths (Adams, 1979). However, many others reported fewer sclerotia surviving when buried deeper in the soil profile (Duncan et al., 2006, Imolehin, 1980, Matheron and Porchas, 2005, Wu and Subbarao, 2008).

Sclerotia carpogenic germination

Despite multiple studies on the topic, the importance of a conditioning phase for *S. sclerotiorum* sclerotia carpogenic germination remains a point of contention. The conditioning phase refers to the period between sclerotia production and germination during which sclerotia are exposed to a cool and moist environment, similar to exposure during winter and spring conditions in temperate regions. Based on work on temperature and moisture, some suggested that such a phase was necessary for carpogenic germination to take place (Abawi, 1979, Phillips, 1986, Saharan and Mehta, 2008). The highest germination rates were obtained with sclerotia conditioned in hydrated environments, whereas limited germination rates occurred following dry conditioning (Dillard, 1995, Foley et al., 2016). Such work suggests that the role of moisture during conditioning of sclerotia is critical for carpogenic germination.

The effect of temperature was also studied, and a wide range of conditioning temperatures was found to promote sclerotia carpogenic germination. Many studies report successful sclerotia conditioning in temperatures below 10°C (Dillard, 1995, Mila et al., 2004, Phillips, 1986, Sun and Yang, 2000), while carpogenic germination also occurred following conditioning temperatures above 10°C and up to 30°C (Dillard, 1995, Foley et al., 2016, Huang et al., 1998). Dillard (1995) studied conditioning temperatures between 4°C and 24°C on the carpogenic germination of 24 isolates of *S. sclerotiorum*. Not one conditioning temperature was optimal for sclerotia carpogenic germination across isolates. Generally, conditioning temperatures between 8°C and 16°C were found to promote carpogenic germination. Foley et al. (2016) observed sclerotia carpogenic germination following conditioning under temperatures between -20°C and 30°C, with the highest germination rates at conditioning temperatures between 0.5°C and 10°C (Foley et al., 2016).

The duration of the conditioning period was also found to affect subsequent carpogenic germination rates of two *S. sclerotiorum* isolates in the United Kingdom. Longer conditioning periods at 4°C resulted in faster carpogenic germination once the isolates were exposed to temperatures between 10°C and 18°C. However, differences were observed among temperature and duration requirements for complete conditioning to be achieved among isolates. In addition, carpogenic germination of conditioned (28 days at 4°C) sclerotia buried in the field starting the previous December until August of the current year showed that apothecia development was reduced for burials made in May and beyond, again with differences among isolates. These results were explained by sclerotia being incompletely conditioned prior to burial. Hence, the sclerotia buried in winter and early spring completed their conditioning by being exposed to cold temperatures and produced apothecia rapidly, while those buried in late spring and summer did not complete conditioning which delayed or prevented their carpogenic germination (Clarkson et al., 2007).

Some studies challenged the necessity of a conditioning phase for sclerotia germination due to disparities in isolates from different geographical origins (Huang et al., 1998, Wu and Subbarao, 2008). For example, Wu and Subbarao (2008) showed that *S. sclerotiorum* isolates from California germinated after being incubated at 18°C in a moist environment. There was no chilling period between sclerotia production and germination. The need for conditioning prior to sclerotia germination might be dependent on many factors, including the *S. sclerotiorum* isolate, sclerotia geographical area of origin, the temperature under which they were produced, and the host from which they were formed (Foley et al., 2016, Huang et al., 1998).

Sclerotia myceliogenic germination

Sclerotia germination can take two forms: myceliogenic or carpogenic. Following either type of germination, sclerotia are no longer viable. Myceliogenic germination produces vegetative hyphae, or mycelium, and is affected by numerous factors. Close contact must be established between the germinating *S. sclerotiorum* sclerotia and the host for an infection to occur successfully. As such, myceliogenic germination is of minimal importance for SSR in soybeans as it rarely occurs under field conditions (Abawi and Grogan, 1975). Myceliogenic germination is influenced by the

integrity of the melanized outer rind, moisture level, and temperature (Huang et al., 1998, Lane et al., 2019). Some investigated the ability of temperature treatments to induce myceliogenic germination over carpogenic germination with conflicting results suggesting that a more detailed examination of the role of temperature in the type of sclerotial germination is required (Lane et al., 2019, Foley et al., 2016, Huang et al., 1998).

Sclerotia carpogenic germination

Carpogenic germination, unlike myceliogenic germination, plays a major role in SSR development on soybean (Abawi and Grogan, 1975). Through this type of germination, the sclerotium initiates stipes which produce ascospores within apothecia in approximately 3 to 4 weeks (Twengström et al., 1998). The initial formation of stipes, also called carpophores, starts on soilborne sclerotia, occurs below the soil surface and does not require light (Bedi, 1962, Coley-Smith and Cooke, 1971, Willetts and Wong, 1980). Dry conditions can hinder carpogenic germination since the stipes cannot pierce through crusted soil (Saharan and Mehta, 2008). The emerging stipes are phototrophic and require 8 to 12 hours of daylight for differentiation to occur. In a process above ground, the stipes differentiate, growing into ascocarps and forming apothecia. Carpogenic germination is unsuccessful when sclerotia are buried at depths below 5 cm from the soil surface; it was found that sclerotia burial depths over 3 cm result in an environment without light exposure, and prevented apothecia formation from stipes (Bedi, 1962). Sclerotia germination where stipes are initiated but fail to produce complete apothecia containing asci and ascospores is referred to as non-functional sclerotial germination (Pethybridge et al., 2020).

The formation of apothecia is affected by atmospheric temperature, relative humidity, and, most importantly, the interaction of these environmental conditions. Apothecia develop in approximately 10 days under high relative humidity and air temperature ranging from 5°C to 25°C (Abawi, 1979, Saharan and Mehta, 2008). Carpogenic germination is reduced under air temperatures below 5°C or exceeding 30°C, even when relative humidity is optimal for apothecia development (Dillard, 1995).

Ascospore dispersal

Each apothecium can produce millions of ascospores, making carpogenic germination the primary mode of infection of soybeans by *S. sclerotiorum* (Abawi and Grogan, 1975, Hartman et al., 2015, Peltier et al., 2012, Saharan and Mehta, 2008, Willbur et al., 2018a). The presence of apothecia in the field signals the beginning of *S. sclerotiorum* activity before detecting disease symptoms on plants. Ascospore discharge from asci of an apothecium was quantified demonstrating that ascospores were released at a maximum rate of 1600 spores/hour. Hence, a total of 7.6×10^5 ascospores could be produced in optimal conditions by a single apothecium over a lifetime of 20 days (Clarkson et al., 2003). In contrast, Abawi and Grogan (1975) estimated that *S. sclerotiorum* apothecia could produce up to 3×10^7 ascospores.

The forceful dispersal of ascospores from the apothecium is readily observable in the laboratory upon changes in relative humidity (Newton and Sequeira, 1972). Such a 'puffing' pattern of dispersal was assumed to be the principal mode of ascospore dispersion under field conditions. However, such rapid fluctuations in environmental conditions are less likely to occur in natural environments. Thus, whether *S. sclerotiorum* ascospores are released continuously or in bursts was investigated over various environmental conditions (Clarkson et al., 2003). Ascospores were continuously released when apothecia were placed in non-saturated (60-65% RH) and almost saturated (90-95% RH) environments. Additionally, rising temperature from 15°C to 20°C or 25°C resulted in an increased discharge of ascospores in both *S. sclerotiorum* and *Sclerotinia trifoliorum* Erikss (Clarkson et al., 2003, Raynal, 1990). Continuous sporulation was observed whether apothecia were exposed to light or dark conditions, establishing that ascospore release is not restricted to dark or light periods. In contrast, work on *S. trifoliorum* showed that ascospore discharge was promoted by light rather than dark (Raynal, 1990).

Previous work on *S. sclerotiorum* survival has shown similarities in the response of ascospores to environmental conditions. High temperature and humidity reduced ascospore viability in a Clarkson et al. study (2003), similar to observations by Caesar and Pearson (1983). However, they noted that ascospores remained viable in the laboratory for much longer (i.e. several weeks) than that reported by Caesar and Pearson (1983) (i.e. a few days) under similar environmental conditions (Caesar and Pearson, 1983).

Transported by wind or water, ascospores may be dispersed over long distances (Li and Kendrick, 1994). The introduction of SSR from contaminated fields to neighbouring ones has been recorded. The high number of ascospores released, their ease of dispersal, and their highly infectious nature make them key agents in *S. sclerotiorum* disease transmission within and across fields. However, most ascospores are deposited near the apothecium from which they were produced (Wegulo et al., 2000). Since carpogenic germination takes place at the ground level, canopy interception of ascospores can limit their wind dispersal to a certain extent (Saharan and Mehta, 2008).

Ascospore dispersal via wind is one of the ways SSR can be disseminated from infected fields to healthy ones. The presence of sclerotia or mycelia on seedlings, infected seeds, various farm equipment, animals, and humans may also cause SSR dispersal. Moreover, the use of plant residues from infected fields as livestock bedding and the subsequent application of manure collected from the same bedding can introduce sclerotia to healthy fields (Saharan and Mehta, 2008).

Ascospore germination and host infection

Environmental conditions influence pathogen infection by affecting ascospore germination and colonization of host tissues. Ascospores can germinate in temperatures ranging from 10°C to 30°C, with optimal germination observed between 20°C and 25°C in bean (Abawi, 1979) and 15°C to 25°C in lettuce (Young et al., 2004). Ascospores can produce hyphae in non-saturated conditions; however, hyphal tissue cannot colonize plants without free water (Abawi and Grogan, 1975). An exogenous source of energy is also required for such colonization to take place, primarily via senescent tissue. In SSR of soybean, nutrients are mainly supplied to *S. sclerotiorum* ascospores by senescent flower tissue. Hence, the flowering period is a crucial development stage influencing the incidence of SSR. *S. sclerotiorum* can also derive the energy necessary to penetrate the host from dead or damaged vegetative plant tissue (Abawi, 1979, Saharan and Mehta, 2008, Willetts and Wong, 1980). Host penetration occurs directly through stomatal openings or by the mechanical action of fungal appressoria on plant tissue surfaces (Davar et al., 2012). During disease initiation, *S. sclerotiorum* induces host cell death by producing oxalic acid, a virulence factor that alters the plant redox environment. Plant wilting is also enhanced by the action of oxalic acid; stomatal

opening is triggered by oxalates and results in increased transpiration rates (Guimaraes and Stotz, 2004). Following the host invasion, hyphae develop into sclerotial initials. The initials further develop into mature sclerotia inside the pith or on the surface of the soybean stem, or on the soil surface, completing the *S. sclerotiorum* growth cycle (Saharan and Mehta, 2008).

Favourable conditions for *S. sclerotiorum* infection of soybean generally occur when the plants are flowering. However, SSR symptoms only become apparent at later growth stages due to a brief latent period. The first visible sign of SSR infection on soybean is wilting, withering and chlorosis of leaves, usually occurring during the early stages of pod development (R3 to R4). Then, various shades of purple to brown lesions form on the stem, nodes, pods, and occasionally on leaves. Upon infection progression, the distinctive *S. sclerotiorum* white and soft rot appear on the lesions. The disease causes the plant to weaken, the foliage to wilt and fall. The disease also disturbs the size of seeds from infected plants, which are smaller than those of healthy plants (Peltier et al., 2012).

Three disease assessment scales were developed to characterize the severity of SSR infections in soybean and to evaluate soybean cultivar resistance (Grau, 1984, Chun, 1987, Cline, 1983). Both Grau (1984) and Chun (1987) designed 0-3 point scales, whereas Cline (1983) rated disease severity over 5 points. A disease severity index (DSI) is derived from the scores obtained by using the assessment scale developed by Grau et al. (1984) and comprises values ranging between 0% and 100% (1984) (Table 2. 2 and Formula 2. 1). The DSI is still widely used by scientists to evaluate cultivar resistance to soybean white mould and to evaluate disease severity and progression.

Table 2. 2. Sclerotinia stem rot disease severity class and associated symptoms on soybean (Grau, 1984).

Severity Class	Disease Symptom
0	No SSR symptom
1	SSR symptoms only on lateral branches
2	SSR symptoms on main stem, without damage on pods
3	Dead plant or showing SSR symptoms on main stem and pods

Formula 2. 1. Disease severity index (%) (Grau, 1984)

$$DSI = \frac{[\Sigma(severity \ class \times number \ of \ plants \ in \ class)] \times 100}{[(total \ number \ of \ plants \times number \ of \ classes \ with \ symptoms)]}$$

2.4.2 Management strategies

No single solution has been effective at controlling SSR in soybean. Rather, an integrated disease management approach can minimize yield losses. Integrated management of Sclerotinia disease employs various control strategies that target the three factors influencing disease incidence: the pathogen (*S. sclerotiorum*), the host crop (*G. max*), and the environment. Targeting the pathogen aims at reducing inoculum pressure by destroying existing soilborne sclerotia and preventing their formation and germination. Host management strategies focus on decreasing the crop's vulnerability to infections. Additionally, modifications to the environment aim at preventing cool and moist temperatures that favour disease development (Peltier et al., 2012, Saharan and Mehta, 2008, Willbur et al., 2018a).

Agronomic practices

Consistent record-keeping from one growing season to the next is an integral aspect of disease management. It involves monitoring the susceptibility of soybean cultivars to SSR, yield performance and scouting areas for sclerotia and apothecia presence, disease incidence, and severity. The data generated can be used to inform disease mitigation strategies (Peltier et al., 2012).

Tillage operations affect the pathogen component of SSR disease in soybean in various ways. Sclerotia germination can be reduced either by burying them through deep tillage or preventing them from being brought to the soil surface through no-till. However, buried sclerotia may remain viable. Thus, subsequent tillage operations may bring sclerotia to zones where germination and emergence of apothecia are possible, leading to sporulation. The effect of tillage systems on various aspects of Sclerotinia stem rot was studied with results found to be inconsistent at times (Mueller et al., 2002, Mila et al., 2004, Kurle et al., 2001, Garza et al., 2002, Workneh and Yang, 2000) (Table 2. 3).

Table 2. 3. Effect of tillage practices on Sclerotinia stem rot.

Location	Effect of no till system on SSR	Reference		
	compared to conventional			
	tillage			
IL, United States	Increases sclerotia quantity	Mueller et al., 2002		
	Increase disease incidence			
	Reduces soybean yields			
IL, IA, MN, MO, OH, United	No significant difference	Mila et al., 2004		
States				
WI, United States	Reduces SSR incidence	Kurle and Grau, 2001		
	Reduces apothecia quantity			
ON, Canada	Reduces apothecia quantity	Gracia-Garza, 2002		
IL, IA, MN, MO, OH, United	Decreases disease prevalence	Workneh and Yang, 2000		
States				

The use of crop rotations is an additional strategy that targets the pathogen element of disease control. Crop rotations were found to decrease the inoculum density of an infected field (Peltier et al., 2012). Non-host crops do not prevent the emergence of apothecia, but rather promote the carpogenic germination of sclerotia and subsequent degradation of the sclerotia, while hindering the formation of new sclerotia and their subsequent return to the soil. Factors influencing the success of crop rotations as SSR control strategies include the choice of non-host crops such as maize, barley, and wheat and a period of three (Garza et al., 2002, Rousseau et al., 2007) to five (Zimmer, 1978) years between soybean plantings. Similarly, non-host cover crops such as small grains were effective at lowering the level of viable field sclerotia. The sporulation of apothecia was promoted, but sclerotial production was prevented due to the absence of crop infection (Willbur et al., 2018a). Recently, rolled-crimped cereal rye was found to successfully reduce weed and SSR pressure in no-till soybean since it either prevented carpogenic germination or resulted in non-functional sclerotia germination, where stipe initiation does not lead to complete apothecia formation, preventing the production of inoculum (Pethybridge et al., 2020).

Weed management is a crucial control strategy partly because many weeds are *Sclerotinia* spp. hosts and have the potential to increase the sclerotial load of a field. As such, the pathogen can infect weeds, increasing the soilborne sclerotia reservoir (Boland and Hall, 1994). Non-host weed control is also essential because they increase the density of the foliage, and in turn, result in less airflow and sun exposure at the soil level, which creates microclimate conditions favourable to the germination of sclerotia leading to infections if the main crop is a host species (Peltier et al., 2012).

Similarly to weed pressure, the plant population affects the rapidity at which the canopy closes, creating environmental conditions suitable for SSR development during vulnerable soybean growth stages in fields with a disease history. For example, there is a reduction in airflow, increase in shade and relative humidity, as well as cooler temperatures under the crop foliage (Peltier et al., 2012). Some studies observed reductions in disease incidence with wider row spacing and lower plant populations (Grau et al., 1982, Lee et al., 2005). Before altering their seeding rates, farmers should consider their field disease history since lower plant populations may reduce yields (Peltier et al., 2012).

Cultivar choice is a crucial disease-management strategy for SSR in soybean. There is no complete resistance to *S. sclerotiorum* in soybean yet. However, some commercially available partially resistant cultivars are less susceptible to infection (Kim and Diers, 2000). Seed companies may provide cultivar information, including SSR resistance level. In Québec, the Réseaux des grandes cultures du Québec (RGCQ) attributes an SSR susceptibility rating to soybean cultivars evaluated in an SSR disease nursery for a minimum of two years. The susceptibility scale ranges from 0 to 10, where 10 is comparable to the highly susceptible cultivar Nattosan (Oleo Quebec, 2019). Recommended cultivars suitable for planting in fields with disease history are associated with a susceptibility rating below 2, whereas cultivars with susceptibility ratings over 4 are not recommended (Faucher et al., 2017).

One persistent challenge to developing entirely resistant cultivars is that multiple genes control SSR disease resistance in soybean (McCaghey et al., 2017). Studies of genetic resistance have identified quantitative trait loci (QTLs) that contribute to SSR resistance in cultivars (Arahana et al., 2001, Guo et al., 2008, Kim and Diers, 2000, Vuong et al., 2008). However, further work is

needed to elucidate the mechanisms of inheritance of SSR partial resistance in soybean. Yearly variations in SSR incidence and field conditions also compromise the screening of cultivars for disease resistance (McCaghey et al., 2017).

In addition to the level of disease resistance, the soybean maturity group of a cultivar can play a role in disease management. Choosing an early-maturing cultivar is associated with lower yield losses compared to those that flower later when climatic conditions are more suitable for disease development due to canopy closure. Those conditions can also be avoided by selecting a cultivar with a low foliage density to slow down canopy closure and promote airflow (Kim and Diers, 2000, Peltier et al., 2012).

Chemical Control

In Québec, the information tool SAgE pesticides provides information related to pesticide toxicological, ecotoxicological characteristics and their persistence in the environment, including pesticides registered for SSR in Québec (Table A. 2). Such pesticides are used either as pre-seeding or foliar treatments, with only the latter being registered as chemical controls for SSR in soybean. Chemical applications aim to protect the soybean flowers against colonization by S. sclerotiorum ascospores (SAgE Pesticides, 2020). Depending on their class, pesticides have different modes of action (Table A. 3). SSR control using fungicides is partial under field conditions and inconsistent among products; they were found to reduce disease incidence by 0-60% (Mueller et al., 2002, Peltier et al., 2012). The main factors influencing fungicide efficacy are the type of product used, the coverage, and the timing of applications. Differences in canopy closure and soil temperatures on the production of apothecia were suggested as factors contributing to the inconsistency of fungicide efficacy when recommendations are based on soybean growth stages (Fall et al., 2018b). Other considerations include the machinery used, the mixing ratio, and the application rate (Willbur et al., 2018a). A study on fungicide timing showed that a preventive fungicide application during flowering (R1) before inoculation was more effective in controlling SSR than an application at R3 after host infection. Once symptoms of disease infection were observable, the efficacy of the chemicals was greatly reduced (Mueller et al., 2004). Inadequate canopy dispersion and incomplete coverage of soybean flowers by chemicals reduce disease control by fungicides. Using flat-fan spray nozzles that produce high-fine to mid-medium droplets

was the most effective sprayer (Mueller et al., 2002, Peltier et al., 2012). Aside from suboptimal coverage or timing of applications, another factor explaining their inconsistency is their systemicity; the chemicals have a low translocation potential and are limited to the point of contact on the plant (Peltier et al., 2012). Chemical herbicides containing lactofen can be used in the management of SSR. Lactofen can indirectly control *S. sclerotiorum* by inducing the production of phytoalexins, antimicrobial chemicals, in soybean, simultaneously conferring them with acquired systemic resistance. In addition, lactofen may modify the canopy development of soybean in a way that delays the flowering window (Nelson et al., 2002).

Biological Control

Aside from chemical means, biological controls of S. sclerotiorum are also commercially available. Biological factors influence sclerotia survival as soil microbial populations include antagonists of Sclerotinia spp. that colonize and degrade sclerotia. Among others, infection by Coniothyrium minitans W. A. Campb. and Trichoderma hamatum (Bonord.) Bainier decrease sclerotia viability under field conditions by producing antifungal metabolites and releasing enzymes with cell wall degrading properties (Adams, 1979, Coley-Smith and Cooke, 1971, Baazeem et al., 2021). The most widely studied and used biological control is C. minitans Strain CON/M/91-08, a pathogenic fungus of S. sclerotiorum, commercially accessible as Contans WG (Bayer CropScience) in Québec. Upon its incorporation in the soil, it parasitizes sclerotia, thus preventing the formation of apothecia from those decayed sclerotia (Del Rio et al., 2002, Zeng et al., 2012). In Michigan, C. minitans reduced the number of S. sclerotiorum sclerotia by 95.3%. Moreover, this biological control agent effectively decreased the disease severity index of soybean 68.5% in the study. Other biological controls used against S. bv same sclerotiorum included Trichoderma harzianum Rifai strain T-39 and Streptomyces lydicus De Boer et al. strain WYEC 108. These were associated with lower DSI reductions than C. minitans, with 35% for T. harzianum, and 43% for S. lydicus (Zeng et al., 2012). Studies within Québec on the efficacy of biological agents namely C. minitans (Contans WG, Bayer Cropscience), Reynoutria sachalinensis (F. Schmidt) Nakai (Regalia Maxx, Marrone Bio Innovations), Bacillus subtilis (Ehrenberg) Cohn (Serenade OPTI, Bayer Cropscience), and Bacillus amyloliquefaciens (ex Fukumoto) Priest (Double Nickel 55, Certis) against Sclerotinia stem rot of soybean were inconclusive in years of low disease severity (Bipfubusa et al., 2020). Despite some promising

results obtained with biocontrols, there is a lack of published results on their use and profitability in cases of severe SSR epidemics in soybean production.

2.5 SSR prediction modelling

The three primary factors influencing Sclerotinia stem rot disease onset are the *S. sclerotiorum* life cycle, prevailing weather conditions, and the soybean growth stage. Infections occur under cool and humid conditions when *S. sclerotiorum* ascospores, produced by germinating soilborne apothecia, colonize soybean flowers. The complex interaction of these components makes their continuous and accurate monitoring challenging. In turn, the capacity of farmers to determine the infection risk level in a specific field during the crop's susceptibility period is limited. The risk of SSR can be predicted through disease forecast models with the capacity to filter information related to several host crop, and environmental parameters. Model risk assessments are based on known conditions suitable for disease onset and can therefore corroborate the need for and the timing of disease management strategies (Peltier et al., 2012).

Format of forecast models

Many different formats of comprehensive disease forecast models have been suggested as tools to combat *Sclerotinia* spp. diseases in various crops across locations (Table 2. 4). The complexity of models for plant disease management ranges from simple empirical models to intricate mechanistic models. Empirical models are based on statistical relationships between SSR incidence and environmental conditions. Developing such models is relatively rapid and simple. Empirically derived models are easy to use and reliable in the growing area where they were developed. Upon adaptations, they can also be used in various locations. Mechanistic models are reliable across locations since they extensively depict the pathogen's response to environmental conditions. However, their complexity lengthens their development (Madden, 2006). Examples of forecast models for diseases caused by *S. sclerotiorum* include risk point tables (Foster et al., 2011, Twengström et al., 1998), carpogenic germination (Clarkson et al., 2007), petal infestation (Bom and Boland, 2000, Turkington, 1993), crop loss (Koch et al., 2007) and logistic regression-based models (Harikrishnan and del Río, 2008, Mila et al., 2004). Regardless of the format, models work to predict inoculum presence or disease incidence and inform the sustainable use of properly timed fungicides.

Table 2. 4. Forecast models developed for Sclerotinia spp. diseases internationally.

Forecast model	Host crop	Location	Variables used in predictions	Reference
format				
	Carrot	Canada	Canopy Growth (%)	Foster et al.,
	(Daucus		Soil Matric Potential (kPa)	2011
	carota L.)		Soil Temperature (°C)	
	Oilseed	Sweden	Number of years since last	Twengström et
	rape		oilseed rape crop	al., 1998
D:-1 :4	(Brassica		Disease incidence in last host	
Risk point system	napus)		crop	
system			Crop density	
			Rain in the last 2 weeks	
			Weather forecast	
			Regional risk for apothecium	
			development (per 100	
			sclerotia)	
	Oilseed	Canada	Petal infestation (%)	Turkington,
	rape			Morall and
Petal infestation-	(Brassica			Gugel, 1991
based model	napus)			
	Oilseed	Canada	Petal infestation (%)	Bom and
	rape		Soil moisture (centibars)	Boland, 2000
	(Brassica			
	napus)			

Table 2. 4 Forecast models developed for Sclerotinia spp. diseases internationally (cont'd).

Host crop	Location	Variables used in predictions	Reference
Lettuce	United	Rate of sclerotia conditioning	Clarkson et al.,
(Lactuca	Kingdom	per day	2007
sativa L.)		Rate of sclerotia germination	
		per day	
		Temperature (°C)	
Oilseed	Germany	Air temperature (°C)	Koch et al.,
rape		Relative humidity (%)	2007
(Brassica		Rainfall (mm)	
napus)		Sunshine duration (h)	
		Crop growth stage	
		Microclimate in the canopy	
Bean	United	Total rainfall (mm)	Harikrishnan
(Phaseolus	States	Average minimum temperature	and del Rio,
vulgaris)		in June, July and August (°C)	2008
		Number of rainy days in the	
		first half of June, July and	
		August	
Soybean	United	Average temperature in July	Fall et al., 2018a
(Glycine	States	(°C)	
max)		Total rainfall in July (mm)	
		Interaction between average	
		temperature in July (°C) and	
		total rainfall in July (mm)	
	Lettuce (Lactuca sativa L.) Oilseed rape (Brassica napus) Bean (Phaseolus vulgaris)	Lettuce United (Lactuca Kingdom sativa L.) Oilseed Germany rape (Brassica napus) Bean United (Phaseolus States vulgaris) Soybean United (Glycine States	Lettuce United Rate of sclerotia conditioning (Lactuca Kingdom per day Rate of sclerotia germination per day Temperature (°C) Oilseed Germany Air temperature (°C) Relative humidity (%) Rainfall (mm) Sunshine duration (h) Crop growth stage Microclimate in the canopy Bean United Total rainfall (mm) (Phaseolus States Average minimum temperature in June, July and August (°C) Number of rainy days in the first half of June, July and August Soybean United Average temperature in July (Glycine States (°C) max) Total rainfall in July (mm) Interaction between average temperature in July (°C) and

Table 2. 4 Forecast models developed for Sclerotinia spp. diseases internationally (cont'd).

Forecast model	Host crop	Location	Variables used in predictions	Reference
format				
	Soybean	United	April precipitation (cm)	Mila et al., 2004
	(Glycine	States	April air temperature (°C)	
	max)		Indicator variable of tillage	
			system	
			Indicator variable of regional	
			effect	
			July precipitation (cm)	
			Average air temperature of	
			July and August (°C)	
			Interaction between average	
Logistic			temperature in July and August	
regression model			Indicator variable of tillage	
(cont'd)			system	
			Indicator variable of regional	
			effect	
	Soybean	United	Row width	Willbur et al.,
	(Glycine	States	30-day moving averages daily	2018
	max)		maximum air temperature (°C)	
			30-day moving averages daily	
			maximum relative humidity	
			(%)	
			Wind speed/1.609 (km/h)	

Recently, SSR forecast models in soybean were developed in the United States of America (Table 2. 4). The models predict the risk of *S. sclerotiorum* apothecial presence at the field level during the crop's most vulnerable growth stages. The models explained the levels of SSR disease incidence observed by using the highest apothecial presence probability during the soybean flowering period. The accuracy of the models ranged from 63.3% to 83.3% depending on the disease incidence threshold used, either 5% or 10% (Willbur et al., 2018c). Overall, management prescriptions from the weather-based apothecia formation models reduced fungicide applications compared to calendar-based programs (Willbur et al., 2018b). The validation results support the theory advanced by Foster et al. (2011) in white mould of carrot that forecasted inoculum presence can be used to predict end-of-season disease levels (Willbur et al., 2018b). The disease threshold selected for a model affects its accuracy and can be modified based on the specificity and sensitivity of the model. For example, Hariskrishnan and del Rio (2008) modeled SSR in dry bean using a disease incidence threshold of 20%, and Fall et al. (2018a) predicted DSI levels above 22 in soybeans. Models that tend to underpredict the occurrence of epidemics can be adjusted by decreasing the disease threshold (Madden, 2006).

2.6 Model validation

Following their development, models are validated to ensure their reliability before farmers adopt them. Efficient forecast models should aim to be both sensitive (correctly predicting the occurrence of epidemics), and specific (correctly predicting the occurrence of non-epidemics). *Sensitivity* refers to the proportion of true positives; the number of correctly predicted presence of events over the total number of events observed. *Specificity* is defined as the proportion of true negatives; the number of correctly predicted absence of events over the total number of events observed. Models that are not sensitive would fail to recommend treatments. Models that are not specific would advise unnecessary treatments, hence additional costs for farmers and unwarranted consequences for the environment. Measures of sensitivity and specificity are commonly reported as percentages; the highest percentages suggesting that the model's predictions are accurate. Another measure of model accuracy is the coefficient of determination (R²), for which values can range between 0 and 1. Accurate models would have R² values approaching 1 (Yuen and Hughes, 2002). Receiver operating characteristic (ROC) curve is an additional statistical method used to evaluate and compare model performance (Metz, 1978). It has long been used to evaluate medical imaging

techniques and has now been adopted in other fields, including in plant pathology (Hughes et al., 1999, Swets, 1979). The performance of two SSR risk point tables for oilseed rape was evaluated by comparing their respective area under the ROC curve (AUC). The table using six parameters predicted the need for fungicide applications better than the one based on eight factors (Twengström et al., 1998). An additional feature of ROC analysis used in model evaluation is the possibility to determine an optimal decision threshold for a model when both sensitivity and specificity are equally valued. Such cut-off point (*J*) is identified as being closest to the coordinate (0, 1) on the ROC graph and can be determined from the Youden index (*J*= sensitivity + specificity -1) (Youden, 1950).

Different methodologies are employed to validate forecast models based on the availability of datasets. In the cross-validation strategy, one arbitrarily sets aside a portion of the data collected for development purposes while the remaining portion is used as a validation set. In such cases, datasets used for development were collected in the same period and location as those for validation (Harikrishnan and del Río, 2008). Another strategy is external validation, where one establishes plots in different locations and collects data for model validation purposes. In cases where external validation is conducted in following years, it is referred to as external and temporal validation (Foster et al., 2011, Willbur et al., 2018b). External validation is also applied to investigate the reliability of models operated in regions outside where the models were initially developed. Within a growing region, various weather conditions and farming practices prevail. Ensuring that the data collected for validation purposes represents such variability is important to accurately assess model reliability in those regions (Giroux et al., 2016).

Often, model validation shows that model performance in different environments is lower than in the setting in which the models were first developed (Bouchard, 2008). This leads to the development of multiple models to predict the same disease, most of which never get directly applied during producers' decision-making processes. Doing so is an inefficient use of data as the valuable knowledge derived from the observations used to develop previous models are not accounted for in the development of new ones (Moons et al., 2012). Instead of re-developing disease prediction models, poor predictive ability in new contexts can be addressed by customizing an original model equation to the new environment in which it will be used. This strategy has the

benefit of integrating findings from previous studies while ensuring that the modified model predictions are adapted to the setting in which the model is applied (Janssen et al., 2008, Steyerberg, 2019).

Disease prediction model customization is common practice in clinical epidemiology where physicians use models developed from patient data from a specific set of hospitals to generate patient prognosis in a different clinical setting (Curtin et al., 2019, Steyerberg and Vergouwe, 2014). In botanical epidemiology, model customization has been done for different pathosystems, including potato late blight (*Phytophthora infestans* (Mont.) de Bary), early blight (*Alternaria* spp.), and tomato grey leaf spot (*Ascochyta lycopersici* Brun.) (Hjelkrem et al., 2021, Meno et al., 2020, Wang et al., 2020). The statistical methodology used to update prediction models comprises multiple strategies. A simple recalibration method consists of a modification of the model intercept, re-estimation involves adjusting all regression coefficients associated with model variables, and the more complex extension approaches result in new variables being added to the model (Steyerberg, 2019, Steyerberg and Vergouwe, 2014, Janssen et al., 2008).

Connecting text between Chapter 2 and Chapter 3

The next chapter's emphasis is on the association between *S. sclerotiorum* carpogenic germination and agro-environmental variables. The influence of weather conditions on the apparition and abundance of apothecia has been documented previously in the literature, but it has not been investigated across soybean production regions of Québec. In addition, weather-based *Sclerotinia*-related prediction models were previously developed in the United States for legume crops, but no model has been developed or tested in Québec. The aim of Chapter 3 is to first study the correlation between environmental variables and carpogenic germination of sclerotia in soybean fields, and then to validate selected *Sclerotinia*-related prediction models for agro-environmental conditions of Québec.

Chapter 3: Effect of agro-environmental variables on Sclerotinia sclerotiorum carpogenic germination and evaluation of SSR bioclimatic prediction models in soybean (Glycine max) in Québec

3.1 Introduction

Sclerotinia stem rot (SSR), caused by the pathogenic fungus *Sclerotinia sclerotiorum* (Lib.) de Bary, affects a wide range of hosts comprising mostly dicotyledonous and some monocotyledonous plants. Across the world, several hosts are economically important oilseed and pulse crops (Boland & Hall, 1994). In Canada, SSR is a major disease of soybean (*Glycine max* (L.) Merr.), canola (*Brassica napus* L.), potato (*Solanum tuberosum* L.), and sunflower (*Helianthus annuus* L.). In Québec, among the top three soybean-producing provinces in Canada, SSR frequently occurs in soybean fields. Prevailing temperature and humidity during the soybean growing season can cause variations in how SSR reduces yields. In Québec, the disease generally causes yield losses ranging from 0-20% (Breault et al., 2017, Rousseau et al., 2004); however, environmental conditions suitable for soybean infections by *S. sclerotiorum* inoculum can exacerbate the problem and affect production even more severely (Breault et al., 2017). SSR epidemics result in reductions in soybean density, and pod and seed quality. In turn, the repercussions of SSR incidence on the producers' revenues and the economy is substantial (Bailey et al., 2004).

Sclerotia are the survival structure of *S. sclerotiorum*, which can germinate myceliogenically, producing mycelium, or carpogenically, producing apothecia. The latter is epidemiologically more important than myceliogenic germination for Sclerotinia stem rot of soybean as the ascospores produced from apothecia are the main source of inoculum (Abawi and Grogan, 1975). Soil-borne sclerotia carpogenic germination, and subsequent apothecia formation, is influenced by agronomic and environmental factors. Conditions conducive to apothecia emergence include a cool and moist climate fostered by a closed canopy (Fall et al., 2018a, Abawi, 1979). In addition, SSR occurs when ascospores colonize senescing host tissues, suggesting that apothecia development and inoculum density during soybean flowering stages and SSR severity may be tightly correlated

(Huzar-Novakowiski and Dorrance, 2018). In soybean, in which no SSR-resistant cultivar yet exists, flower petals are the nutrient source of choice for ascospores. Previous reports indicate that soybeans are particularly susceptible to infection during the flowering period (Abawi and Grogan, 1975, Cook, 1975).

Sclerotinia disease epidemiology has been previously studied and reviewed in various crops, including soybean (Abawi and Grogan, 1975, Saharan and Mehta, 2008, Peltier et al., 2012, Willbur et al., 2018a); however, the effect of environmental and agronomic variables on *S. sclerotiorum* carpogenic germination of sclerotia and disease severity has not been investigated in Québec. In addition, the association between the timing of apothecia presence and DSI levels has not been examined in Québec. This study is separated into distinct yet complementary objectives. The first goal was to use data from soybean-producing regions in Québec to confirm the importance of SSR risk factors among previously studied environmental and agronomic variables. The second goal was to identify additional environmental predictors of the risk of sclerotia germination and apothecia formation among previously unstudied factors and establish their relevance to disease management challenges. The final goal was to assess whether previously published inoculum and SSR disease prediction models could adequately predict SSR disease severity under Québec soybean growing conditions.

3.2 Materials and Methods

3.2.1 Experimental sites and data collection

Commercial soybean fields were identified as study sites in partnership with the Québec Ministry of Agriculture, Fisheries and Food (MAPAQ) based on three main criteria; field history of SSR, producer's willingness to abstain from using fungicides, and proximity to an Agrometeo weather station. To include agro-environmental conditions representative of the Québec soybean industry, the number of field sites for each region was prorated based on the regional share of the soybean provincial production. Additional fields were also established at research centres within the province. The research sites were located at the Emile A. Lods Agronomy Research Centre of McGill University in Sainte-Anne-de-Bellevue, the Agronomy Research Station of Laval University in Saint-Augustin-de-Desmaures, the Centre de recherche sur les grains, inc. (CÉROM) in Saint-Mathieu-de-Beloeil, and the Institut de recherche et développement en agroenvironnement

(IRDA) in Saint-Lambert-de-Lauzon. The soybean cultivar chosen for each site was selected based on the agro-environmental zone in which the fields were located. Soybeans were seeded from mid-May to mid-June and harvest was done in late September, with some variation from one site to another attributable mainly to local environmental conditions. Table A. 4 shows the number and type of fields scouted from 2019 to 2021.

3.2.2 Experimental design

Experimental sites were artificially inoculated with sclerotia deposits. Sclerotia were preconditioned by being exposed to a cool (4°C) and moist environment for 12 weeks following their production under laboratory conditions at CÉROM. The sclerotia deposits consisted of 2.0 × 12.7 × 25.4 cm wooden frames, bottom-lined with mosquito netting, in which 14 *S. sclerotiorum* isolate NB-5 (provided by Sylvie Rioux, CÉROM) sclerotia were placed and covered by 1.5 cm of soil.

At the commercial sites, the row spacing in experimental plots was either 17.8-, 38.1-, 76.2-cm or twin rows (17.8- and 55.9-cm) based on the standard seeding equipment used by the producer at that site. Soybean rows were planted in the east-west direction to promote wind dispersal of *S. sclerotiorum* ascospores. Soybean seeding rates at each experimental site were determined based on cultivar and regional recommendations.

In each commercial field surveyed, four sclerotia deposits were artificially buried in experimental plots following plant emergence (beginning to mid-June) to observe carpogenic germination under field conditions. Deposits were placed on the north side of a soybean row representative of the plot, where the shade and humidity would promote carpogenic germination of sclerotia. Each deposit represented one field repetition for a total of four repetitions in each commercial field scouted. From one repetition to another, soybean deposits were separated by a minimum width of 3 rows and a minimum length of 50 m in regions representative of the field (Figure A. 1).

At the research centres, the experiment used a randomized complete block design with four blocks. In each block, experimental validation plots of approximately $6 \text{ m} \times 8 \text{ m}$ were established using three row spacings (17.8-, 38.1- and 76.2-cm), representing the experimental factor under study.

In total, there were 12 plots per site (three row spacings × four blocks). Zones of 76.2 cm between each experimental plot and 12 m spacing in between each block acted as buffer zones. Borders were planted around each block and the field to simulate standard environmental field conditions in the experimental plots, including wind and moisture conditions. Row orientation and buffer zones were as specified for the commercial fields. In research fields, one deposit containing 14 pre-conditioned *S. sclerotiorum* isolate NB-5 sclerotia was artificially buried in a single row at the centre of each plot at plant emergence (beginning to mid- June) for a total of 12 deposits per research centre site. Each deposit was placed on the north side of a soybean row representative of the plot (Figure A. 2).

3.2.3 Data collection

3.2.3.1 Weather data

Weather data was obtained for each of the growing seasons from 2019 to 2021 through the Agrometeo weather station network (Solutions Mesonet, 2021). Each experimental site was matched with the closest network weather station based on its GPS coordinates. Meteorological data recorded included air temperature (AT (°C)), relative humidity (RH (%)), wind speed (WS (km/h)) and rainfall (mm). An additional variable, the Abundant and Well-Distributed Rainfall index (AWDR) was created from the raw rainfall data (Tremblay et al., 2012). Weather data was also obtained from on-site Vantage Vue weather stations (Davis Instruments Corporation, United States, cat. #6351) in commercial sites located far from the local Agrometeo weather stations.

3.2.3.2 Apothecia scouting data

From 2019 to 2021, in commercial and research sites, scouting for apothecia formation in the deposits was performed twice a week from the end of June until the apparition of the first apothecium, and once a week subsequently until the R5 soybean developmental stage (variable date depending on the growing region). The number of germinated sclerotia, and the number and level of maturity (immature or mature) of apothecia was recorded for each scouting visit at each commercial and experimental site. The number of scouting visits varied from 4 to 16 for each site for a total of 789 visits over the three years of data collection (Table 3. 1).

Table 3. 1. Number and type of site for data collection in Québec from 2019 to 2021.

Dogion	Voor	Number (of sites	Number of		
Region	Year	Commercial	Research	apothecia scouting visits		
Capitale-Nationale	2019	1	1	22		
	2020	2	1	28		
	2021	2	1	34		
Centre-du-Québec	2019	1	0	10		
	2020	2	0	27		
	2021	2	0	18		
Chaudière-Appalaches	2019	2	1	45		
	2020	2	1	32		
	2021	1	1	26		
Estrie	2019	1	0	7		
	2020	2	0	20		
	2021	2	0	16		
Lanaudière	2019	2	0	8		
	2020	2	0	32		
	2021	2	0	22		
Laurentides	2019	1	0	10		
	2020	1	0	9		
	2021	1	0	11		
Mauricie	2019	1	0	10		
	2020	1	0	8		
	2021	1	0	15		
Montérégie-Est	2019	6	1	86		
	2020	5	1	83		
	2021	3	1	48		
Montérégie-Ouest	2019	2	0	18		
	2020	3	0	45		
	2021	3	0	47		

Table 3. 1 Number and type of site for data collection in Québec from 2019 to 2021 (cont'd).

Dogian	Year	Number	of sites	Number of	
Region	Year	Commercial	Research	apothecia scouting visits	
Montréal	2019	0	1	14	
	2020	0	1	16	
	2021	0	1	14	
Outaouais	2019	1	0	8	
Total		55	12	789	

For each scouting visit, the developmental stage of soybean plants was noted (Fehr and Caviness, 1977), along with plant height (cm) (mean of two plants per row, up to the apex). Other data collected included plant population and the level of canopy closure (cm), measured as the distance between two rows where the soil was visible.

At R5 and R8 soybean growth stages, a disease severity index (DSI) was recorded by taking the percentage of plants displaying symptoms of SSR and the severity of the symptoms displayed out of 30 plants in each experimental plot (two rows of 15 plants) at the commercial and research sites (Table 3. 2, Formula 3. 1). Control plots in both commercial and research fields were identified at the R5 soybean growth stage and consisted of 30 soybean plants (two rows of 15 plants) located in proximity of a sclerotia deposit, but not in the same row, in which the DSI was recorded at R5 and R8. The location of the control plot was chosen based on the area most representative of the crop conditions in the entire plot.

Table 3. 2. Sclerotinia stem rot disease severity class and associated symptoms on soybeans (Grau, 1984).

Severity Class	Disease Symptom
0	No SSR symptom
1	SSR symptoms only on lateral branches
2	SSR symptoms on main stem, without damage on pods
3	Dead plant or showing SSR symptoms on main stem and pods

The DSI for the plot was calculated using the following formula:

Formula 3. 1. Disease severity index (%) (Grau, 1984).

$$DSI = \frac{[\Sigma(severity \ class \times number \ of \ plants \ in \ class)] \times 100}{[(total \ number \ of \ plants \times number \ of \ classes \ with \ symptoms)]}$$

3.2.4 Data analysis

3.2.4.1 Associations between apothecia, SSR severity and selected weather variables

Statistical analyses were conducted in R statistics v.1.4.1717 (R Foundation for Statistical Computing, Austria) at the $\alpha=0.05$ significance level ('stats' package) (R Core Team, 2021). The relationship between apothecia observed at distinct soybean growth stages and end-of-season SSR severity was evaluated through Pearson correlation analyses. The association between apothecia and weather variables was assessed using Kendall's correlation matrix. The selected weather variables were maximum, mean, and minimum values of temperature and relative humidity, maximum and mean values of wind speed and the AWDR parameter. Those weather variables were selected based on pre-established relationships between carpogenic germination and temperature and humidity parameters such as rainfall and relative humidity (Willbur et al., 2018b). Kendall's correlation analyses were conducted using a binary apothecia variable and moving averages of weather variables with durations ranging from 10- to 40-days. The binary apothecia variable was created from the mean number of apothecia counted in each deposit in each experimental site. When the mean apothecia per site was above 0.25 (an average of 1 apothecium/4 deposits at one site), the binary variable was equal to 1, otherwise it was equal to 0.

The relationship between end-of-season disease severity index and weather variables were analysed through Pearson correlation analyses. The selected weather variables were maximum, mean and minimum temperature and relative humidity, maximum and mean wind speed, and the total rainfall for the months of June, July, and August. Those variables were chosen because they have been reported as influencing SSR disease development (Harikrishnan and del Río, 2008, Fall et al., 2018a).

3.2.4.2 Effect of the growing season, location and row spacing on timing of apothecia formation A time-to-event approach was used to characterize the duration of time between installing the sclerotia deposits in the field and the first carpogenic germination occurrence at the research sites from 2019 to 2021. This statistical methodology, borrowing from the survival analyses in biomedical epidemiology, allows for the analysis of censored data (Scherm and Ojiambo, 2004). The apothecia data are censored in two ways. They are interval-censored since the deposits were not continuously monitored. Instead, data were collected twice weekly. There is thus an interval of time, the period in between two subsequent scouting visits, as opposed to a single day, associated with each germination observation. In some cases, where no apothecia were produced in a deposit by the end of the growing season, the data is right-censored. Despite the time-to-event duration not established for those deposits, this information is valuable and can contribute to the understanding of carpogenic germination under Québec's climate. The time-to-event analysis was conducted by year and by research centre to describe the effect of row spacing on the speed of carpogenic germination. The estimated values for the number of days until the presence of one apothecium was observed in half of the sclerotia deposits (50% carpogenic germination, T50) were compared among the 17.8-, 38.1-, and 76.2-cm spaced plots in R ('drc' package) (Onofri et al., 2019, Ritz et al., 2015).

3.2.4.3 Effect of the growing season, location and row spacing on abundance of apothecia

3.2.4.3.1 Inoculum progress curve approach

The effect of year, location and row spacing on apothecia formation at the four research centres from 2019 to 2021 was evaluated using an analysis of variance of the area under the inoculum progress curve (AUIPC) calculated using the 'epifitter' package in R (Alves and Del Ponte, 2021). The ANOVA was performed in SAS v.9. 4 (SAS Institute, United States) using PROC GLM. As the pattern of apothecia formation was expected to vary from one research centre to another and from one year to the next, we anticipated differences in the number of scouting visits during which apothecia would be observed and in the maximum number of apothecia observed in each scouting visit. For each research centre and row spacing from 2019 to 2021, the area under the IPC (AUIPC) was calculated to simultaneously compare those two components (Carisse et al., 2014).

3.2.4.3.2 GLMM approach

In addition to the IPC approach, the effect of the row spacing on the production of apothecia was analysed using a generalized linear mixed-model (GLMM) approach using the data collected at the research centres under the RCBD design. This analysis was performed in SAS v.9. 4 (SAS Institute, United States of America) using PROC GLIMMIX (Gbur et al., 2012). The row spacing experiment was conducted at four research centres (IRDA, CÉROM, Laval University, and McGill University) from 2019 to 2021. However, CÉROM, Laval University and McGill University had low levels of carpogenic germination with many zero apothecia counts and low numbers of apothecia observed in all years of data collection. Since these sites did not provide enough data points, only observations from IRDA were used in the GLMM analysis. The statistical model for the analysis of apothecia data observed in the research centre from 2019 to 2021 was a repeated measures model of count data. The row spacing, the scouting visit and their interaction were treated as fixed effects, while the deposit and the replicate were treated as random effects. The GLMM approach was chosen to test the data using the analysis of variance framework despite not following the basic assumptions of normality, independence of data and homogeneity of variances. The response variable in the study was the number of apothecia observed in each deposit, which are non-negative integers. In GLMM, the basis for model parameters estimation is maximum likelihood. While both pseudo-likelihood and integral approximation methods can be used to estimate conditional GLMMs models, the integral approximation technique Laplace was chosen here to obtain a true log-likelihood function (Gbur et al., 2012). By default, PROC GLIMMIX estimation method is the restricted pseudo-likelihood (RSPL). The estimation method was changed using the "method=Laplace" option to override the default setting. This allowed for the fit statistics to be calculated and the goodness-of-fit of different models to be compared through the ratio of the Pearson chi-square to its degrees of freedom (Pearson Chi-Square/DF). The final model parameter estimates were those found to minimize the negative log-likelihood function.

Both the Poisson and the negative binomial distributions were considered as potentially appropriate to estimate model parameters. The Poisson distribution assumes that the data is evenly and randomly distributed within the experimental units (Pearson Chi-Square/DF = 1). If this was not the case, the negative binomial distribution was considered more appropriate since the scale parameter allows the variance to be different than the mean.

The apothecia observations were counted over time in the three years of data collection, thus showing dependency. The correlation in the responses was addressed by using a repeated measures analysis. The use of the Laplace estimation technique prevents the modelling of the R-side effects. The dependency of the responses was thus modeled by specifying a G-side covariance structure using the "random" statement. Both Compound Symmetry (cs) and First-Order Autoregressive (ar1) covariance matrix structures were investigated.

3.2.4.4 Effect of row spacing on disease severity index

The effect of row spacing on end-of-season disease severity index (DSI) was evaluated using an analysis of variance with the row spacing as a fixed effect. The fields at CÉROM, Laval University and McGill University showed no disease symptoms for most experimental plots in all years of data collection. The IRDA fields showed disease symptoms only in 2021. Since all sites in 2019 and 2020, and three of the sites in 2021 did not provide enough DSI data points, only DSI observations from IRDA in 2021 were used in this analysis. The ANOVA was performed in SAS v.9. 4 (SAS Institute, United States of America) using PROC GLM.

3.2.4.5 Validation of Sclerotinia-related prediction models

The performance of five *Sclerotinia* prediction models initially developed in the United States to predict *Sclerotinia*-related indicators such as *S. sclerotiorum* apothecia presence, SSR incidence and SSR severity was validated through receiver operator characteristic curve (ROC) analyses for their predictive ability regarding SSR severity. While many SSR disease forecasters exist, models tested here were selected based on the crop and location in which they were developed and the accessibility of predictor variables to Québec soybean farmers. Models developed for legume crops and in climates similar to Québec's continental conditions were retained. The first three models were developed using soybean from data collected in Iowa, Michigan, and Wisconsin in the United States (Willbur et al., 2018b). They are apothecia formation models that can help predict end-of-season SSR incidence based on carpogenic germination of sclerotia during the soybean flowering stages (Willbur et al., 2018c). Weather variables used as predictors are 30-day moving averages of maximum temperature (Willbur 1, Formula 3. 2), and maximum wind speed (Willbur 2, Formula 3. 3) and maximum relative humidity (Willbur 3, Formula 3. 4). The fourth model was

developed using data collected in soybean fields in the Midwest of the United States (Fall et al., 2018a). This model predicts the probability of DSI above 22 using the average temperature in July, the total precipitation in July and the interaction between those two variables (Fall, Formula 3. 5). The fifth model was developed on common bean (*Phaseolus vulgaris* L.) in North Dakota in the United States (Harikrishnan and del Río, 2008). It was hypothesized that the similarities between soybean and bean crops, including indeterminate growth habits and mid-May to early June planting periods, would potentially make the Harikrishnan model applicable to soybean in Québec. It predicts the risk of SSR incidence using the total precipitation in the first half of June, the average minimum temperature in the first half of July and the number of days with precipitations in the first half of August (Harikrishnan, Formula 3. 6). All five models were developed from logistic regression analyses and probabilities were obtained using the logit equation (Formula 3. 7).

All models were evaluated for their predictive ability regarding SSR disease severity even if, among the five models of interest, only the Fall model was originally derived to predict a DSI outcome. This choice was based on the associations between apothecia presence during the soybean flowering period, in-season weather variables and end-of-season DSI observations. This raised the question whether the Willbur model series and the Harikrishnan models could also be used to predict SSR disease severity in Québec. Additionally, disease severity and its impact on yield losses is perhaps more of concern than apothecia presence and disease incidence to soybean producers looking for disease management guidelines. Model performance was evaluated through receiver operating characteristic (ROC) curve analyses at the $\alpha = 0.05$ significance level in R ('verification' and 'pROC' packages) (Manubens et al., 2018, Robin et al., 2011).

Formula 3. 2. Willbur 1 model equation.

 $Logit(\mu) = -0.68(MaxT_{30MA}) + 17.19$

Where MaxT_{30MA} is the 30-day moving average of the maximum value of air temperature (°C).

Formula 3. 3. Willbur 2 model equation.

 $Logit(\mu) = -0.47(MaxT_{30MA}) - 1.01(MaxWS_{30MA}/1.609) + 16.65$

Where $MaxT_{30MA}$ is the 30-day moving average of the maximum value of air temperature (°C), and $MaxWS_{30MA}$ is the 30-day moving average of the maximum of wind speed (km/h).

Formula 3. 4. Willbur 3 model equation.

 $Logit(\mu) = -0.56(MaxT_{30MA}) + 0.10(MaxRH_{30MA}) - 0.75(MaxWS_{30MA}/1.609) + 8.20$

Where MaxT_{30MA} is the 30-day moving average of the maximum value of air temperature (°C),

MaxWS_{30MA} is the 30-day moving average of the maximum of wind speed (km/h),

And MaxRH_{30MA} is the 30-day moving average of the maximum of relative humidity (%).

Formula3. 5. Fall model equation.

$$Logit(\mu) = -9.77(Tp.J) - 1.76(PP.J) + 0.09(Tp.J*PP.J) + 197.33$$

Where Tp.J is the average temperature in July (°C),

PP.J is the total rainfall in July (mm),

and Tp.J*PP.J is the interaction between the average temperature and rainfall in July.

The coefficient for the PP.J was modified from 176 to 1.76 following an error in the original manuscript (M. L. Fall, personal communication, October 2021).

Formula 3. 6. Harikrishnan model equation.

$$Logit(\mu) = 1.70(TRFJ1) + 1.50(MinTJu1) - 0.05(RDAug1) - 26.00$$

Where TRFJ1 is the total rainfall during the first half of June (mm),

MinTJul is the average minimum temperature in the first half of July (°C),

and RDAug1 is the number of rainy days in the first half of August.

Formula 3. 7. Logit equation to calculate the probability disease severity.

Probability =
$$\frac{e^{logit(\mu)}}{(1 + e^{logit(\mu)})}$$

A new binary SSR severity variable was created from the DSI ratings in each experimental site in each year of data collection in Québec. When the DSI in the experimental plot was above 10, the binary variable was equal to 1, otherwise it was equal to 0. The DSI value of 10 was chosen as a disease indicator based on the SSR severity rates observed in Québec from 2019 to 2021 and severity values reported to be of concern for soybean producers (Willbur et al., 2018c).

In the first phase of analysis, the accuracy of each model was evaluated through a z statistic testing the null hypothesis that the area under the receiver operator characteristic curve (AUC) of the model under evaluation was not significantly different from 0.500, which represents the AUC of the line of no-discrimination on a ROC graph. This procedure was used to test whether the models forecasted SSR severity significantly better than chance ($\alpha = 0.05$). Models with an AUC not significantly different than 0.500 were considered poor predictors of SSR severity (Hughes et al., 1999).

In the second phase of analysis, comparisons of the models were performed through pairwise $\chi 2$ statistic tests at a family-wise error rate of 0.05, with degrees of freedom of N-1 where N is the number of AUCs derived from the covariance matrices of the Mann-Whitney U-statistic (Bamber, 1975, DeLong et al., 1988, Hanley and McNeil, 1982). Using the Delong (1988) method, the covariance matrices accounted for the correlated nature of the ROC curves generated from the same data sets. This analysis was used to test whether a model forecasted SSR severity significantly better than the other models (DeLong et al., 1988).

3.2.4.5.1 Threshold selection

3.2.4.5.1.1 Youden index

In the third phase of analysis, the accuracy, sensitivity and specificity of models were assessed at their respective optimal threshold derived from the Youden index (*J*) and from a published probability action threshold of 40% from the development and validation phases of the Willbur models (Formula 3. 8) (Youden, 1950, Willbur et al., 2018b, Willbur et al., 2018c). The Youden index is identified as being closest to the coordinate (0, 1) on the ROC graph and equally values sensitivity and specificity. An action threshold appropriate to the agro-environmental context of Québec must be identified for the model equations to be used in an integrated decision support system for producers. The action threshold is a model probability value above which a fungicide application would be indicated to prevent the colonization of soybean tissues by ascospores and yield-reducing end-of-season disease severity. Such an action threshold value must strike a balance between over and under-spraying. The action threshold should be high enough that fungicides are not sprayed unnecessarily, for example when the risk of disease development is low. However, the

action threshold should be low enough that fungicides applications are not delayed, for example when the risk of SSR severity is high.

Formula 3. 8. Equation to calculate the Youden index of the models (Youden, 1950).

J= sensitivity + specificity -1

The percentage of correct predictions obtained for each model was used as a measure of model accuracy. The percentage of correct predictions was calculated by dividing the number of model successes by the total number of observations and multiplying by 100. Sensitivity and specificity were used to assess a model's tendency to over-predict or under-predict SSR severity. Sensitivity was measured by the proportion of true positives; the number of correctly predicted instances of disease presence over the total number of instances of disease presence. Specificity was measured by the proportion of true negatives; the number of correctly predicted instances of absence of disease over the total number of instances of disease absence observations.

3.2.4.5.1.2 Published threshold

The selection of an appropriate threshold to use with each model under study was based on the likelihood ratios from the Youden index and the published 40% threshold derived from each model's ROC curve (Willbur et al., 2018b). The likelihood ratio of a positive prediction (LR+) corresponds to sensitivity/(1-specificity), while the likelihood ratio of a negative prediction (LR-) corresponds to (1-sensitivity)/specificity. The predictive ability of a model increases either as LR+ increases or LR- decreases. As the LR+ of a model increases, the model accuracy in apothecia presence situations increases. As the LR- of a model decreases, the model accuracy in the absence of apothecia increases. At an appropriate action threshold, a model with good predictive power would be associated with an LR+>1 and an LR- <1 (Biggerstaff, 2000).

3.3 Results

3.3.1 Association between apothecia at selected soybean growth stages and DSI

Figure 3. 1 shows the experimental sites where *S. sclerotiorum* apothecia were observed in the deposits placed in the experimental plots during each soybean growth stage in 2019, 2020 and

2021. Random noise was added through a jittering effect to avoid overplotting the data represented in Figures 3. 1 and 3. 2. In the three years of scouting, no apothecia were observed in the deposits during the vegetative growth stages. The first apothecia were observed at the R3 growth stage in one experimental site in the Laurentides in 2019, at the R2 growth stage in one experimental site in Montérégie-Est in 2020, while they were observed earlier, starting at the R1 growth stage in five experimental sites in Montérégie-Est and Montérégie-Ouest in 2021. There were no apothecia at the experimental site in the Outaouais region which was surveyed in 2019 only (Figure 3. 1).

SSR symptoms were observed only at a few experimental sites over the three years of data collection, as shown in Figure 3. 2. In 2019, SSR severity was greater than the 10% DSI threshold in four experimental sites in the Montérégie-Est, Laurentides, and Chaudière-Appalaches regions. The highest DSI observed in a plot in 2019 was 94.4% in Chaudière-Appalaches, where apothecia were first observed in the deposit at the R4 growth stage. In 2020, SSR severity was above the 10% DSI threshold in three experimental sites in the Centre-du-Québec and Estrie regions. The highest DSI observed for a plot in 2020 was 43.3% in Centre-du-Québec, where apothecia production in the deposit started at the R4 growth stage. In 2021, SSR severity was above the 10% DSI threshold in three experimental sites in the Centre-du-Québec, Estrie, and Chaudière-Appalaches regions. The highest DSI observed in 2021 was 63.3% in a plot in Estrie, where apothecia were first observed in the deposit at the R2 growth stage, and the peak apothecia formation occurred between the R4 and R5 growth stages (Figure 3. 2).

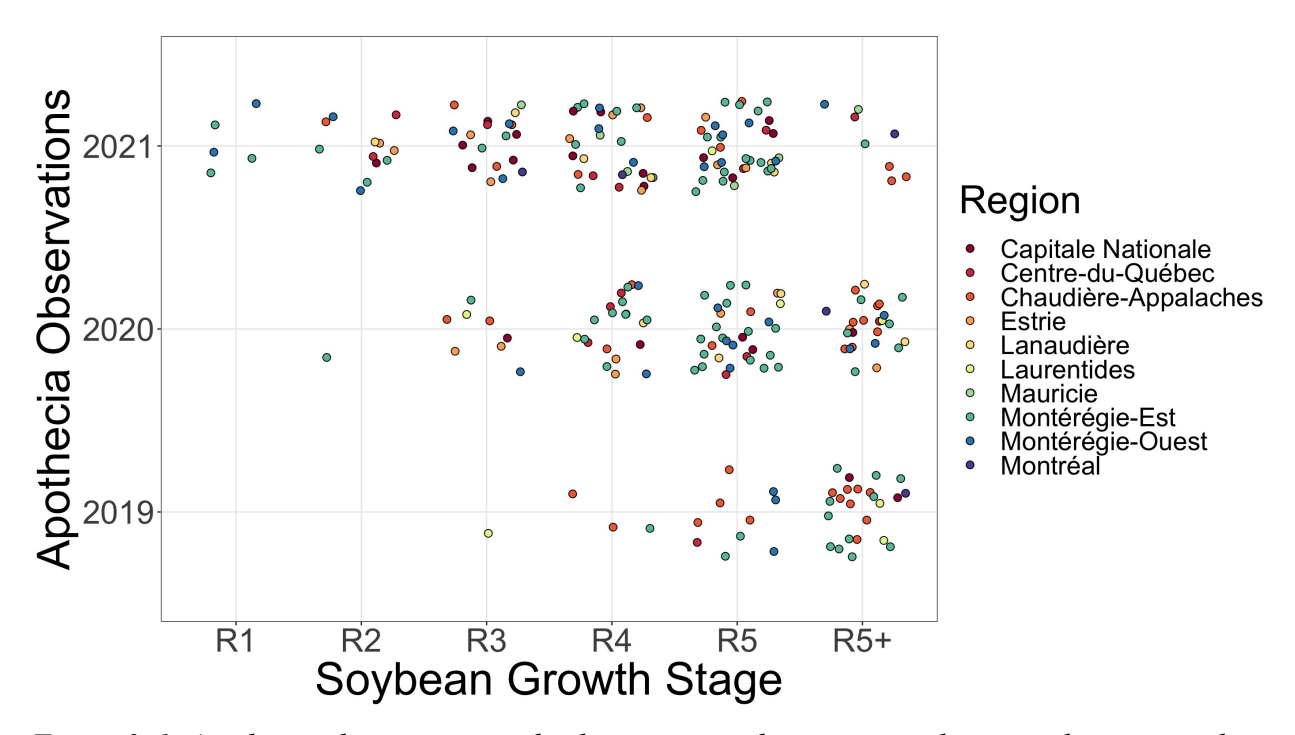


Figure 3. 1. Apothecia observations in the deposits at each experimental site in relation to soybean growth stages in Québec from 2019 to 2021. Each dot represents one experimental site where at least one apothecium was present, and the dot colour identifies the experimental site's region.

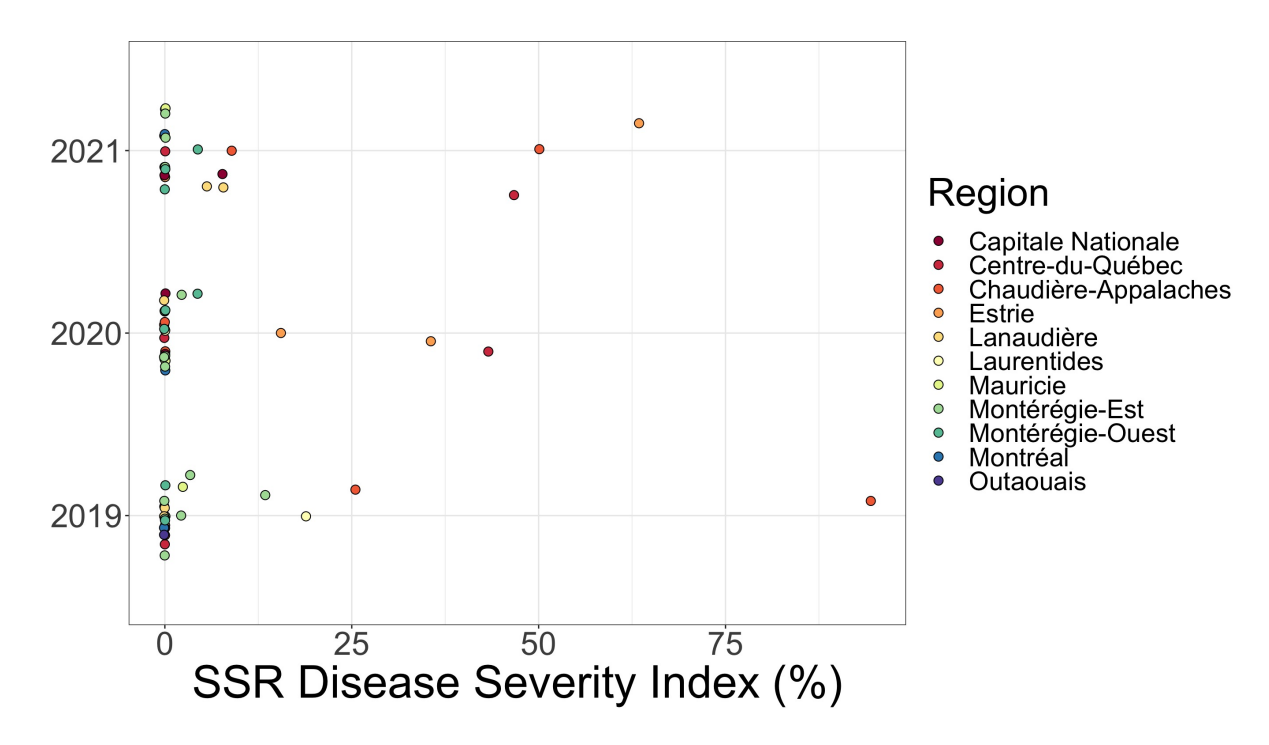


Figure 3. 2. Disease severity index (%) of inoculated soybean plots at experimental sites from 2019 to 2021 in Québec. Each dot represents one experimental site, and the dot colour identifies the experimental site's region.

Sclerotinia stem rot severity was positively associated with apothecia observed in the deposits between the R2 and R5 growth stages. The DSI was very weakly negatively correlated with apothecia produced during the R1 growth stage and beyond the R5 growth stage. The apothecia produced during the R2, R3, and R4 growth stages had a significant relationship with DSI (r > 0.27, P < 0.05), with R3 apothecia having the largest correlation coefficient (r = 0.34, P < 0.05) between 2019 and 2021 (Figure 3. 3).

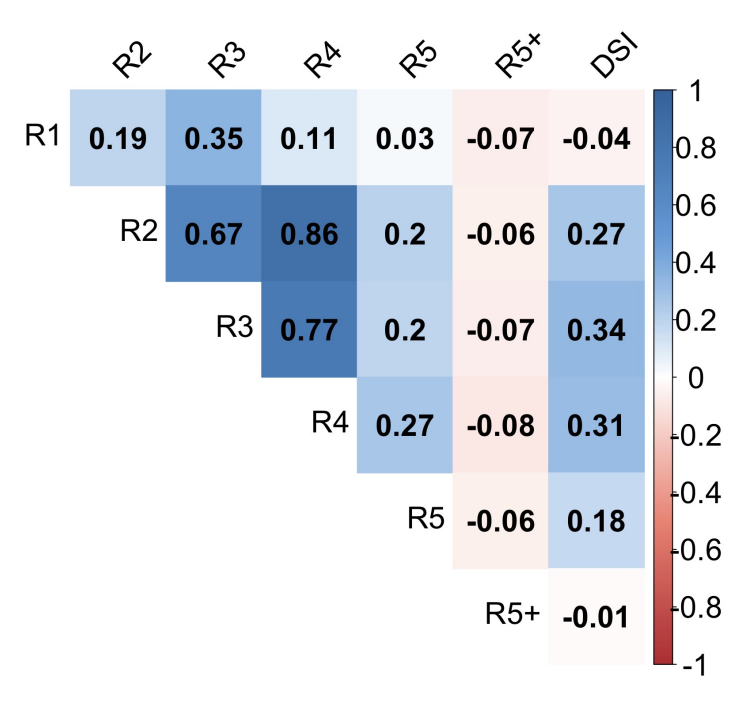


Figure 3. 3. Correlation matrix showing the Pearson correlations between apothecia observed during the soybean growth stages R1 to R5 and beyond (R5+) and the disease severity index (DSI)(%) from 2019 to 2021 in experimental sites in Québec. The blue colour indicates a positive correlation and the red color shows a negative correlation.

3.3.2 Association between apothecia and selected weather variables

The relationship between apothecia formation and weather variables was assessed through a correlation analysis. A value of 0.25 mean apothecia/deposit was initially used as a threshold to construct the apothecia binary variable used in correlation analyses as it corresponds to the presence of a single apothecium observed in only one of the four deposits placed in each experimental site. The optimal moving average durations were identified based on the number of variables correlated with the resulting binary variable and the strength of the relationship (Table

A. 5). The moving average duration with the most weather variables strongly correlated with the binary apothecia variable were 10-day, 20-day and 30-day periods. In addition to 0.25 mean apothecia/deposit, values of 0.50, 0.75 and 1.00 mean apothecia/deposit were analysed as potential thresholds to construct the binary apothecia variable to identify optimal moving average durations (Table A. 6). There were no differences in the strength or the number of correlated variables based on the value of the threshold, and as such, a value of 0.25 mean apothecia/deposit was used for the remainder of the analyses.

Figure 3. 4 shows that the associations between weather variables and apothecia presence were similar in strength and direction for 10-day, 20-day and 30-day moving averages and different for some variables for the 40-day moving average duration over the three years of data collection. The presence of apothecia was positively associated with maximum, mean, and minimum values of relative humidity and the rainfall AWDR parameter. There was a negative correlation between apothecial presence and maximum, mean, and minimum values of temperature and maximum and mean values of wind speed. From 2019 to 2021, the variables most strongly associated with the presence of apothecia were mean relative humidity (r > 0.39, P < 0.05) and maximum daily temperature (r > 0.30, P < 0.05) for 10-day, 20-day and 30-day moving average durations. The relative humidity associations were strongest at the 40-day and 30-day moving average durations, while the temperature coefficients were greater for the 10-day and 20-day periods (Figure 3. 4).

There were some differences in the strength of the association between apothecia formation and weather variables from one year to the next. The association between apothecia formation and relative humidity, especially mean values, was the most consistent. However, the association between carpogenic germination and other weather variables such as temperature and wind speed fluctuated from 2019 to 2021. Maximum temperature was most strongly associated with apothecia formation in 2019 (r = -0.60, P < 0.05), and less in 2020 (r = -0.22, P < 0.05) and 2021 (r = -0.03, P > 0.05). It was the opposite for maximum wind speed as the correlation with apothecia was strongest in 2021 (r = -0.36, P < 0.05) (Figure A. 3).

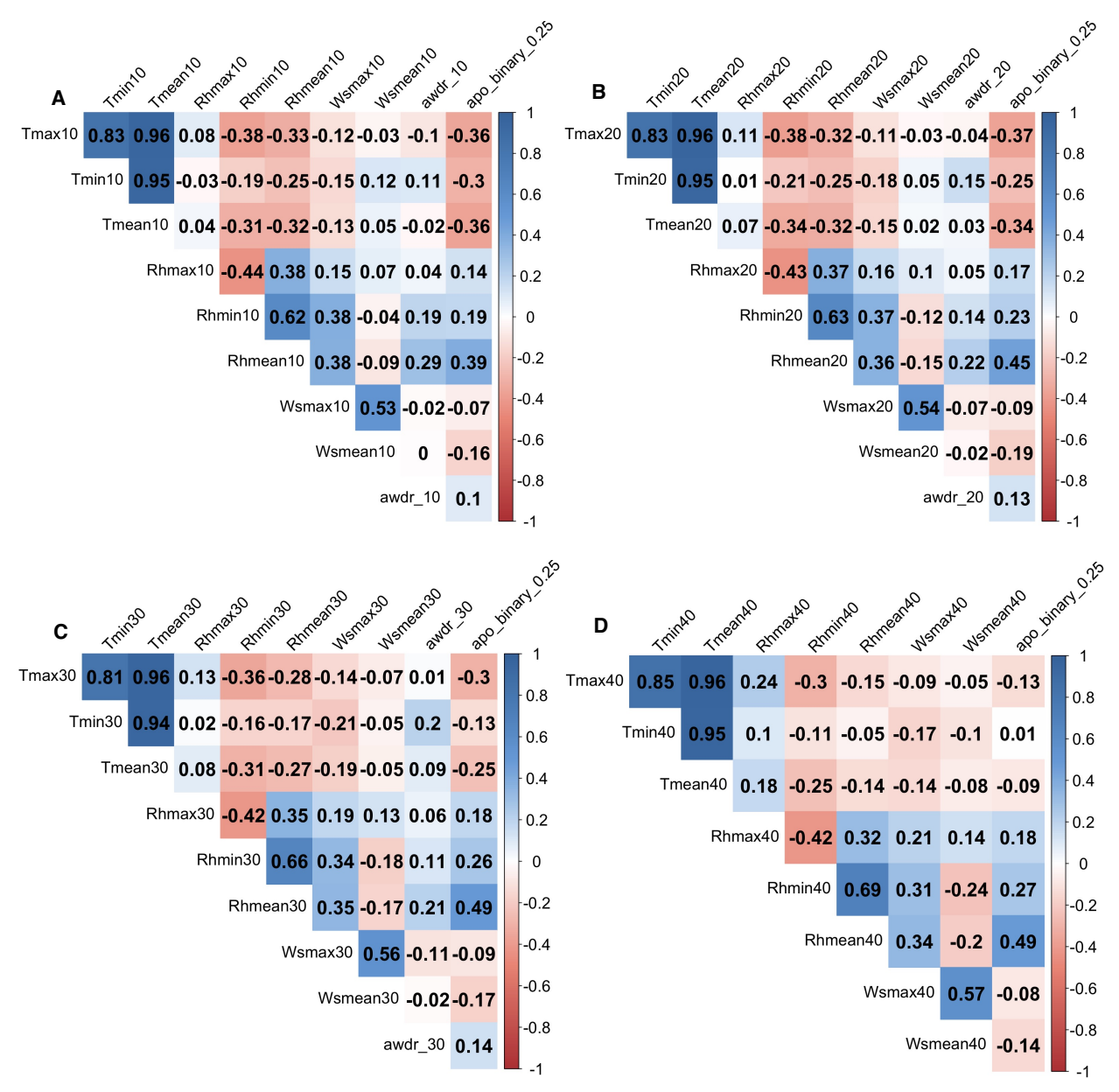


Figure 3. 4. Correlation matrices showing the correlation coefficients for Kendall correlations between A) 10-day, B) 20-day C) 30-day and D) 40-day moving averages of weather variables and the apothecia binary variable created based on a threshold of 0.25 mean apothecia/deposit in Québec from 2019 to 2021. The blue colour indicates a positive correlation and the red colour shows a negative correlation.

3.3.3 Association between SSR severity and selected weather variables

The relationship between SSR severity and weather variables during selected periods of the growing season was assessed through correlation analyses. June was the month with the most weather variables strongly and significantly correlated with SSR severity (Figure 3. 5; Table A.

7). Relationships between selected weather variables in August and SSR severity were weak and not statistically significant. SSR severity was most strongly associated negatively with mean (r = -0.26, P < 0.05) and maximum (r = -0.34, P < 0.05) temperature in June, mean (r = -0.25, P < 0.05) and minimum temperature in July (r = -0.33, P < 0.05), mean temperature in September (r = -0.26, P < 0.05) and with total rain in July (r = -0.23, P > 0.05). Among the positive relationships, SSR severity was most strongly associated with moisture parameters such as total rainfall, mean relative humidity, and all AWDR values in June and mean relative humidity in September (Figure 3. 5). Precipitations after July were weakly associated with SSR severity as the correlation coefficients for rain and DSI were low in August and September. Despite the significant relationship between disease severity and mean wind speed in June, the coefficient was low (r = 0.16, P = 1.027E-08) (Figure 3. 5).

3.3.4 Effect row spacing and location on timing and abundance of apothecia formation

Figure 3. 6 shows the number of *S. sclerotiorum* apothecia observed at each research centre for the 17.8-, 38.1- and 76.2-cm row spacing plots from 2019 to 2021. In each year of data collection, apothecia were observed at all research centres in at least one plot. However, apothecia were not observed in each of the three row spacing plots. No apothecia were observed in the 17.8- and 76.2-cm spaced plots at CÉROM in 2019, in the 17.8-cm spaced plots at McGill University and CÉROM, the 76.2-cm spaced plots at McGill University in 2020 and in the 17.8-cm spaced plots at McGill University in 2021. Apothecia formation occurred when the canopy was on average 94.4% closed across all commercial and research sites scouted. In addition, no apothecia were observed prior to the canopy being at least 46.3% closed, which occurred in a 55.9-cm row spacing experimental site in Centre-du-Québec on July 12th, 2021.

From 2019 to 2021, at the research centres, the maximum number of apothecia observed was highest at IRDA (Figure 3.6D) with a mean peak value of 17.4 apothecia/deposit, compared to 3.9 apothecia/deposit at Laval University (Figure 3.6A), 1.6 apothecia/deposit at CÉROM (Figure 3.6C) and 2.4 apothecia/deposit at McGill University (Figure 3.6B). At IRDA, apothecia were observed in all the deposits in each year of data collection (Figure 3.6D).

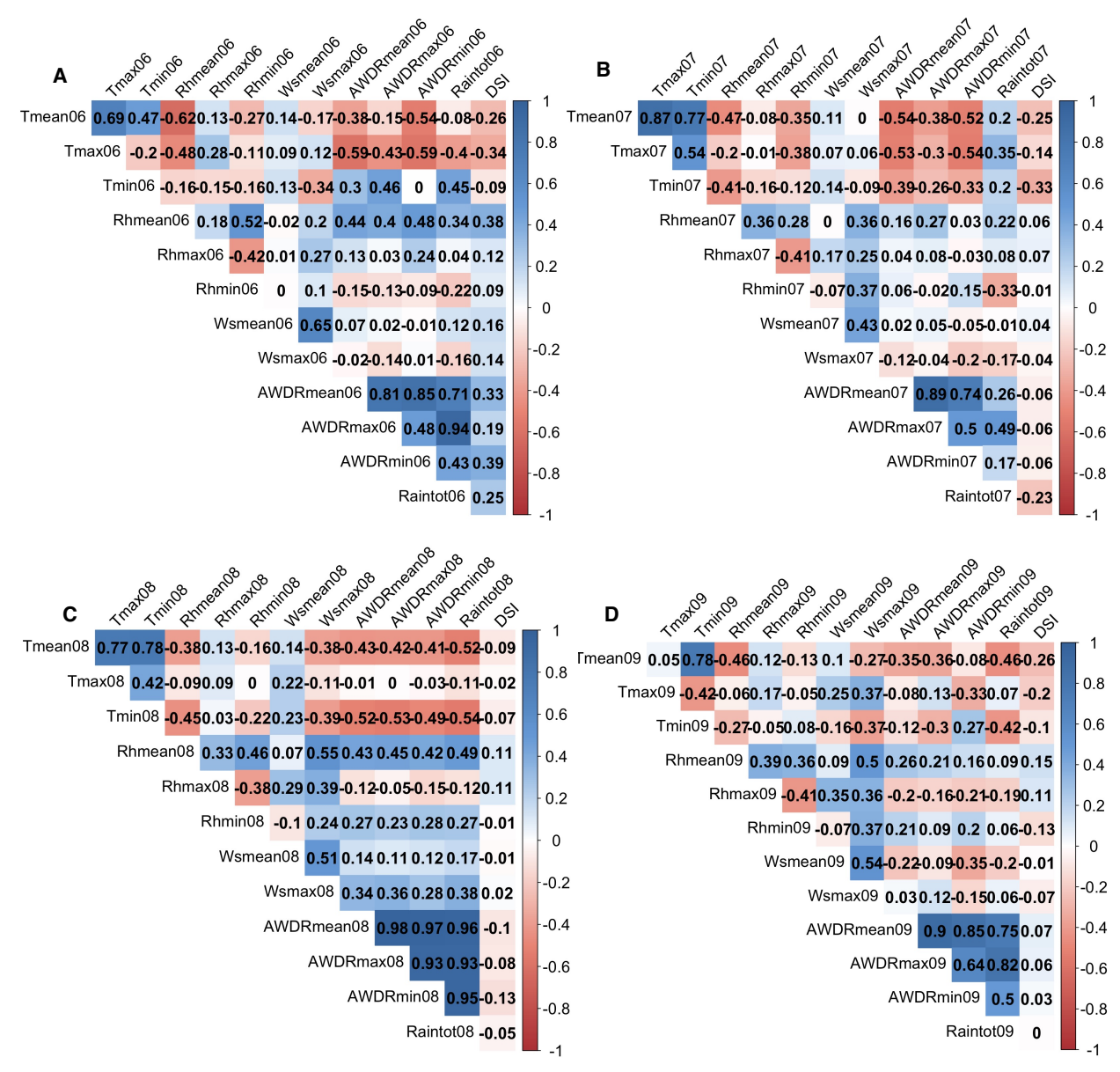


Figure 3. 5. Pearson correlations between A) June, B) July, C) August, and D) September weather variables and the DSI (%) for soybean fields from 2019 to 2021. The blue colour indicates a positive correlation and the red colour shows a negative correlation.

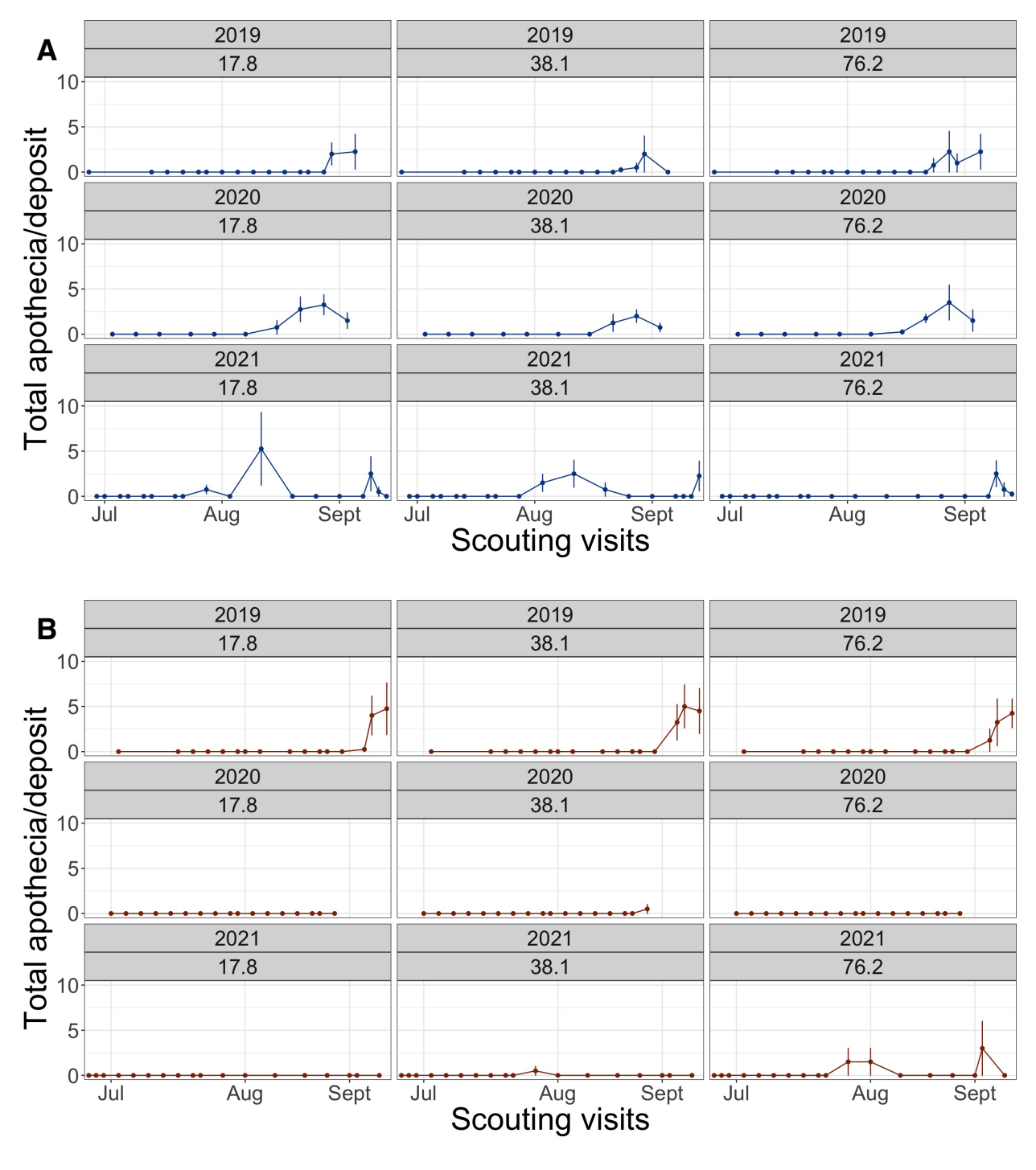


Figure 3. 6. Total apothecia observations in deposits in 17.8-, 38.1-, and 76.2-cm row spacing plots at A) Saint-Augustin-de-Desmaures (Laval University), B) Sainte-Anne-de-Bellevue (McGill University), C) Saint-Mathieu-de-Beloeil (CÉROM), and D) Saint-Lambert-de-Lauzon (IRDA) from 2019 to 2021. Each dot is a mean of apothecia counts from each of the four deposits for each row spacing and the vertical lines represent the standard error.

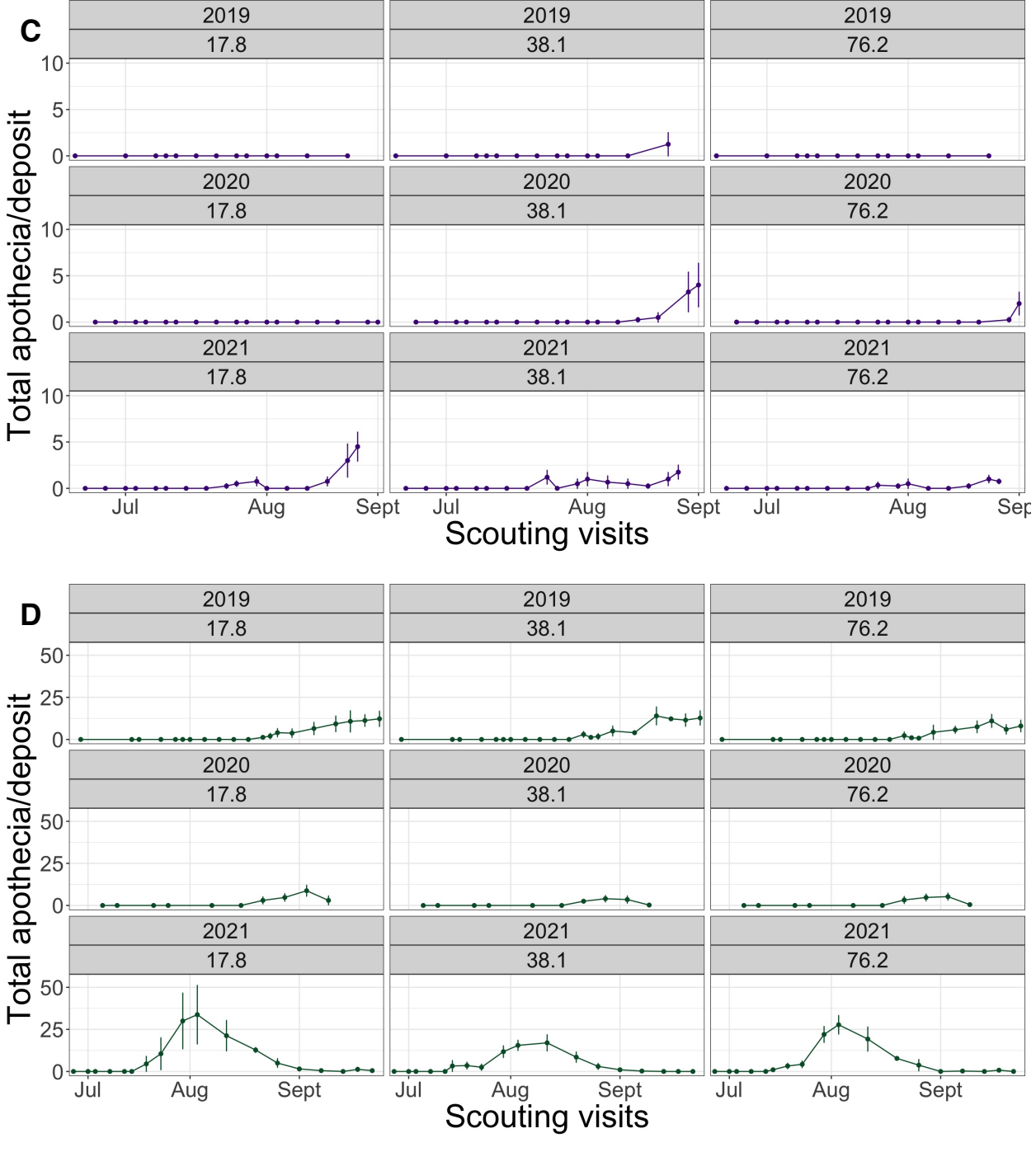


Figure 3. 6. Total apothecia observations in deposits in 17.8-, 38.1-, and 76.2-cm row spacing plots at A) Saint-Augustin-de-Desmaures (Laval University), B) Sainte-Anne-de-Bellevue (McGill University), C) Saint-Mathieu-de-Beloeil (CÉROM), and D) Saint-Lambert-de-Lauzon (IRDA) from 2019 to 2021 (cont'd). Each dot is a mean of apothecia counts from each of the four deposits for each row spacing and the vertical lines represent the standard error.

Within each research centre, apothecia first appeared at similar times during the growing season despite the three different row spacings used at planting. In the plots where apothecia were observed in at least one deposit, the survival analysis results showed that the difference in the length of time before the apparition of the first apothecia was not statistically significant based on row spacing in each year of data collection (Table A. 8).

The area under the inoculum progress curve (AUIPC) was calculated for the apothecia formation at each experimental plot at the four research centres from 2019 to 2021. The 3-term interaction between the row spacing, research centre and year was not significant and was removed from the statistical model. The 2-term interactions between row spacing and research centre, and row spacing, and year were not statistically significant. However, the 2-term interaction between the research centre and the year was statistically significant (Table 3. 3). The largest AUIPCs were observed at IRDA in 2021 and at IRDA in 2019 (Table A. 9).

Table 3. 3. Type III tests of fixed effects for the effect of row spacing on the area under the inoculum progress curve at research centres in Québec from 2019 to 2021.

Main effects and interactions	F value	$Pr > F^1$
Row spacing	0.59	0.5550
Research centre	46.74	< 0.0001
Year	11.32	< 0.0001
Row spacing * Research centre	0.80	0.5688
Row spacing * Year	0.85	0.4991
Research centre * Year	10.51	< 0.0001

¹The p-value for the F statistic (a = 0.05).

The effect of row spacing on apothecia formation was further evaluated at IRDA, where carpogenic germination was observed in all experimental plots in 2019, 2020 and 2021. A GLMM analysis with temporal repeated measures (scouting visits) was performed with Poisson and negative binomial distributions, and with compound symmetry and first order autoregressive covariance structures. Based on the optimal AIC and Pearson chi-square/DF values, the model using Negative binomial distribution and a first-order autoregressive covariance structure was

retained for the analysis (Table A. 10). The results showed no significant difference in the abundance of apothecia in the plots with different row spacing at IRDA in 2019, 2020 and 2021 (Table 3. 4).

Table 3. 4. Type III tests of fixed effects for the effect of row spacing on apothecia formation at IRDA from 2019 to 2021.

Main effects and interactions	F Value	$Pr > F^1$
Row spacing	0.09	0.9105
Visit	7.27	< 0.0001
Year	1.31	0.2725
Row spacing*Visit	0.55	0.9879
Row spacing * Year	0.20	0.9377

¹The p-value for the F statistic (a = 0.05).

3.3.5 Disease severity index at the research centres from 2019 to 2021

Disease severity indices were calculated for each experimental plot at the four research centres from 2019 to 2021. In 2019, out of the four research sites surveyed, disease symptoms were only observed at the Laval University site located in the Capitale-Nationale region. At that site, only one experimental plot, planted with 76.2-cm row spacing, showed disease symptoms with a DSI value of 5.6%. The other 11 experimental plots at the Laval University research site had DSI values of 0.0% in 2019. In 2020, among research centres, disease symptoms were only observed at the CÉROM location in the Montérégie-Est region. Out of the 12 experimental plots at CÉROM, only one 17.8-cm spaced plot showed very minimal disease symptoms with a DSI value of 1.1%. In 2021, disease symptoms were observed at IRDA, in the Chaudière-Appalaches region, while the three other research centres had no sign of disease (Figure 3. 2 and Figure 3. 7). DSI was the highest in the 38.1-cm spaced plots with a mean value of 19.2%, while the mean DSI was 7.5% and 5.0% in the 17.8- cm and 76.2-cm spaced plots respectively at IRDA in 2021. The difference in DSI between the three row spacings was not significantly different (Table A. 11).

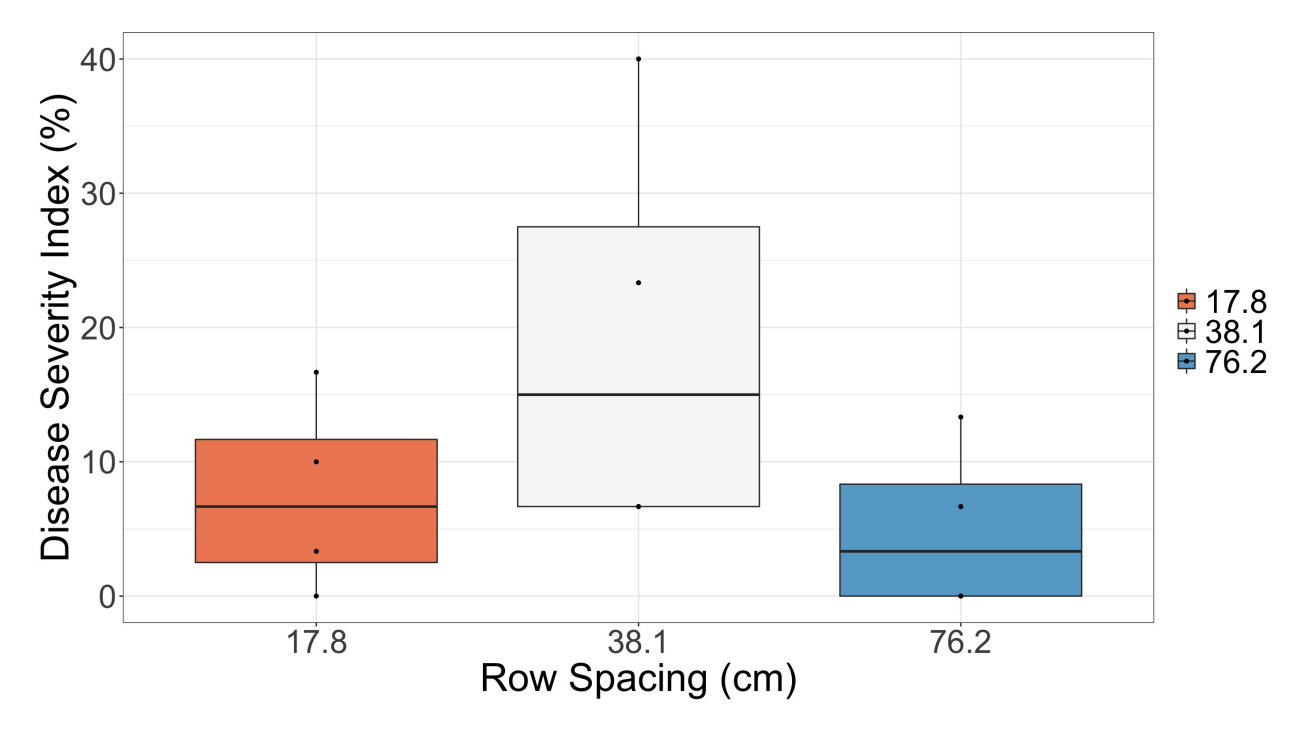


Figure 3. 7 Disease severity index (%) at R8 for 17.8-, 38.1-, and 76.2-cm spaced experimental plots at the IRDA research centre in 2021.

3.3.6 Validation of Sclerotinia-related prediction models

Over the three years of data collection, SSR severity in Québec varied between DSI values of 0.0 and 94.4% at the field level. The sites surveyed were artificially inoculated with sclerotia and had an established history of Sclerotinia stem rot. However, 85.1% of fields showed little to no disease symptoms (DSI < 10%) and were considered controls in the model validation dataset. The proportion of cases, fields with a DSI of 10% and above, was highest in 2019 (18.2%) and lowest in 2020 (12.5%) as seen in Table 3. 5.

Table 3. 5. Proportion of cases and controls in Québec from 2019 to 2021 based on a DSI threshold of 10%.

Vaan	Sites	Disease	Disease	Casas (0/)1	Controls (9/)2	
Year	Scouted	Presence	Absence	Cases (%) ¹	Controls (%) ²	
2019	22	4	18	18.2	81.8	
2020	24	3	21	12.5	87.5	
2021	21	3	18	14.3	85.7	
Total	67	10	57	14.9	85.1	

¹Cases are fields with a disease severity index of 10% and above.

3.3.6.1 AUC pairwise comparisons

Selected SSR models were evaluated for their capacity to predict disease severity at the 10% DSI level through AUC analyses as shown in Figure 3. 8. The models' ability to determine whether an occurrence of a disease severity index of 10% or above varied throughout the three years of data collection. The models' performances were generally better in 2020 and 2021 compared to 2019. In 2019, none of the models' AUC was significantly greater than the AUC of the no-discrimination line (0.500) with values ranging from 0.403 to 0.639 (Figure 3. 8A). In 2020, Willbur 1, Willbur 2, Willbur 3 and Harikrishnan models had AUCs significantly larger than the no-discrimination line with values ranging between 0.810 and 0.921 (Figure 3. 8B; Table 3. 6). The Fall model erroneously predicted high probability of disease incidence for most fields and had an AUC of 0.444 in 2020 (Figure 3. 8B; Table 3. 6); however, its AUC was not significantly lower than the four other models. In 2021, Willbur 1 and Fall were the only models with a predictive ability significantly better than chance with an AUC of 0.898 and 0.935, respectively (Figure 3. 8C; Table 3. 6). The other model AUCs ranged between 0.482 and 0.648. That year, the Fall model was significantly better than the Harikrishnan model (Table 3. 6).

Model performance was also tested over the data collected at all sites scouted in Québec from 2019 to 2021, inclusively. The Willbur 1 model had an AUC significantly greater than the no-discrimination line, a value of 0.715, indicating a classification ability significantly superior to that of chance. The Willbur 2, Willbur 3, Harikrishnan and Fall models had AUCs of 0.626, 0.653,

²Controls are fields with a disease severity index below 10%.

0.602, and 0.506, respectively, which were not significantly larger than the no-discrimination line over the three years of data collection (Table 3. 6). The models' performances over data from the three years were not superior to the classification ability analyzed with data from each year individually (Table 3. 6).

The AUCs of the Willbur models were compared for probabilities obtained during the soybean growth stages from beginning bloom to beginning pod formation (R1-R3) and those obtained from beginning bloom to full pod formation (R1-R4) with no significant differences in model classification ability (Table A. 12).

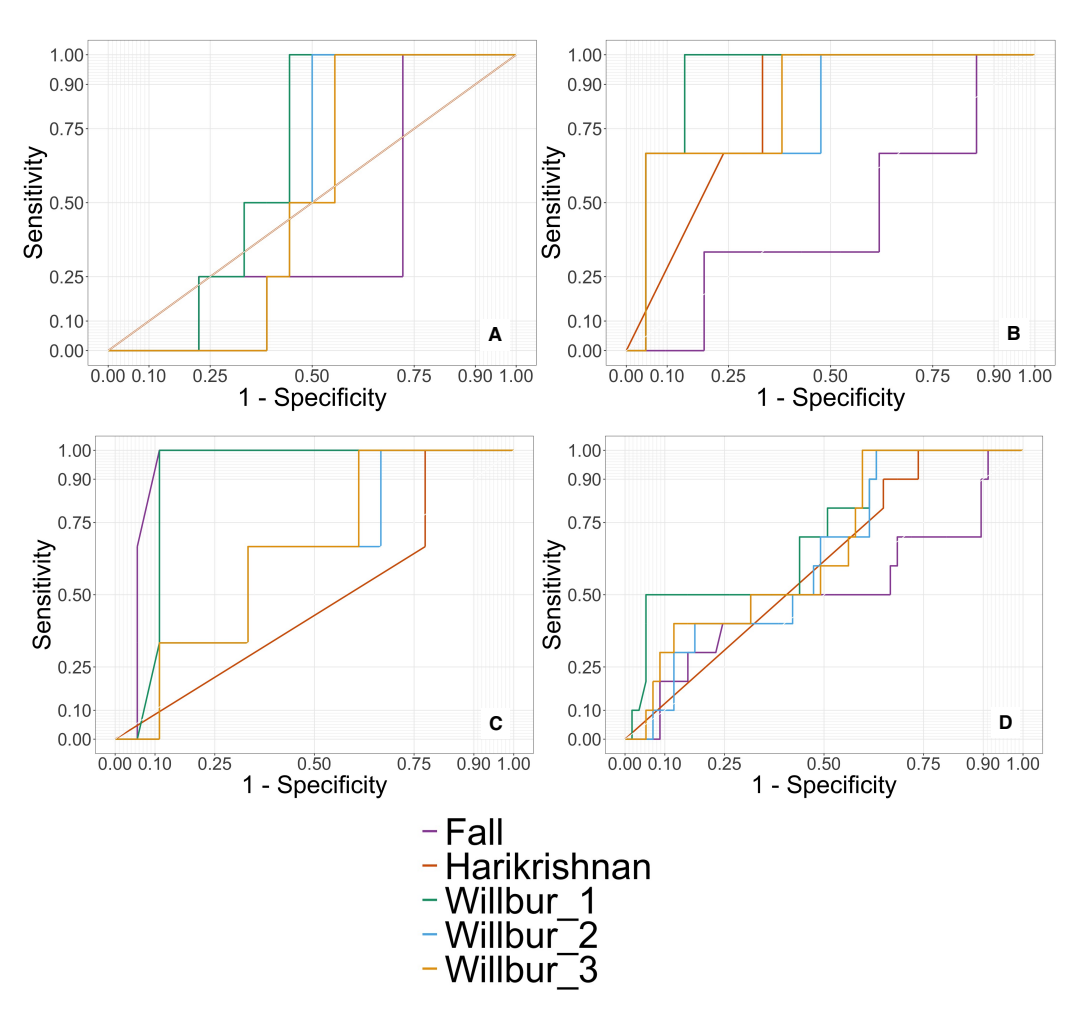


Figure 3. 8. Receiver operating characteristic curve for various Sclerotinia models to predict 10% disease severity in Québec in A) 2019, B) 2020, C) 2021 and D) 2019-2021.

Table 3. 6. Comparisons between the AUCs and the line of no-discrimination of Sclerotinia-related prediction models using 10% DSI as a disease indicator in Québec from 2019 to 2021.

Year	Model	AUC ¹	SE ²	Z-Statistic	P-value ³
	Willbur 1	0.639 a	0.014	0.78	0.217
	Willbur 2	0.542 a	0.014	0.21	0.416
2019	Willbur 3	0.514 a	0.014	0.04	0.483
	Harikrishnan	0.500 a	0.000	-141.42	1.000
	Fall	0.403 a	0.024	-0.64	0.739
	Willbur 1	0.921 a	0.004	2.27	0.012
	Willbur 2	0.810 a	0.023	1.66	0.048
2020	Willbur 3	0.841 a	0.015	1.84	0.033
	Harikrishnan	0.810 a	0.009	1.68	0.046
	Fall	0.444 a	0.043	-0.35	0.637
	Willbur 1	0.898 ab	0.005	2.11	0.017
2021	Willbur 2	0.630 ab	0.033	0.65	0.257
	Willbur 3	0.648 ab	0.028	0.75	0.225
	Harikrishnan	0.482 b	0.021	-0.20	0.580
	Fall	0.935 a	0.003	2.32	0.010
2019-2021	Willbur 1	0.715 a	0.008	2.15	0.016
	Willbur 2	0.626 a	0.007	1.26	0.104
	Willbur 3	0.653 a	0.008	1.52	0.064
	Harikrishnan	0.602 a	0.004	1.21	0.113
	Fall	0.506 a	0.013	0.05	0.479

 $^{^{1}}$ AUC: Area under the Receiver Operating Characteristic curve. For each year individually and the 2019-2021 pooled year analyses, the AUC followed by the same letter are not statistically different (a=0.05).

²Standard Error of the model AUC.

³Probability associated with the Z-statistic given a null hypothesis of no difference between the model AUC and an AUC of 0.5 being true ($\alpha = 0.05$).

3.3.6.1.1 Performance parameters at selected thresholds for pooled years and regions

For each model, the accuracy, sensitivity, specificity, and likelihood ratios of positive (LR+) and negative (LR-) predictions at the published probability threshold of 40% and the Youden index, are presented in Table 3. 7. The models with the highest Youden indices were the Harikrishnan and Fall models with indices of 1.00 and the Willbur 1 model with an index of 0.749. The Youden index of the Willbur 2 and 3 models were very low at 0.006 and 0.019, respectively. These indices reflect that the Fall and Harikrishnan models mostly gave very high probabilities of disease, while Willbur 2 and Willbur 3 probabilities were mainly very low for all sites (Figure 3. 9).

At the Youden index, the most accurate model was Willbur 1, which accurately predicted 88.1% of the disease severity observations in all regions from 2019 to 2021 (Table 3. 7). The accuracy of the other models varied between 37.3% and 65.7%, with the Harikrishnan model being on the lower end and the Fall model on the higher end of the range. The Willbur 2, Willbur 3 and Harikrishnan models were generally better at correctly predicting the fields with disease than identifying healthy fields since model sensitivity was 100.0% while the specificity was between 26.3% and 40.4% (Table 3. 7). In comparison, the Willbur 1 and Fall models both had a sensitivity of 50.0% and specificities of 94.7% and 68.4%, respectively. This is also seen by the positive and negative likelihood ratios of the models. Models with high predictive abilities are associated with LR+>1, the value representing correctly predicted disease severity, and LR-<1, the value denoting erroneously predicted disease severity. At the Youden index, Willbur 1 model had the highest LR+ (9.5) (Table 3. 7).

The probability action threshold of 40% was not close to any of the models' Youden indices. As such, the performance parameters of the models at the 40% threshold differed largely from their performance at their Youden index. At 40%, the most accurate models were Willbur 2 and Willbur 3, which accurately predicted 82.1% and 80.6% of the disease severity observations in all sites from 2019 to 2021, respectively (Table 3. 7). The accuracy of the other models varied between 14.9% and 56.7%, with the Harikrishnan model being on the lower end and the Willbur 1 model on the higher end of the range. Willbur 2 and 3 were highly specific since they generated probabilities of disease presence below 40% for most experimental sites scouted (Figure 3. 9). As such, they correctly identified situations where disease development did not occur, which was the

case for most of the observations in the dataset. However, at the 0.40 threshold, they failed to identify all situations where the DSI was equal to or greater than 10% which resulted in their sensitivity being 0.0%. Since disease situations were the minority in the dataset, it created the illusion that the Willbur 2 and 3 models were accurate overall. However, their LR+ of 0.000 and LR- of 1.036 and 1.056 reflect their flaws. On the contrary, at a threshold of 40%, lower than their Youden Index, the Willbur 1, Fall, and Harikrishnan models had high sensitivity (>70.0%) and low specificity (<54.4%) (Table 3. 7).

Table 3. 7. Model performance indicators at their Youden index and at a probability threshold of 40% in Québec from 2019 to 2021 for different Sclerotinia models.

Model	Threshold	Accuracy	Sensitivity	Specificity	LR+2	LR- ³
	Youden Index					
Willbur 1	0.7491	0.881	0.500	0.947	9.500	0.528
Willbur 2	0.006^{1}	0.463	1.000	0.368	1.583	0.000
Willbur 3	0.019^{1}	0.493	1.000	0.404	1.676	0.000
Harikrishnan	1.000^{1}	0.373	1.000	0.263	1.357	0.000
Fall	1.000^{1}	0.657	0.500	0.684	1.583	0.731
	Published					
	threshold					
Willbur 1	0.400	0.567	0.700	0.544	1.535	0.552
Willbur 2	0.400	0.821	0.000	0.965	0.000	1.036
Willbur 3	0.400	0.806	0.000	0.947	0.000	1.056
Harikrishnan	0.400	0.149	1.000	0.000	1.000	NaN
Fall	0.400	0.224	0.700	0.140	0.814	2.138

¹Youden index.

NaN: Not a Number, the likelihood ratio is invalid due to a division by 0.

²Likelihood Ratio of a positive prediction (diseased field).

³Likelihood Ratio of a negative prediction (healthy field).

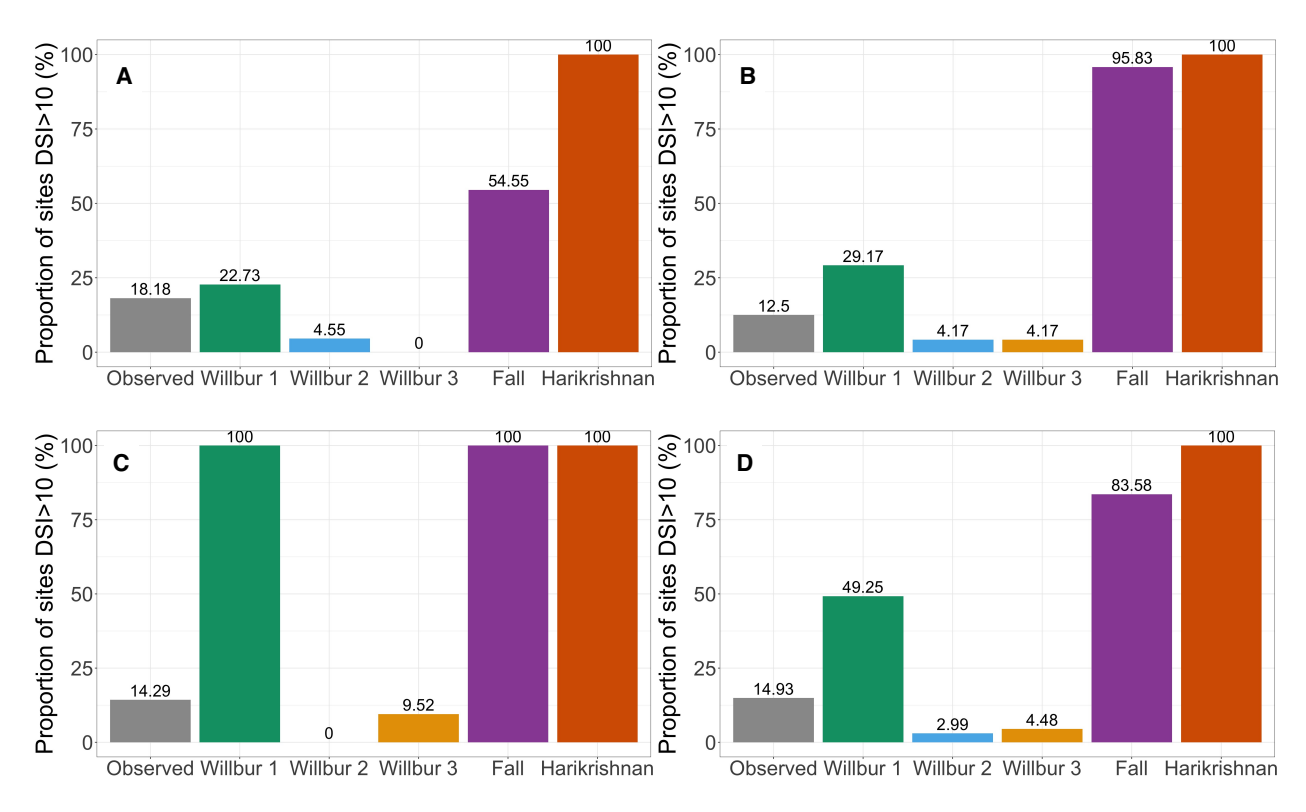


Figure 3. 9. Observed frequencies and predicted probabilities (shown above the respective model bars) of disease severity for a probability threshold of 40% and disease severity index above 10% in A) 2019, B) 2020, C) 2021 and D) 2019 to 2021 in Québec soybean fields.

3.4 Discussion

Understanding the intricate associations between the environmental conditions, the soybean susceptibility period, and *S. sclerotiorum* inoculum production in Québec is essential in moving away from managing the sporadic disease through preventative, calendar-based fungicide spray programs and towards risk-based integrated SSR management strategies. In this study, the production of apothecia was first observed and linked to prevailing environmental conditions and disease severity. Then, the predictive ability of selected bioclimatic *Sclerotinia*-related predictions models developed in the United States was tested to evaluate their ability to predict SSR severity. While apothecia were present in most experimental sites surveyed, only a few fields showed disease symptoms above a DSI of 10% in Québec from 2019 to 2021.

One reason for the low disease severity observed in Québec in the past few years is the presence of apothecia occurring late in the growing season. While apothecia were observed during the flowering period in some regions, when dying flower petals make soybean vulnerable to SSR infections, apothecia were mostly observed during the later soybean growth stages. This suggests that the peak of ascospore pressure was not aligned with the soybean susceptibility window in most fields surveyed. The correlation results from 2019 to 2021 showed that the apothecia produced at the R5 growth stage and beyond were not associated with disease observations. Rather, the apothecia produced during the R2, R3, and R4 growth stages were most strongly associated with SSR severity in Québec. This observed association led us to further investigate whether apothecia presence during the blooming period had a predictive role regarding end-of-season disease severity rates observed in Québec.

The association between the apothecia observed early during the flowering period (i.e. at the R1 growth stage) although reported as influential for disease development (Peltier et al., 2012), was not strongly correlated with disease symptoms in Québec. Correlation analyses were not meant to infer causal relationships, nor should the results be interpreted as such. Instead, these results highlight the late timing of carpogenic germination in Québec in relation to the host vulnerability window, especially in 2019 and 2020. During these two summers, there was no apothecia formation in the R1 soybean growth stages, which could explain the lack of a strong association with disease severity. Earlier research had identified the R3 growth stage as the end of the vulnerable soybean period for infection by *S. sclerotiorum* (Peltier et al., 2012). In this study, apothecia produced during the full pod period (R4) also seemed associated with disease development later in the growing season. The presence of senescing tissues on the crop during that period perhaps allowed ascospores released by apothecia to colonize the plants, thus explaining the association observed. Inoculum pressure at the R4 soybean growth stage had also been previously linked to SSR disease development in the United States (Willbur et al., 2018c).

The environment is a crucial aspect in inoculum production, initial plant infection and disease progression. As many have noted before, apothecia formation is positively associated with high relative humidity and negatively correlated with temperature (Workneh and Yang, 2000, Young et al., 2004). The correlation analysis results between weather variables and apothecia formation in Québec mainly echoed previous findings; however, some differences were noticed. For example, while a negative association between maximum wind speed and carpogenic germination

had been observed in the United States in non-irrigated fields (Willbur et al., 2018b), it was the case only in 2021 in Québec. The fluctuations in environmental conditions across years may explain some of the differences in associations between apothecia formation and weather variables. Given the distance between weather stations from which data were recorded and experimental field locations in Québec, the accuracy of the environmental measurements may also have affected the relationships obtained. The distance between experimental sites and weather stations in Québec was on average 8.28 km but was not uniform from one site to another. In the United States, the Willbur models utilized weather-gridded data at a 5-km resolution, increasing the precision of model predictions at the field level (Willbur et al., 2018b). Among weather variables recorded using the Québec Agrometeo network, wind speed, especially maximum values, is perhaps the variable most likely to be affected by microclimate variations at the soil level where the apothecia were located.

The limited disease observations in Québec from 2019 to 2021 restricted the analysis of the relationship between environmental conditions and disease severity. Among the weather variables selected, temperature in Québec was the factor most consistently correlated to disease severity throughout the growing season, in agreement with findings from historical data in the United States (Fall et al. 2018a). The association between rainfall in June and July and disease severity at the end of the growing season varied in strength and direction from 2019 to 2021 and no consistent trend was observed. This research was a short-term study and epidemiological studies often include years of historical data (Fall et al., 2018a). Additional observations should be collected to shed more light on the influence of specific environmental conditions on SSR disease severity in soybean-producing regions of Québec

While environmental conditions may favour carpogenic germination and disease development, these processes are also influenced by interactions with other factors. For example, row spacing has been shown to influence disease development (Lee et al., 2005, Rousseau et al., 2007). The effect of row spacing on apothecia formation was analyzed as an agronomic aspect at the Québec research centres from 2019 to 2021. The hypothesis was that a narrower row spacing would create a favourable shaded, cool and humid microclimate earlier in the growing season and thus promote rapid and abundant apothecia formation (Sun and Yang, 2000). It had previously been observed

that less carpogenic germination was observed at further distances from the soybean row (Fall et al., 2018b). In Québec, the sclerotia deposits were purposefully placed near the soybean row, as opposed to the centre of the row, to create conditions promoting carpogenic germination early in the growing season. While the rate of canopy closure was, on average, faster for narrower row spacings, total canopy closure is not required for sclerotia to produce apothecia, especially given the positioning of the sclerotia close to the plants in experimental sites in Québec. Fall et al. (2018b) observed the highest number of apothecia produced following 50% canopy closure in soybean in Michigan, USA. In Québec, most of the apothecia were observed late in the growing season when the canopy was near or at complete closure. In the three years of data collection, the initial row spacing of the plots did not result in significant differences in either the timing of carpogenic germination or the number of apothecia observed in the deposits.

As for the impact of row spacing on disease development and severity, the row spacings of 17.8-cm and 76.2-cm were associated with the lowest DSI values, while the 38.1-cm plots had the most disease symptoms at IRDA in 2021. Despite not being statistically significant, this effect had been previously observed in trials conducted in Québec (Bipfubusa et al., 2020). These observations suggest that wider row spacing could reduce disease severity. Also, narrow rows could limit the spread of airborne inoculum in the field due to canopy interception in years when the environment is favourable to carpogenic germination and inoculum is present in the field (T. Copley, personal communication, October 2021).

Bioclimatic modelling is a strategy that can enhance disease control since environmental conditions influence SSR development and severity. The correlation analyses presented here suggest that weather variables are similarly associated with inoculum production and disease severity in Québec and in the north-east of the United States (Willbur et al., 2018b). Weather-based algorithms predicting the risk of apothecia development and SSR development have been developed and integrated into disease management tools used by agronomists and farmers. Among others, logistic regression *S. sclerotiorum* forecasting models have been developed in the United States to predict the risk of apothecia presence, SSR incidence and severity in soybeans and dry beans (Harikrishnan and del Río, 2008, Fall et al., 2018a, Willbur et al., 2018b). For those models to successfully inform producers' decision-making process, the equations need to be studied and

validated under Québec agro-environmental conditions first, and appropriate action thresholds must be identified. To date, such work had not been carried out in Québec. This report evaluated the performance of five S. sclerotiorum models to predict end-of-season SSR severity under Québec soybean growing conditions from 2019 to 2021. Various DSI values have been reported as disease indicators in the literature (Fall et al., 2018a, Willbur et al., 2019). Among others, DSI values of 22% and above were linked to significant yield losses in soybean in the United States (Fall et al., 2018a). However, given that only eight fields in the sites surveyed in Québec reached this value over the three years of data collection, a lower value of 10% DSI was used to categorize experimental sites between cases and controls. SSR disease development on specific plant structures influences the extent to which soybean yield is reduced (Willbur et al., 2019). For example, infection of the stem is expected to cause more yield losses than lateral branch colonization (Fall et al., 2018a). By ranking the importance of disease symptoms based on their location on the crop tissues, the DSI (Grau, 1984), as opposed to disease incidence, is of particular interest for SSR disease management purposes. Also, producers may want to manage the disease for reasons other than preventing yield losses. Particularly in the case of SSR, infected plants become reservoirs for new sclerotia production, increasing the field load, thus perpetuating, and exacerbating the disease pressure within a specific location.

Model performance was assessed through ROC curve analysis, which evaluates a model's ability to discriminate between cases and controls for all possible probability threshold values (Metz, 1978). Model ROC curves can be used to compare the accuracy of various models at potential action thresholds. Probability threshold selection considers the balance between model specificity and sensitivity that is most appropriate to the context in which the model is used (Biggerstaff, 2000). At a disease indicator of 10% DSI, Willbur 1 had the highest AUC over the three years of data collection. This model was the most parsimonious, being based only on maximum temperature during the soybean flowering period. In comparison, models that also included moisture-related parameters, such as Willbur 2 and Willbur 3 with maximum wind speed and relative humidity, Fall with rainfall in July, and Harikrishnan with rainfall in June and August generally had lower AUCs. Given the relationship between moisture variables, apothecia formation, and disease development, it was expected that moisture-related predictors would improve model predictive ability. However, this was not the case in Québec from 2019 to 2021.

This result can be explained by the impact of local model development conditions on the choice of selected final variables, the period considered, and the weight given to each model input. Rain patterns, used in the Fall and Harikrishnan models, and wind speed, included in the Willbur 2 and 3 models, are perhaps more likely to vary across regions and within growing seasons compared to temperature. Thus, using models based on such predictors outside of their local contexts is suboptimal without proper calibration.

The predictive abilities of the models were evaluated based on their error types at specific probability threshold values. The threshold values obtained using the optimal Youden index calculated individually for each model had large variations. Models like Willbur 2 and 3, which generally showed a low probability of disease development, had minimal Youden index values, while models like Fall and Harikrishnan, with generally high probabilities of disease development, had larger Youden index values. Model end-users ultimately make decisions based on the probability action threshold value, and, as such, it should be readily interpretable, which was not the case with the Youden index values obtained for most models tested here. A probability threshold value of 0.40 has a more practical use since any probability above it can be interpreted as a high risk of disease development and thus indicates a potential need for disease management measures. While Willbur 2 and 3 showed high accuracy at a probability threshold of 0.40, their sensitivity of 0% should not be overlooked. It indicates that they failed to identify environmental conditions conducive to disease development. While such conditions were rare in Québec sites scouted from 2019 to 2021, producers need models that can signal both situations where disease development is likely and unlikely with high reliability. The Willbur 2 model equation was validated in the United States and while the model displayed high accuracy, most model errors were also underprediction mistakes (Willbur et al., 2018c).

On the contrary, the Fall and Harikrishnan generally overestimated the risk of disease severity. While they perfectly identified all the fields that had a DSI greater than or equal to 10%, they also misidentified a large proportion of healthy fields. If producers used these models to decide whether to chemically manage the disease, they would over-apply fungicides when conditions are unfavorable to disease development. At the 40% probability action threshold, this type of error was very costly given that there were more healthy than diseased fields in Québec in this study. In

comparison, Willbur 1 model had the best disease development discerning capacity. Despite making some errors, its sensitivity and specificity were never below 50.0% at the Youden index and the 0.40 probability threshold.

Based on the ROC curve and threshold analyses, some models appeared superior for use in Québec. The Willbur models, especially Willbur 1, had the highest AUC from 2019 to 2021 and had a high AUC in each of the three years of data collection. The other models did not display the same consistency in performance. For example, the Harikrishnan model performed well only in 2020, and the Fall model successfully classified diseased and healthy fields only in 2021. Additionally, the Fall model uses July data, and the Harikrishnan model requires data until mid-August to generate predictions. However, the soybean flowering period in Québec generally occurs in July, and timely action, generally at R1, R3 or both, is essential for adequate control of SSR. This delay in obtaining model predictions could have tremendous implications for disease development in high-risk years. The Willbur models were developed to use weather variables prevailing during the flowering period to calculate the risk of inoculum presence during which soybean is susceptible to infections (Willbur et al., 2018b). Compared to the Fall and Harikrishnan models, it seems that the Willbur models, by predicting apothecia formation instead of disease development and by using crop-based cues rather than calendar timing, seized more dependably the conditions leading to SSR development at the field level in Québec from 2019 to 2021. The models mostly captured weather-based aspects; however, additional elements such as differences in field isolate aggressiveness and load, plant population, cultivar SSR disease tolerance, nitrogen at planting, soil texture, tillage, and residue density may be factors that also impact disease development in Québec (Peltier et al., 2012).

3.5 Conclusion

Environmental and agronomic conditions for apothecia formation, disease development, and severity were assessed in Québec from 2019 to 2021. Previously published models that used weather variables during the vulnerable period of soybean to predict apothecial presence showed some potential to be used in Québec as decision-making tools to manage Sclerotinia stem rot. However, before producers adopt these models, the equations should be modified to improve

accuracy and provide more reliable apothecia formation and disease severity predictions. For example, the logistic regression coefficients associated with the weather variables could be revised using data collected in Québec. In addition, the use of weather variables with weak associations to inoculum production and disease severity should be re-evaluated.

Connecting text between Chapter 3 and Chapter 4

The previous chapter identified the potential of the Willbur apothecia formation model series for use under Québec conditions to predict end-of-season disease severity. *S. sclerotiorum* is the causal agent of Sclerotinia stem rot and is one of the most concerning pathogens for soybean producers in the region. The first aim of Chapter 4 is to validate the Willbur weather-based models for their capacity to identify apothecia presence during the soybean growing season. The second objective is to adapt the Willbur models to improve their performance in the Quebec soybean production context.

Chapter 4: Validation and modification of Sclerotinia sclerotiorum carpogenic germination prediction models in soybean (Glycine max) in Québec

4.1 Introduction

Protecting crops against diseases is a complex process. It requires monitoring multiple aspects related to the environment, the crop, and the pathogen to evaluate the prospect that disease will occur. Managing plant diseases is especially challenging when an intervention needs to be performed before disease symptoms appear on the crop. Farmers and their advisors will weigh the cost of treatment, such as applying a pesticide, against the potential loss of yield to devise a management strategy. For example, in some cases, farmers will choose to spray pesticides preventatively to avoid potential crops losses due to disease epidemics that may or may not arise (Gent et al., 2011). Many plant disease prediction models assist farmers in evaluating the likelihood of disease development. These models are mathematical equations, often based on environmental variables, sometimes including crop or pathogen-related factors that predict disease incidence (Bourgeois et al., 2005). For example, forecasting Sclerotinia stem rot (SSR) disease incidence by predicting the presence of Sclerotinia sclerotiorum (Lib.) de Bary inoculum is a management strategy gaining popularity among soybean growers (Willbur et al., 2018b, Willbur et al., 2018c). Soybean (Glycine max (L.) Merr.) is a crop for which yield losses to SSR are frequent in Québec (Breault et al., 2017). Recent advances in modelling technologies allow the development of precise and efficient tools to inform the use and timing of fungicide applications. Among others, forecasting models for SSR of common bean (*Phaseolus vulgaris* L.) and soybean have been developed in the United States (Harikrishnan & del Rio 2008; Fall et al., 2018a; Willbur et al., 2018b). However, no SSR model has been developed or validated for SSR of soybean under the weather conditions of Québec.

Models range in scale from predicting disease risk regionally to the field level (Twengström et al., 1998, Mila et al., 2004, Willbur et al., 2018b). Since models can be used to identify situations where disease incidence is unlikely, they can help farmers economically and environmentally by reducing unnecessary pesticide use (Willbur et al., 2018c, Small et al., 2015). Despite the many prediction models developed, some challenges remain regarding their adoption by producers and agronomists. One issue is the availability of model equations or prediction rules outside of the

network that initially developed the forecasters (Carisse and Fall, 2021). Also, before producers can rely on prediction models as part of their disease management plan, the predictive ability of those models needs to be validated in the local context. When these models are not widely accessible, it directly limits their uptake in new environments. Another concern is that model performance in different environments is often lower than in the setting in which the models were initially derived (Bouchard, 2008). This leads to the development of multiple models to predict the same disease, most of which never get directly applied during producers' decision-making process. Doing so is an inefficient use of data, as the valuable knowledge derived from the observations used to develop previous models are not accounted for in the development of new ones (Moons et al., 2012). Instead of re-developing disease prediction models, poor predictive ability in new contexts can be addressed by customizing an original model equation to the new environment in which it will be used. This strategy benefits from integrating findings from previous studies while ensuring that the modified model predictions are adapted to the setting in which the model is applied (Janssen et al., 2008, Steyerberg, 2019).

Disease prediction model customization is common practice in clinical epidemiology, where physicians use models developed from patient data from a specific set of hospitals to generate patient prognosis in a different clinical setting (Curtin et al., 2019, Steyerberg and Vergouwe, 2014). The statistical methodology used to update prediction models comprises multiple strategies. A simple recalibration method consists of a modification of the model intercept, re-estimation involves adjusting all regression coefficients associated with model variables, and the more complex extension approaches result in new variables being added to the model (Steyerberg and Vergouwe, 2014, Steyerberg, 2019, Janssen et al., 2008).

The first objective of this study is to evaluate and compare the effectiveness of three *S. sclerotiorum* apothecia formation models, initially developed in the United States, under Québec growing conditions and agronomic practices. Then, the second objective is to provide a phytopathological assessment of the application of the prediction model updating methodology using data collected from 2019 to 2021 in Québec soybean-producing regions. Finally, the third objective is to identify the most promising apothecia formation models for Québec soybean

growers by validating the modified models and comparing their apothecia prediction capacity to the original models using data collected in Québec in 2017 and 2018.

4.2 Materials and methods

4.2.1 Experimental sites and data collection

4.2.1.1 Original model validation and model modifications

Data were collected from 55 commercial location-years and 12 research location-years in Québec from 2019 to 2021. Throughout the growing season, data collected included weather conditions, apothecia observations (789 scouting visits), soybean growth stages (Fehr and Caviness, 1977), soybean plant height (cm) (mean of two plants per row, up to the apex), and the level of canopy closure (cm). Disease incidence, severity of symptoms, and yield at harvest were collected in plots where disease development had been observed during the growing season. Weather variables used in model validation and modification were maximum temperature (Tmax, (°C)), maximum wind speed (Wsmax, (km/h)), maximum relative humidity (Rhmax, (%)), mean relative humidity (Rhmean, (%)) and the Abundant and Well-Distributed Rainfall index (AWDR) (Tremblay et al., 2012). Experimental design at the commercial and research sites and data collection methods were described in Chapter 3 (Morier-Gxoyiya et al., in preparation).

4.2.1.2 External validation of modified models

Data were collected during the R1, R2 and R3 soybean growth stages from 23 commercial location-years in Québec in 2017 and 2018 (Table 4. 1). The sites were artificially inoculated with sclerotia deposits as outlined in Chapter 3 (Morier-Gxoyiya et al., in preparation). Data collected included weather conditions, apothecia observations (117 scouting visits), and soybean growth indicators as mentioned above. Experimental design and data collection methods at the commercial sites were described in Chapter 3 (Morier-Gxoyiya et al., in preparation).

Table 4. 1. Regions and number of sites for data collection in Québec in 2017 and 2018.

Region	Year	Number of sites	Apothecia scouting visits
Centre-du-Québec	2017	2	10
	2018	2	6
Chaudière-Appalaches	2017	2	7
	2018	1	3
Estrie	2017	2	12
	2018	1	3
Lanaudière	2017	2	11
	2018	2	12
Montérégie-Est	2017	2	12
	2018	3	15
Montérégie-Ouest	2017	2	7
	2018	2	19
Total		23	117

4.2.2 Statistical Analysis

4.2.2.1 Validation of original Willbur apothecia formation models

Statistical analyses were conducted in R v.1.4.1717 (R Foundation for Statistical Computing, Austria). The performance of three weather-based apothecia formation logistic regression models, Willbur 1, Willbur 2 and Willbur 3 (Formulae 3.2, 3.3 and 3.4, Morier-Gxoyiya et al., in preparation) originally developed in soybean in the United States of America (Willbur et al., 2018b), in predicting apothecia presence in Québec was validated through receiver operator characteristic curve (ROC) analysis. In this case, the classification capacity of the three models was evaluated specifically with regards to observations of apothecia presence and absence during each scouting visit from 2019 to 2021 (n = 789) rather than for DSI observations at the end of the growing season as in Chapter 3 (Morier-Gxoyiya et al., in preparation). The ROC analyses were conducted according to the statistical methods described in Chapter 3 (Morier-Gxoyiya et al., in preparation). Models with an area under the ROC curve (AUC) not significantly different than 0.500, representing the area under the line of no-discrimination on a ROC graph, were considered poor predictors of apothecial presence (Hughes et al., 1999). Pairwise comparisons of the models

were performed to test whether a model forecasted apothecial presence significantly better than another model (DeLong et al., 1988). The ROC analyses of apothecia formation models were completed with pooled data from the three years (2019-2021) and by individual year.

4.2.2.2 Comparison of model performance at two thresholds

The accuracy, sensitivity and specificity of models were assessed at their respective optimal thresholds derived from the Youden index (*J*) (Formula 3. 1, Chapter 3 Morier-Gxoyiya et al., in preparation). For each model, the likelihood ratios obtained from the Youden index and from the published threshold of 40% were compared as described in Chapter 3 (Morier-Gxoyiya et al., in preparation) (Willbur et al. 2018b).

4.2.2.3 Calibration performance

The calibration of the three Willbur models was evaluated graphically on the data collected in Québec from 2019 to 2021. The goal of the calibration analysis was to verify the reliability of predicted probabilities in reference to observed frequencies of apothecia presence in Québec. Poor model calibration can occur either when models consistently overestimate or underestimate the risk of the event of interest, in this case, carpogenic germination of sclerotia. In other words, adequately calibrated models should provide higher probabilities for scouting visits during which apothecia were observed than for visits when there was no apothecia formation. In addition, poor calibration can prevent the model's useful application in decision-making, even if the model has a high AUC, especially when a probability action threshold must be identified. As the models were initially developed in the United States, the frequency of apothecia presence there may vary from what is observed in Québec. Thus, the original models may systematically distort the predicted risk of apothecia presence when used in a new setting. A perfectly calibrated model should have an intercept of 0 and a slope of 1 on a graph of the predicted probability against the observed proportion of apothecia presence events (Van Calster et al., 2019).

4.2.3 Modification of Willbur models for Québec conditions

Willbur models were modified to increase their predictive performance under Québec agroenvironmental conditions. Modification methods are summarised in Table 4. 2 and the workflow of model modification, fit evaluation and validation is shown in Figure 4. 1. Model modifications were conducted using a training dataset containing a random sample of 70% of the data collected in Québec from 2019 to 2021. The proportion of apothecia presence observations in the training dataset was 33.9%, a distribution similar to that of the full sample (34.6%) (Figure 4. 2).

Modifications ranged from simple to more elaborate methods and were adapted from the clinical prediction modelling methodology (Steyerberg, 2019, Steyerberg et al., 2004, Steyerberg and Vergouwe, 2014, Van Calster et al., 2019, Curtin et al., 2019). For each model, the linear predictor was the starting point for modifications. The linear predictor of each model was obtained, for each scouting visit, by using the model equation and its respective input variables available in Formulae 3.2, 3.3 and 3.4 in Chapter 3 (Morier-Gxoyiya et al., in preparation). The two simplest model modifications consisted of "Recalibration-in-the-large" and "Logistic recalibration" (Steyerberg, 2019). In the first method, only one parameter, the intercept of the model, was adjusted while the model linear predictor was fixed with a coefficient of 1. The aim of Recalibration-in-the-large is for the average of the recalibrated model probabilities to return the overall apothecia presence rate observed in Québec from 2019 to 2021. In the second method, two parameters were estimated: the intercept and the coefficient of the model linear predictor. Through logistic recalibration, the coefficients of models with multiple variables (Willbur 2 and Willbur 3) were modified by a common factor (Steyerberg, 2019). These recalibration methods were conducted using maximum values of weather variables for both 20-day and 30-day moving average durations.

A more altering modification method was the revision in which the number of parameters reestimated was equal to the intercept plus the number of input variables in the model. Revision was conducted by re-estimating the regression coefficients associated with the variables in the models freely through logistic regression (Steyerberg, 2019). Model revision was conducted using maximum values of model variables and both 20-day and 30-day moving average durations. Revised models were fitted through 10-fold cross-validation in the 'caret' package in R (Kuhn, 2011, R Core Team, 2021).

Finally, the most extensive modification method was the extension, in which model variables were added, and all regression coefficients and the model intercept were freely re-estimated (Steyerberg, 2019). Model extension was conducted using maximum and mean values of model variables and

both 20-day and 30-day moving average durations. The extended model equations were fitted using 10-fold cross-validation in the 'caret' package in R (Kuhn, 2011, R Core Team, 2021). Additional variables included in model equations during the extension phase were 30-day moving averages of either mean values of wind speed, mean values of relative humidity or the abundant and well-distributed rainfall (AWDR) index. The AWDR was included as a representation of soil moisture over a period of 30 days (Tremblay et al., 2012). The duration of the period was chosen following a preliminary correlation analysis between AWDR durations ranging from 10 to 30-days and apothecia observations in Québec from 2019 to 2021 as reported in Chapter 3 (Morier-Gxoyiya et al., in preparation).

The fit of the modified models was evaluated on the data used for model modifications, the training dataset, and included the Akaike information criterion (AIC), the coefficient of determination (R²), and the Kappa statistic. Additionally, predictive performance metrics reported included model AUC, accuracy, sensitivity, specificity, false positive and false negative rates, and likelihood ratios of positive and negative predictions of selected modified models at their respective Youden index.

Following the modifications of the Willbur models, the calibration of modified Willbur models was re-evaluated graphically by plotting their calibration plots on the modification dataset (Figure 4. 2). The calibration was conducted to assess the reliability of the revised Willbur model probabilities when compared to the magnitude of the risk of apothecia presence in Québec.

Table 4. 2. Modification methods used to customize the Willbur apothecia formation models for Québec agro-environmental conditions (Steyerberg, 2019).

		Model changes	
Modification method	Intercept	Regression coefficient(s)	Addition of
			variable(s)
Recalibration-in-the-large	Yes	No	No
Logistic recalibration	Yes	Yes, by a common factor	No
Revision	Yes	Yes, by an individual factor	No
Extension	Yes	Yes	Yes, when s.s. ^b

^bs.s. stands for statistically significant ($\alpha = 0.05$).

4.2.4 Validation of modified Willbur models

4.2.4.1 Internal validation

The modified Willbur models were validated using a test dataset comprised of a random sample of 30% of the data collected in Québec from 2019 to 2021. This validation is referred to as internal; while observations in the dataset were not used for model modifications, they were not entirely independent from the training set, since both sets were randomly partitioned from one common dataset. The training and internal test datasets respectively contained 33.9% and 36.7% scouting visits during which apothecia were observed. In addition to the modified model equations, the original Willbur model equations were also evaluated using the internal test set to provide comparable validation results. Predictive performance metrics for internal validation included model AUC, and the accuracy, sensitivity and specificity of models at their respective Youden index.

4.2.4.2 External validation

The performance of the original and modified Willbur models was validated externally using a test dataset comprising data collected in Québec during the soybean flowering period in 2017 and 2018. These observations were collected from 12 commercial sites located across Québec soybean producing-regions in which sclerotia were artificially buried. The 2017 and 2018 observations were collected independently from data observed from 2019 to 2021 which were used for model

updating and internal validation (Figure 4. 2). The external validation dataset contained 35.0% of scouting visits during which apothecia were observed. Predictive performance metrics included model AUC, and the accuracy, sensitivity and specificity of models at their respective Youden index.

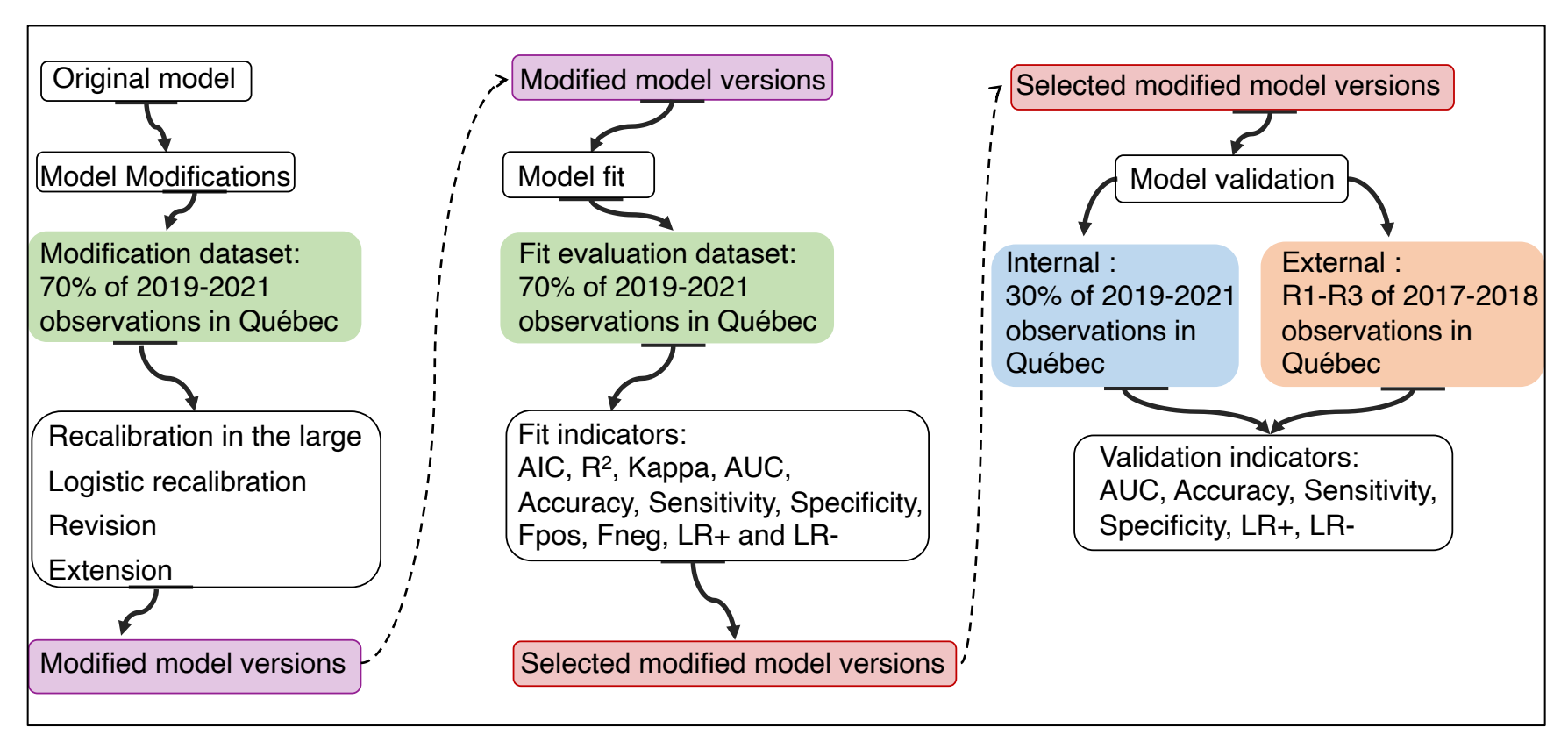


Figure 4. 1. Workflow of model modifications, fit evaluation, and validations. Abbreviations: AIC, Akaike Information Criterion; R², coefficient of determination; Kappa, Kappa statistic; AUC, Area under the Receiver Operating Curve; Fpos, False positive rate; Fneg, False negative rate; LR+, Positive Likelihood Ratio; LR-, Negative Likelihood Ratio; R1-R3, beginning of blooming to beginning of pod development soybean growth stages.

Development Dataset¹

Modification Dataset

Inclusion

2014-2016

Location

Iowa, Michigan, Wisconsin (US)

Sample composition

3866 observations

Apothecia presence

Not available

Inclusion

70% of 2019-2021 observations

Location

Québec (CAN)

Sample composition

552 scouting dates

Apothecia presence

Incidence 33.9%

Validation Datasets

Internal

Inclusion

30% of 2019-2021 observations

Location

Québec (CAN)

Sample composition

237 scouting dates

Apothecia presence

Incidence 36.7%

External

Inclusion

R1-R3 2017-2018 observations

Location

Québec (CAN)

Sample composition

117 scouting dates

Apothecia presence

Incidence 35.0%

Figure 4. 2. Sample composition for datasets used for modifying and validating apothecia formation models in Québec soybean fields from 2019 to 2021. R1-R3: beginning bloom to beginning pod soybean growth stages. ¹The Development Dataset refers to data used to develop the Willbur et al. (2018b) models.

4.2.4.3 Dominance analysis

After model modifications, a dominance analysis was conducted to compare the relative contribution of each variable to the prediction of apothecia using the two most complex modified models (set of four predictors). These models were chosen as the reference models to evaluate and relate the importance of all predictors of interest. The first model included 30-day moving average values of maximum temperature, maximum wind speed, maximum relative humidity and AWDR variables. The second model included 30-day moving average values of maximum temperature, maximum wind speed, mean relative humidity and AWDR variables. The contribution of each

predictor was assessed based on the change in model fit, for all possible subset models, following the addition of the predictor as measured through the McFadden index (R²_M) (Azen and Traxel, 2009). The dominance analysis was conducted for each year of data collection from 2019 to 2021 individually and for the three years pooled using the package 'dominanceanalysis' in R (Bustos Navarrete and Coutinho Soares, 2020).

4.3 Results

4.3.1 Proportion of cases and controls

Observations from the scouting visits at each experimental site were grouped into "cases" and "controls" based on the mean number of apothecia observed in the four deposits at each of the commercial sites, and 12 deposits at each of the research sites (Willbur et al., 2018b). The proportion of observations in those two groups varied each year and in the different regions of Québec where data was collected. Overall, there was a tendency to observe a greater number of control situations (absence of apothecia), compared to case situations (presence of apothecia). Using a disease indicator of 0.25 mean total apothecia/deposit, the prevalence of cases was highest in 2021 at 49.8%. The prevalence of cases was lowest in 2019 at 17.7% (Table 4. 3). The region with the highest prevalence of cases on average over the three years of data collection was the Laurentides at 53.3%, followed by Estrie at 46.5%. The prevalence of cases was lowest in the Montréal and Outaouais (one site in 2019) regions at 11.4% and 0.0%, respectively (Table 4. 4).

Table 4. 3. Proportion of cases and controls in each data collection year from 2019 to 2021.

Year	Scouting	Apothecia	Apothecia	Cases	Controls
r ear	Visits	Presence	Absence	$(\%)^1$	$(\%)^2$
2019	238	42	196	17.7	82.4
2020	302	107	195	35.4	64.6
2021	249	124	125	49.8	50.2
Total	789	273	516	34.6	65.4

¹Cases are scouting visits with at least 1 apothecium/deposit.

²Controls are scouting visits with no apothecia observed.

Table 4. 4. Proportion of cases and controls in each data collection region from 2019 to 2021.

Region	Number of location-years	Scouting Visits	Apothecia Presence	Apothecia Absence	Cases (%) ¹	Controls (%) ²
Capitale Nationale	8	84	27	57	32.1	67.9
Centre-du-Québec	5	55	22	33	40.0	60.0
Chaudière- Appalaches	8	103	46	57	44.7	55.3
Estrie	5	43	20	23	46.5	53.5
Lanaudière	6	62	24	38	38.7	61.3
Laurentides	3	30	16	14	53.3	46.7
Mauricie	3	33	6	27	18.2	81.8
Montérégie-Est	17	217	58	159	26.7	73.3
Montérégie-Ouest	8	110	49	61	44.6	55.5
Montréal	3	44	5	39	11.4	88.6
Outaouais	1	8	0	8	0.0	100.0

¹Cases are scouting visits with at least 1 apothecium/deposit.

4.3.2 Validation of original Willbur apothecia formation models

4.3.2.1 AUC pairwise comparisons from 2019 to 2021

The original model equations developed by Willbur et al. (2018b) were first evaluated for their capacity to predict apothecial development over the three data collection years from 2019 to 2021 through AUC analyses. Model performance was assessed over the data collected at all sites scouted in Québec from 2019 to 2021. Models were evaluated for their capacity to identify the presence of apothecia at different maturity levels; immature apothecia (IA), mature apothecia (MA) and all maturity levels combined (TA). All model AUCs, regardless of apothecia maturity, were significantly greater than 0.500, with values between 0.636 and 0.718, indicating a classification ability significantly superior to that of chance (Table A. 13).

²Controls are scouting visits with no apothecia observed.

Across all apothecia maturity levels and over the data from all the experimental sites and years, Willbur 3 model showed a better ability to determine whether apothecia were present or absent compared to Willbur 1 and Willbur 2 models. The Willbur 3 AUC curve was consistently the highest, with values of 0.677, 0.698, and 0.718, for IA, MA, and TA, respectively (Table A. 13). The curvature of the Willbur 3 ROC curve was the closest to the (0, 1) coordinates on the plot showing a better trade-off between sensitivity and specificity compared to the other models (Figure A. 4). The model showing the second-best predictive ability across IA, MA and TA was Willbur 1 with AUCs of 0.657, 0.680 and 0.685, respectively (Table A. 13). Willbur 2 ROC curves were the closest to the line of no-discrimination for all apothecia maturity levels with areas of 0.636, 0.654 and 0.675 for IA, MA, and TA, respectively (Table A. 13). All the model AUCs were higher using TA compared to using IA or MA as an indicator. However, the differences between the AUCs of the same model versions due to apothecia maturity levels were not statistically significant $(\alpha = 0.05)$ (Figure A. 4). Thus, the following analyses were carried out using TA as an indicator.

4.3.2.2 Youden index from 2019 to 2021

For each Willbur model, the optimal threshold for the TA indicator calculated using the Youden index and the 0.40 published probability action threshold are presented in Table 4. 5 along with each model's accuracy, sensitivity, specificity, and likelihood ratios of positive (LR+) and negative (LR-) predictions at those thresholds. The model with the highest Youden index was Willbur 1, while the Youden indices of Willbur 2 and 3 were very low (Table 4.5). At the Youden index, the most accurate model was Willbur 3, which accurately predicted 68.0% of the apothecial development observations in all regions from 2019 to 2021. The second most accurate model was Willbur 2, and the least accurate model was Willbur 1. The Willbur 3 model was generally better at classifying instances of apothecial absence than apothecial presence since its specificity was higher than its sensitivity. The opposite was true for Willbur 1 and Willbur 2 which were more sensitive than specific (Table 4. 5). This is also represented by the LR+ and LR- values of the models with Willbur 3 showing the highest LR+, while Willbur 1 and 2 had lower LR+ and LR-values. The lower specificity of the Willbur 1 model was a key factor differentiating its predictive ability at the Youden index given that the dataset contained more instances of apothecia absences, which gave more weight to its weakness (Table 4. 5).

At a probability action threshold of 40%, the most accurate models from 2019 to 2021 were Willbur 1 and Willbur 3. In this case, all three models were better at classifying instances of apothecial absence than apothecial presence since sensitivity was lower than specificity for all three Willbur models (Table 4.5). Again, the model with the highest LR+ was Willbur 3. At a 0.40 threshold, the Willbur 1 LR- value was the lowest, followed by Willbur 3 and Willbur 2 (Table 4.5).

Table 4. 5. Performance parameters of apothecia formation of the Willbur models with the Youden index and a threshold of 0.40 using total apothecia as an indicator from 2019 to 2021.

Model	Threshold	Accuracy	Sensitivity	Specificity	LR+ ²	LR- ²
Willbur 1	0.25^{1}	0.61	0.75	0.54	1.62	0.46
Willbur 2	0.01^{1}	0.64	0.70	0.60	1.75	0.50
Willbur 3	0.05^{1}	0.68	0.65	0.70	2.13	0.51
Willbur 1	0.40	0.66	0.55	0.72	1.98	0.62
Willbur 2	0.40	0.64	0.03	0.96	0.80	1.01
Willbur 3	0.40	0.66	0.08	0.97	2.97	0.95

¹Youden index

4.3.2.3 AUC pairwise comparisons by year

The models' abilities to determine whether apothecia were present varied throughout the three years of data collection. Willbur 1, the model based only on 30-day moving average of maximum daily temperature, had the highest discrimination ability in 2019, which was significantly higher than Willbur 2 and 3, the two models based on temperature and moisture variable(s) (Table 4. 6, Figure 4. 3A). In 2020, the presence or absence of apothecia was best determined by Willbur 1 and Willbur 3 (Figure 4. 3B), while in 2021, Willbur 3 was also the most performant model, followed by Willbur 2, with both being significantly better than Willbur 1 (Figure 4. 3C).

4.3.2.4 AUC pairwise comparisons during the flowering period

The most important risk period for *S. sclerotiorum* infections is during the soybean flowering period corresponding to the growth stages R1 to R3. From 2019 to 2021, all three Willbur models

²LR+, Positive Likelihood Ratio; LR-, Negative Likelihood Ratio.

showed discrimination abilities significantly superior to that of chance during the soybean vulnerable stages, with AUCs ranging from 0.720 to 0.790 (Table 4. 6). Willbur 1 and Willbur 3, using 30-day moving averages of maximum daily temperature (Willbur 1), and relative humidity and wind speed (Willbur 3) had the highest discrimination ability (Figure 4.3E). However, only Willbur 3 was significantly better than Willbur 2 (Figure 4. 3E).

Table 4. 6. Comparisons between the AUCs and the line of no-discrimination of apothecia prediction models in Québec from 2019 to 2021.

Year	Model	AUC^1	SE^2	Z-Statistic	P-value ³
	Willbur 1	0.893 a	0.001	7.970	7.34E-16
2019	Willbur 2	0.633 с	0.003	2.710	3.40E-3
	Willbur 3	0.707 b	0.003	4.200	1.31E-5
	Willbur 1	0.649 ab	0.001	4.280	9.29E-06
2020	Willbur 2	0.639 b	0.001	3.990	3.24E-5
	Willbur 3	0.672 a	0.001	4.940	3.94E-07
	Willbur 1	0.517 b	0.001	0.450	0.33
2021	Willbur 2	0.733 a	0.001	6.360	1.02E-10
	Willbur 3	0.750 a	0.001	6.810	4.99E-12
	Willbur 1	0.685 ab	0.0004	141.420	5.45E-18
2019-2021	Willbur 2	0.675 b	0.0004	8.080	2.86E-16
	Willbur 3	0.718 a	0.0004	141.420	2.72E-24
	Willbur 1	0.790 ab	0.004	3.770	8.31E-5
2019-2021, R1-R3 ⁴	Willbur 2	0.720 b	0.005	2.850	2.19E-3
	Willbur 3	0.781 a	0.004	3.650	1.31E-4

¹Area under the Receiver Operator Curve (AUC) was calculated using the Delong et. al. (1988) method. AUCs followed by the same letter within a given year(s) of analysis are not statistically different ($\alpha = 0.05$). ²SE: Standard error.

³Significance between model AUC and the AUC of the line of no-discrimination (0.5) was determined at $\alpha = 0.05$.

⁴2019-2021, R1-R3 indicates analyses performed with data collected only during the flowering periods in 2019, 2020 and 2021.

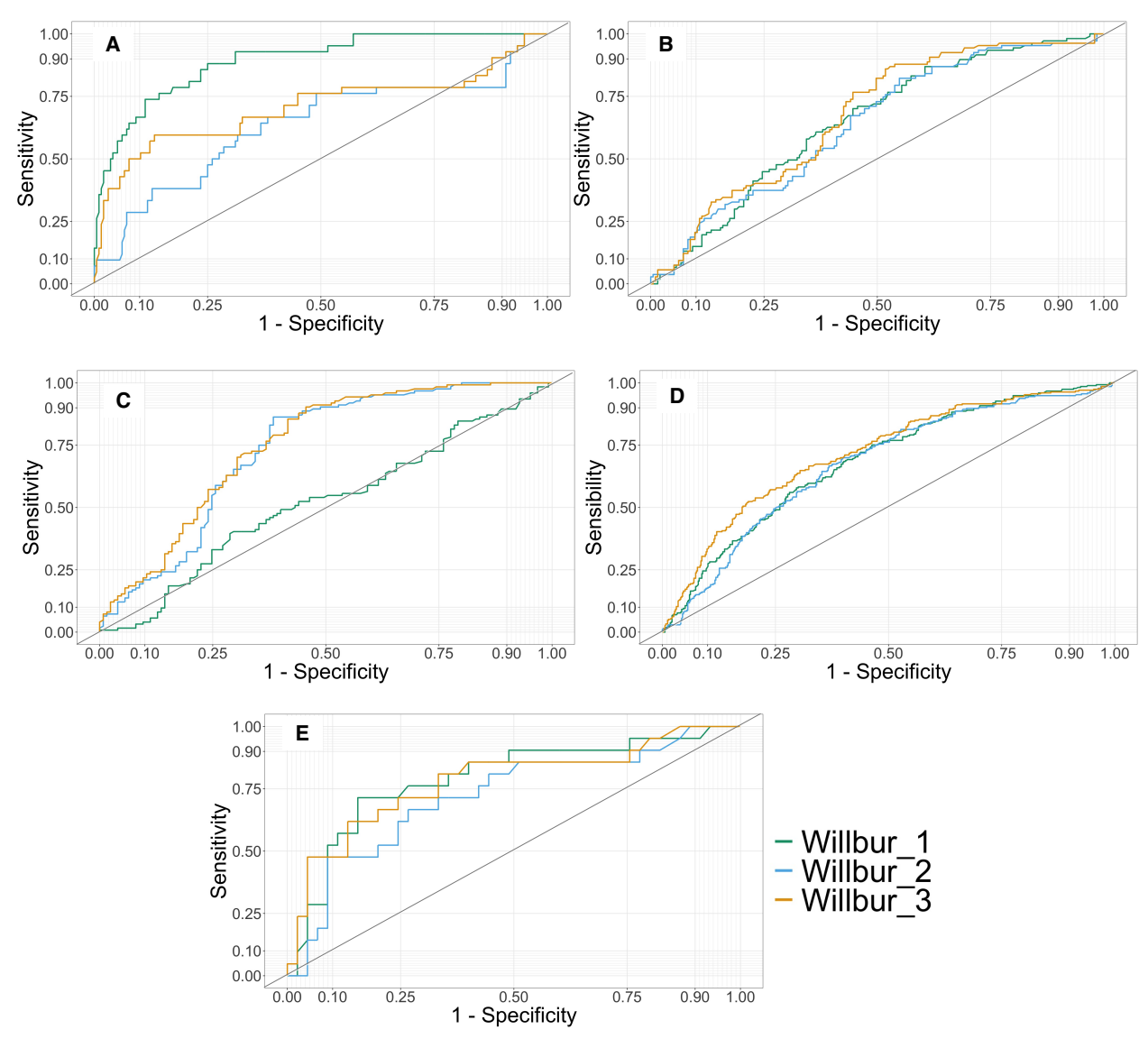


Figure 4. 3. Receiver operating characteristic curves for the original Willbur apothecia formation models in A) 2019, B) 2020, C) 2021, D) 2019 to 2021 and E) the flowering period (R1-R3) from 2019 to 2021.

4.3.3 Calibration plots of original Willbur models

The original Willbur models' calibration was evaluated using the data collected in Québec from 2019 to 2021. The calibration plots for all three original models show that predicted probabilities generated by the models were not in line with the observed probabilities of apothecia presence in Québec. Willbur 1 predictions are inversed compared to the observed probabilities. Willbur 2 and 3 predictions are concentrated at very low probability values (Figure 4. 4B and C). These plots

suggest that recalibration is required for these models to be reliably used to predict apothecia presence in Québec.

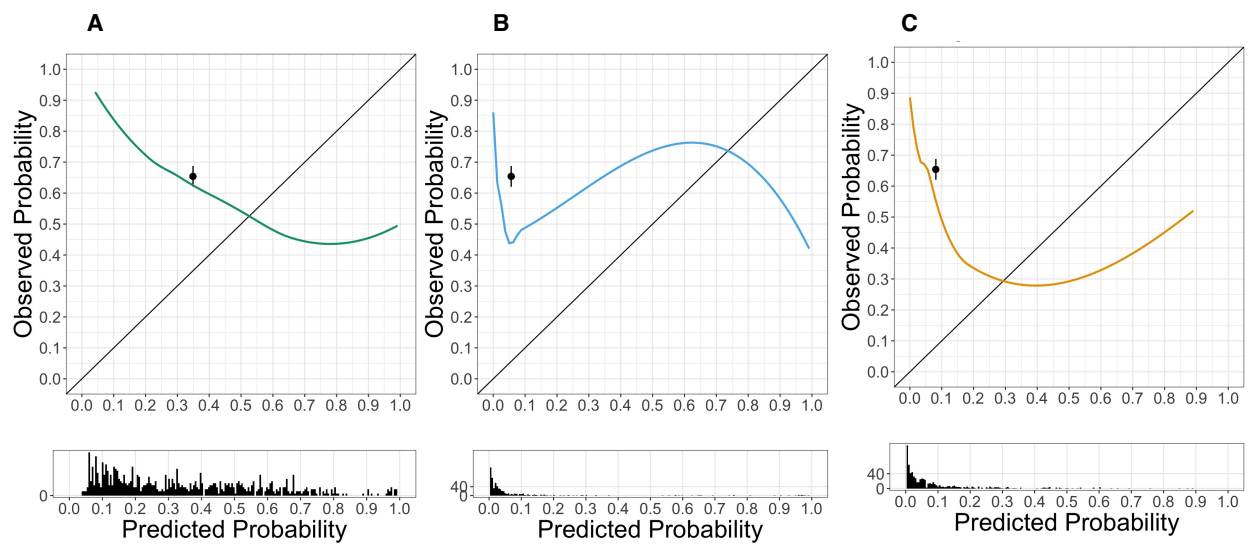


Figure 4. 4. Calibration plots for the A) Willbur 1, B) Willbur 2 and C) Willbur 3 models in Québec from 2019 to 2021. The predicted probability represents the logistic regression model probability values and the observed probability represents the corresponding frequency of apothecia presence observed in Québec from 2019 to 2021. The diagonal line shows optimal calibration and the model calibration is represented by the coloured curves. The histogram below the x-axis shows the distribution of model predicted probabilities.

4.3.4 Modified model fit (70% 2019-2021)

Modified model fit was assessed on the training dataset (70% of the 2019 to 2021 data) through a combination of metrics including the AIC, R², Kappa, and AUC (Table 4. 7), as well as the accuracy, sensitivity, specificity, false positive and false negative rates at each model's Youden index (Table 4. 8). The recalibrated equations for all three Willbur models did not show improvement in classification ability compared to the original model equations in both the internal and external validation datasets and were not retained for the remainder of the analyses (Table A. 14 and Table A. 15). All modified models retained were revised or extended equations that showed acceptable to excellent classification ability with AUCs between 0.693 and 0.865. The best fitting models included a combination of maximum temperature (Tmax) and moisture variables. Moisture variables included maximum relative humidity (RHmax), mean relative humidity (RHmean) and AWDR and were chosen based on previous correlation analyses performed in Chapter 3 (Morier-Gxoyiya et al., in preparation). All models that used 30-day moving averages of daily mean relative

humidity had the highest discrimination (AUC>0.840), R² values (>0.430) and lowest AIC (<504) (Table 4. 7). In particular, the two-parameter model based on 30-day moving average of daily maximum temperature and mean relative humidity, Willbur 1x.2, was among the most parsimonious models, while simultaneously being among the most accurate (77.5% for a probability level of 25.7% calculated through the Youden Index), and showing a low false negative rate (8.6%) (Table 4. 8).

The Kappa statistic was used to assess the models' performances given the unbalanced dataset collected in Québec from 2019 to 2021, which had a relatively low apothecia presence rate of 33.9% (Figure 4. 2). This means that models could overly predict the absence of apothecia yet still achieve high accuracy. The four models with the highest Kappa statistic (>0.422) included 30-day moving average of daily maximum temperature and mean relative humidity in their predictors (Table 4. 7). Models were modified either with 20-day or 30-day moving averages of weather variables. The models using 20-day moving average durations generally did not outperform those modified with 30-day moving averages (Table A. 16), despite the shorter moving average duration showing stronger correlation with temperature and the binary apothecia variable as shown in Chapter 3 (Morier-Gxoyiya et al., in preparation).

In all revised and extended models, the variables chosen as predictors were statistically significant (P < 0.05), except for the model using maximum temperature and wind speed, mean relative humidity and AWDR (Willbur 3x.2), where the AWDR variable was not statistically significant (P = 0.0748) (Table 4. 9). Temperature and wind speed had negative coefficients while relative humidity and AWDR had positive coefficients, suggesting that apothecia presence is linked to decreases in temperature and wind speed and increases in relative humidity and AWDR. All other variables being held constant, scouting visits with either higher maximum relative humidity, mean relative humidity or AWDR are more likely to have apothecia since these variable estimates are positive. Also, all other variables being held constant, scouting visits with lower maximum temperature or maximum wind speed are more likely to have apothecia since these variable estimates are negative (Table 4. 9, Formulae 4.1 to 4.10, and Table A. 17).

Table 4. 7. Modified apothecia formation model fit metrics for various combinations of 30-day moving average durations of weather variables.

Model	Variables	AIC	R2	Kappa	AUC
Wilbur 1r ¹	Tmax	662.300	0.114	0.129	0.693
Willbur 2r ¹	Tmax, WSmax	648.300	0.150	0.168	0.699
Willbur 3r ¹	Tmax, WSmax, RHmax	611.000	0.235	0.283	0.745
Willbur 1x.1 ²	Tmax, AWDR	642.600	0.163	0.136	0.702
Willbur 1x.2 ²	Tmax, RHmean	504.000	0.434	0.453	0.853
Willbur 1x.3 ²	Tmax, RHmean, AWDR	501.400	0.442	0.422	0.840
Willbur 2x.1 ²	Tmax, WSmax, AWDR	630.000	0.194	0.173	0.705
Willbur 2x.2 ²	Tmax, WSmax, RHmean	461.900	0.507	0.512	0.865
Willbur 3x.1 ²	Tmax, WSmax, RHmax, AWDR	594.100	0.274	0.311	0.739
Willbur 3x.2 ²	Tmax, WSmax, RHmean, AWDR	460.700	0.512	0.490	0.856

¹Revised Willbur et al. (2018) equations updated using 70% of the data collected in Québec from 2019 to 2021, Formulae 4.1, 4.2 and 4.3 below, the significance of regression coefficients is available in Table A. 17.

Abbreviations: Tmax, Maximum Temperature (°C); WSmax, Maximum Wind Speed (km/h); RHmax, Maximum Relative Humidity (%); RHmean, Mean Relative Humidity (%); AWDR, Abundant and Well-Distributed Rainfall (mm). All weather variables are 30-day moving averages.

²Extended Willbur et al. (2018) equations updated using 70% of the data collected in Québec from 2019 to 2021, Formulae 4.4 to 4.10 below, the significance of regression coefficients is available in Table A. 17.

Table 4. 8. Performance parameters of modified apothecia formation models at their Youden index using 70% of the data collected from 2019 to 2021 in Québec.

Model	Threshold	Accuracy	Sensitivity	Specificity	Fpos	Fneg	LR+	LR-
Wilbur 1r ¹	0.365	0.681	0.591	0.727	0.273	0.409	2.165	0.562
Willbur 2r ¹	0.356	0.701	0.651	0.727	0.273	0.349	2.381	0.481
Willbur 3r ¹	0.351	0.741	0.710	0.757	0.243	0.290	2.918	0.384
Willbur 1x.1 ²	0.239	0.658	0.952	0.508	0.492	0.048	1.935	0.095
Willbur 1x.2 ²	0.257	0.775	0.914	0.705	0.295	0.086	3.097	0.122
Willbur 1x.3 ²	0.221	0.754	0.946	0.656	0.344	0.054	2.749	0.082
Willbur 2x.1 ²	0.257	0.685	0.898	0.577	0.424	0.102	2.120	0.177
Willbur 2x.2 ²	0.197	0.745	0.930	0.650	0.350	0.070	2.660	0.107
Willbur 3x.1 ²	0.284	0.725	0.860	0.656	0.344	0.140	2.499	0.213
Willbur 3x.2 ²	0.337	0.788	0.807	0.779	0.221	0.194	3.644	0.249

¹Revised Willbur et al. (2018) equations updated using 70% of the data collected in Québec from 2019 to 2021.

Abbreviations: Fpos: False positive rate, Fneg: False negative rate, LR+: Positive Likelihood Ratio, LR-: Negative Likelihood Ratio.

²Extended Willbur et al. (2018) equations updated using 70% of the data collected in Québec from 2019 to 2021.

Table 4. 9. Range of variable logistic regression coefficients for modified apothecia formation models obtained using 70% of the data collected from 2019 to 2021 in Québec.

Variable			R	lange		
	Coe	efficient	Stanc	lard Error	P-	value
Tmax	-0.419	-0.172	0.0538	0.0661	< 0.0001	0.0062
WSmax	-0.383	-0.168	0.0449	0.0593	< 0.0001	0.0003
AWDR	0.005	0.011	0.0025	0.0030	< 0.0001	0.0748
RHmax	0.130	0.130	0.0269	0.0271	< 0.0001	< 0.0001
RHmean	0.299	0.363	0.0316	0.0353	< 0.0001	< 0.0001

Abbreviations: Tmax: Maximum Temperature (°C), WSmax: Maximum Wind Speed/1.609 (km/h), AWDR: Abundant and Well-Distributed Rainfall (mm), RHmax: Maximum Relative Humidity (%), RHmean: Mean Relative Humidity (%). All weather variables are 30-day moving averages.

Formula 4. 1. Willbur 1r, revised model equation.

 $Logit(\mu) = -0.345(MaxT_{30MA}) + 8.417$

Where MaxT_{30MA} is the 30-day moving average of the maximum value of air temperature (°C).

Formula 4. 2. Willbur 2r, revised model equation.

$$Logit(\mu) = -0.374(MaxT_{30MA}) - 0.171(MaxWS_{30MA}/1.609) + 10.657$$

Where MaxT_{30MA} is the 30-day moving average of the maximum value of air temperature (°C), and MaxWS_{30MA} is the 30-day moving average of the maximum of wind speed (km/h).

Formula 4. 3. Willbur 3r, revised model equation.

$$Logit(\mu) = -0.413(MaxT_{30MA}) + 0.13(MaxRH_{30MA}) - 0.235(MaxWS_{30MA}/1.609) - 0.31$$

Where MaxT_{30MA} is the 30-day moving average of the maximum value of air temperature (°C), MaxRH_{30MA} is the 30-day moving average of the maximum of relative humidity (%), and MaxWS_{30MA} is the 30-day moving average of the maximum of wind speed (km/h).

Formula 4. 4. Willbur 1x.1, extended model equation.

$$Logit(\mu) = -0.351(MaxT_{30MA}) + 0.011(AWDR) + 7.843$$

Where MaxT_{30MA} is the 30-day moving average of the maximum value of air temperature (°C) and AWDR is the 30-day moving average of the abundant and well-distributed rainfall index (mm).

Formula 4. 5. Willbur 1x.2, extended model equation.

$$Logit(\mu) = -0.172(MaxT_{30MA}) + 0.31(MeanRH_{30MA}) - 19.812$$

Where MaxT_{30MA} is the 30-day moving average of the maximum value of air temperature (°C) and MeanRH_{30MA} is the 30-day moving average of mean relative humidity (%).

Formula 4. 6. Willbur 1x.3, extended model equation.

$$Logit(\mu) = -0.191(MaxT_{30MA}) + 0.299(MeanRH_{30MA}) + 0.006(AWDR) - 18.925$$

Where MaxT_{30MA} is the 30-day moving average of the maximum value of air temperature (°C), MeanRH_{30MA} is the 30-day moving average of mean relative humidity (%), and AWDR is the 30-day moving average of the abundant and well-distributed rainfall index (mm).

Formula 4. 7. Willbur 2x.1, extended model equation.

$$Logit(\mu) = -0.38(MaxT_{30MA}) - 0.168(MaxWS_{30MA}/1.609) + 0.011(AWDR) + 10.07$$

Where MaxT_{30MA} is the 30-day moving average of the maximum value of air temperature (°C), and MaxWS_{30MA} is the 30-day moving average of the maximum of wind speed (km/h), and AWDR is the 30-day moving average of the abundant and well-distributed rainfall index (mm).

Formula 4. 8. Willbur 2x.2, extended model equation.

$$Logit(\mu) = -0.188(MaxT_{30MA}) - 0.383(MaxWS_{30MA}/1.609) + 0.363(MeanRH_{30MA}) - 20.286$$

Where MaxT_{30MA} is the 30-day moving average of the maximum value of air temperature (°C), and MaxWS_{30MA} is the 30-day moving average of the maximum of wind speed (km/h), and MeanRH_{30MA} is the 30-day moving average of mean relative humidity (%).

Formula 4. 9. Willbur 3x.1, extended model equation.

$$\label{eq:Logit} \begin{split} Logit(\mu) &= \text{-}0.419 (Max T_{30MA}) - 0.239 (Max W S_{30MA}/1.609) + 0.13 (Max R H_{30MA}) + 0.011 (AWDR) \\ &- 0.815 \end{split}$$

Where MaxT_{30MA} is the 30-day moving average of the maximum value of air temperature (°C), and MaxWS_{30MA} is the 30-day moving average of the maximum of wind speed (km/h), MaxRH_{30MA} is the 30-day moving average of maximum relative humidity (%), and AWDR is the 30-day moving average of the abundant and well-distributed rainfall index (mm).

Formula 4. 10. Willbur 3x.2, extended model equation.

$$\label{eq:logit} Logit(\mu) = -0.205(MaxT_{30MA}) - 0.374(MaxWS_{30MA}/1.609) + 0.354(MeanRH_{30MA}) + 0.005(AWDR) - 19.617$$

Where MaxT_{30MA} is the 30-day moving average of the maximum value of air temperature (°C), and MaxWS_{30MA} is the 30-day moving average of the maximum of wind speed (km/h), MeanRH_{30MA} is the 30-day moving average of mean relative humidity (%), and AWDR is the 30-day moving average of the abundant and well-distributed rainfall index (mm).

4.3.4.1 Calibration plots of modified Willbur apothecia formation models

For each modified Willbur model, the calibration plot was obtained by plotting the frequency of observed apothecia presence in the 70% dataset collected from 2019 to 2021 against model predicted probability. Simple recalibration methods such as "Recalibration-in-the-large" and "Logistic recalibration" did not improve model calibration compared to the original Willbur models (data not shown). Rather, modified models showed some modest improvement in calibration when models were modified through the Revision method, in which each model predictor's coefficient was refitted to the data observed in Québec from 2019 to 2021. All three revised Willbur models show some underestimation at very low and very high model predicted probabilities as shown by the model curves crossing above the ideal calibration diagonal line. This indicates that the risk of apothecia presence predicted by the revised Willbur models is lower than the observed rate of apothecia presence in Québec (Figure 4. 5 A, B and C). Some variations in calibration were observed for models modified using the Extension method. For the Willbur 1 model extension, calibration was not improved by the addition of only the AWDR, but rather using RHmean, with or without AWDR (Figure 4. 5 D, E, F). This was also true for extended Willbur 2

and Willbur 3 model versions, where the curves for the models extended with AWDR do not follow the diagonal line as opposed to the curves for the models extended also with RHmean (Figure 4. 5 G, H, I and J).

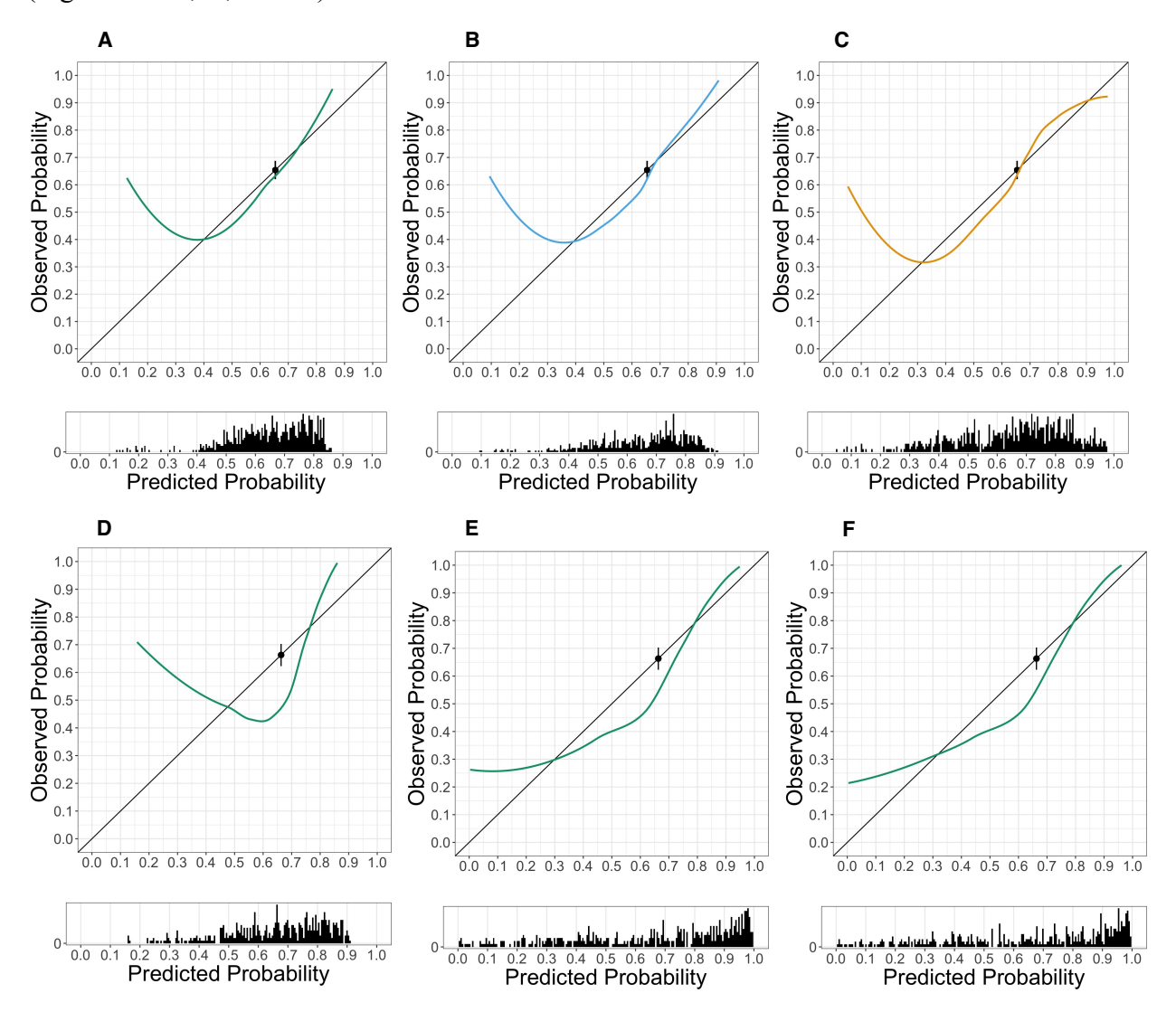


Figure 4. 5. Calibration plots for the A) Willbur 1r, B) Willbur 2r and C) Willbur 3r (Revised models), D) Willbur 1x.1, E) Willbur 1x.2, F) Willbur 1x.3, G) Willbur 2x.1, H) Willbur 2x.2, I) Willbur 3x.1, and J) Willbur 3x.2 (Extended models) in Québec using 70% 2019-2021 dataset. The predicted probability represents the logistic regression model probability values and the corresponding observed probability represents the frequency of apothecia presence observed in Québec from 2019 to 2021. The diagonal line shows optimal calibration and the model calibration is represented by the coloured curves. The histogram below the x-axis shows the distribution of model predicted probabilities.

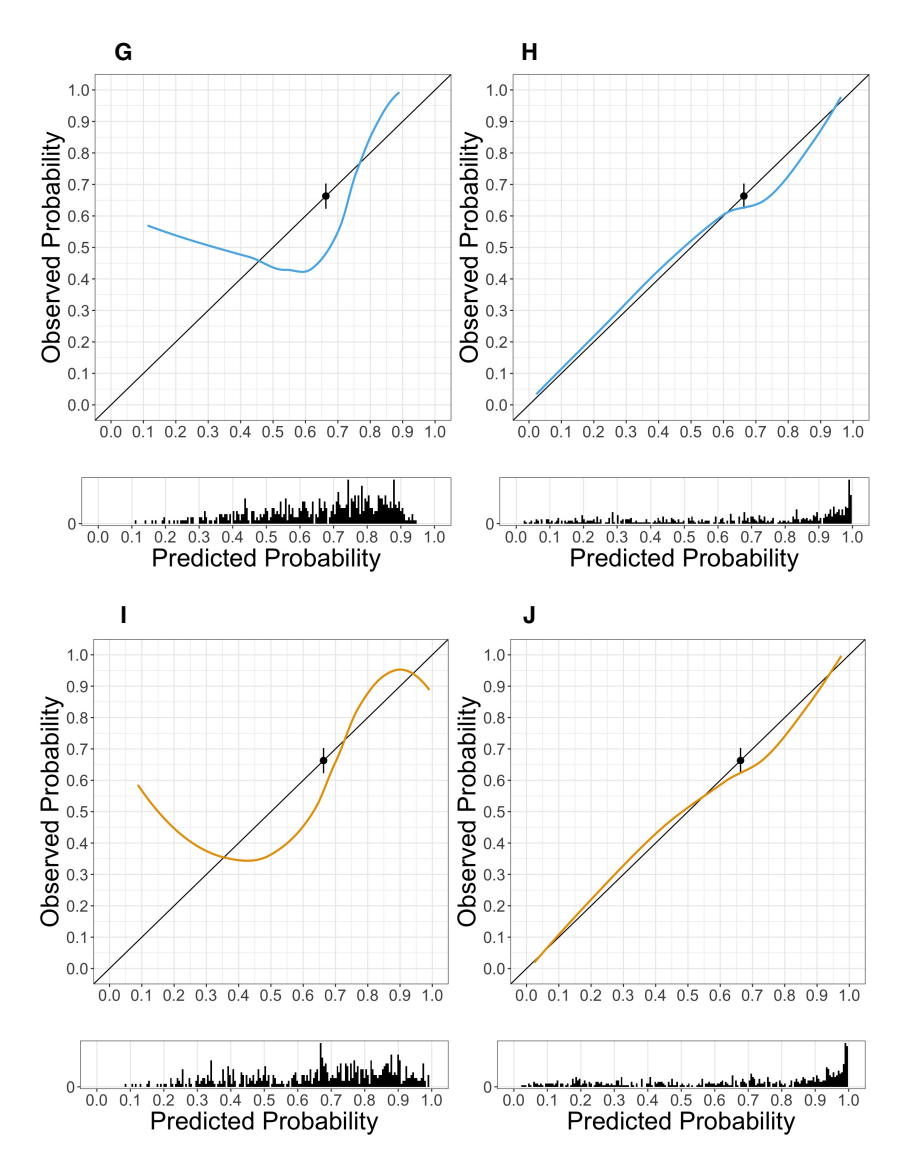


Figure 4. 5. Calibration plots for the A) Willbur 1r, B) Willbur 2r and C) Willbur 3r (Revised models), D) Willbur 1x.1, E) Willbur 1x.2, F) Willbur 1x.3, G) Willbur 2x.1, H) Willbur 2x.2, I) Willbur 3x.1, and J) Willbur 3x.2 (Extended models) in Québec using 70% 2019-2021 dataset (cont'd). The predicted probability represents the logistic regression model probability values and the corresponding observed probability represents the frequency of apothecia presence observed in Québec from 2019 to 2021. The diagonal line shows optimal calibration and the model calibration is represented by the coloured curves. The histogram below the x-axis shows the distribution of model predicted probabilities.

4.3.5 Modified apothecia formation models

4.3.5.1 Internal validation (30% 2019-2021)

The extent to which the original Willbur models were modified influenced their classification performance on the validation dataset composed of the remaining 30% data collected in Québec from 2019 to 2021. The AUCs of the original Willbur models were the same as the versions obtained following the simplest modification methods, the recalibration-in-the-large and the logistic recalibration. This observation was true across Willbur 1, 2 and 3 equations. For example, the ROC curves of the recalibrated models for Willbur 1, had an AUC value of 0.664. The AUC value of the recalibrated models for Willbur 2 was 0.632 and the of the recalibrated models AUC value for Willbur 3 was 0.673 (Table A. 15).

All modified models showed better classification ability than chance since their AUCs were greater than 0.500 ($\alpha = 0.05$). However, improvement compared to the classification ability of the original model equations was not achieved using the recalibration methods. Significant improvement was achieved by extending Willbur 1 by adding 30-day moving average of mean daily relative humidity to the maximum daily temperature (Willbur 1x.2). The addition of other humidity parameters such as the AWDR (Willbur 1x.1) to the model originally based on maximum temperature alone improved its performance, but not significantly. The best-fitted models also performed best in the external validation; the four models with the highest classification ability (AUC>0.815) all included maximum temperature and mean relative humidity as predictors (Table 4. 10).

4.3.5.2 Youden index for internal validation (30% 2019-2021)

The Youden index for the original and best modified models, calculated with 30% of the data from 2019 to 2021, is presented in Table 4. 11 along with model accuracy, sensitivity, specificity, and likelihood ratios of positive (LR+) and negative (LR-) predictions. For Willbur 1, the original and modified models are associated with similar Youden index values. For Willbur 2 and 3, the modified models' Youden index values increased compared to the original equations. While the accuracy of the original models was between 59.9% and 70.0%, the accuracy of modified models was generally higher, ranging from 59.9% to 77.2% (Table 4. 11). All original and modified models showed LR+ values above 1 and LR- below 1. The model using maximum temperature,

mean relative humidity and AWDR (Willbur 1x.3) was the most accurate modified model and had the highest LR+ value. The lowest LR- value was associated with the model using maximum temperature and mean relative humidity (Willbur 1x.1). Most models were more sensitive than specific at their Youden index, which shows that they had a better capacity at classifying instances of apothecial presence than apothecial absence (Table 4. 11).

Table 4. 10. Comparisons between the AUCs and the line of no-discrimination of original and modified apothecia prediction models in Québec using 30% of the data from 2019 to 2021.

Model	Variables	AUC	SE	Z- statistic	P-value ⁴
Willbur 1 ¹	Tmax	0.664	0.001	4.200	1.35E-05
Willbur 2 ¹	Tmax, WSmax	0.632	0.001	3.380	3.57E-04
Willbur 3 ¹	Tmax, WSmax, RHmax	0.673	0.001	4.450	4.39E-06
Wilbur 1r ²	Tmax	0.664	0.001	4.200	1.35E-05
Willbur 2r ²	Tmax, WSmax	0.681	0.001	4.650	1.66E-06
Willbur 3r ²	Tmax, WSmax, RHmax	0.719	0.001	5.630	9.09E-09
Willbur 1x.1 ³	Tmax, AWDR	0.718	0.001	5.580	1.17E-08
Willbur 1x.2 ³	Tmax, RHmean	0.817	0.001	8.130	2.28E-16
Willbur 1x.3 ³	Tmax, RHmean, AWDR	0.815	0.001	8.080	3.41E-16
Willbur 2x.1 ³	Tmax, WSmax, AWDR	0.724	0.001	5.750	4.56E-09
Willbur 2x.2 ³	Tmax, WSmax, RHmean	0.831	0.001	141.420	1.05E-17
Willbur 3x.1 ³	Tmax, WSmax, RHmax, AWDR	0.752	0.001	6.460	5.37E-11
Willbur 3x.2 ³	Tmax, WSmax, RHmean, AWDR	0.833	0.001	141.420	6.29E-18

¹Original Willbur et al. (2018) equations.

Abbreviations: AUC: Area under the Receiver Operator Curve, and SE: Standard Error, Tmax: Maximum Temperature (°C), WSmax: Maximum Wind Speed (km/h), RHmax: Maximum Relative Humidity (%), RHmean: Mean Relative Humidity (%), AWDR: Abundant and Well-Distributed Rainfall (mm). All weather variables are 30-day moving averages.

²Revised Willbur et al. (2018) equations updated using 70% of the data collected in Québec from 2019 to 2021.

³Extended Willbur et al. (2018) equations updated using 70% of the data collected in Québec from 2019 to 2021.

⁴Significance between model AUC and the AUC of the line of no-discrimination (0.5) was determined at $\alpha = 0.05$.

Table 4. 11 Performance parameters of apothecia formation of original and modified Willbur model versions at their Youden index from 2019 to 2021.

Model	Variables	Threshold	Accuracy	Sensitivity	Specificity	LR+	LR-
Willbur 1 ¹	Tmax	0.257	0.599	0.782	0.493	1.543	0.443
Willbur 2 ¹	Tmax, WSmax	0.012	0.599	0.690	0.547	1.521	0.568
Willbur 3 ¹	Tmax, WSmax, RHmax	0.104	0.700	0.460	0.840	2.874	0.643
Wilbur 1r ²	Tmax	0.299	0.599	0.782	0.493	1.543	0.443
Willbur 2r ²	Tmax, WSmax	0.305	0.637	0.724	0.587	1.752	0.470
Willbur 3r ²	Tmax, WSmax, RHmax	0.350	0.675	0.655	0.687	2.091	0.502
Willbur 1x.1 ³	Tmax, AWDR	0.239	0.616	0.954	0.420	1.645	0.110
Willbur 1x.2 ³	Tmax, RHmean	0.280	0.755	0.862	0.693	2.811	0.199
Willbur 1x.3 ³	Tmax, RHmean, AWDR	0.280	0.772	0.885	0.707	3.017	0.163
Willbur 2x.1 ³	Tmax, WSmax, AWDR	0.249	0.633	0.931	0.460	1.724	0.150
Willbur 2x.2 ³	Tmax, WSmax, RHmean	0.224	0.713	0.920	0.593	2.261	0.136
Willbur 3x.1 ³	Tmax, WSmax, RHmax, AWDR	0.299	0.696	0.828	0.620	2.178	0.278
Willbur 3x.2 ³	Tmax, WSmax, RHmean, AWDR	0.247	0.722	0.920	0.607	2.338	0.133

¹Original Willbur et al. (2018) equations.

Abbreviations: LR+, Positive Likelihood Ratio; LR-, Negative Likelihood Ratio; Tmax, Maximum Temperature (°C); WSmax, Maximum Wind Speed (km/h); RHmax, Maximum Relative Humidity (%); RHmean, Mean Relative Humidity (%); AWDR, Abundant and Well-Distributed Rainfall. All weather variables are 30-day moving averages.

²Revised Willbur et al. (2018) equations updated using 70% of the data collected in Québec from 2019 to 2021.

³Extended Willbur et al. (2018) equations updated using 70% of the data collected in Québec from 2019 to 2021.

4.3.5.3 External validation 2017-2018

During the soybean flowering periods in 2017 and 2018, both original and modified models predicted apothecia presence better than chance ($\alpha = 0.05$) and had acceptable to excellent discrimination abilities (0.753<AUC<0.839). Willbur 3 was the original model with the highest AUC (0.795), while the best modified model was Willbur 3r (AUC=0.839). Both models used maximum temperature, maximum wind speed and maximum relative humidity, but the Willbur 3r model had revised coefficients. The models with the highest classification ability based on AUC all included maximum temperature and either maximum or mean relative humidity as predictors (Table 4. 12).

4.3.5.4 Youden index for external validation in 2017-2018

For each original and modified version of the model equations, the optimal Youden threshold, calculated with the data collected during the soybean flowering period in 2017 and 2018, is presented in Table 4. 13, along with the model's accuracy, sensitivity, specificity, and likelihood ratios of positive (LR+) and negative (LR-) predictions. The value of the Youden index for the modified versions increased compared to the original versions of Willbur 2 and 3. The Youden index for the original Willbur 1 model was higher than the Youden index values of modified Willbur 1 equations. The accuracy of the original models ranged between 73.5% and 82.1%, while the accuracy of modified models went from 73.5% to 80.9%. The models using maximum temperature, maximum wind speed, and either maximum or mean relative humidity were the most accurate. The models were once again more sensitive than specific at their Youden index (Table 4. 13).

Table 4. 12. Comparisons between the AUCs and the line of no-discrimination of original and modified apothecia prediction models in Québec using the data from the flowering period in 2017 and 2018.

Model	Variables	AUC	SE	Z- statistic	P-value ⁴
				statistic	
Willbur 1 ¹	Tmax	0.779	0.002	4.960	3.54E-07
Willbur 2 ¹	Tmax, WSmax	0.753	0.002	4.490	3.51E-06
Willbur 3 ¹	Tmax, WSmax, RHmax	0.795	0.002	5.240	7.95E-08
Wilbur 1r ²	Tmax	0.779	0.002	4.960	3.54E-07
Willbur 2r ²	Tmax, WSmax	0.769	0.002	4.790	8.32E-07
Willbur 3r ²	Tmax, WSmax, RHmax	0.839	0.001	6.040	7.90E-10
Willbur 1x.1 ³	Tmax, AWDR	0.782	0.002	5.000	2.85E-07
Willbur 1x.2 ³	Tmax, RHmean	0.817	0.002	5.640	8.42E-09
Willbur 1x.3 ³	Tmax, RHmean, AWDR	0.802	0.002	5.350	4.36E-08
Willbur 2x.1 ³	Tmax, WSmax, AWDR	0.791	0.002	5.150	1.28E-07
Willbur 2x.2 ³	Tmax, WSmax, RHmean	0.821	0.002	5.720	5.45E-09
Willbur 3x.1 ³	Tmax, WSmax, RHmax, AWDR	0.806	0.002	5.420	3.05E-08
Willbur 3x.2 ³	Tmax, WSmax, RHmean, AWDR	0.810	0.002	5.500	1.92E-08

¹Original Willbur et al. (2018) equations.

Abbreviations: AUC, Area under the Receiver Operator Curve; SE, Standard Error; Tmax, Maximum Temperature (°C); WSmax, Maximum Wind Speed (km/h); RHmax, Maximum Relative Humidity (%); RHmean, Mean Relative Humidity (%); AWDR, Abundant and Well-Distributed Rainfall (mm). All weather variables are 30-day moving averages.

²Revised Willbur et al. (2018) equations updated using 70% of the data collected in Québec from 2019 to 2021.

³Extended Willbur et al. (2018) equations updated using 70% of the data collected in Québec from 2019 to 2021.

⁴Significance between model AUC and the AUC of the line of no-discrimination (0.5) was determined at $\alpha = 0.05$.

*Table 4. 13. Performance parameters of apothecia formation Willbur models original*¹ *and modified versions at their Youden index from 2017 to 2018.*

Model	Variables	Youden Index	Accuracy	Sensitivity	Specificity	LR+	LR-
Willbur 1 ¹	Tmax ¹	0.418	0.735	0.927	0.632	2.516	0.116
Willbur 2 ¹	Tmax, WSmax ¹	0.007	0.761	0.878	0.697	2.901	0.175
Willbur 3 ¹	Tmax, WSmax, RHmax ¹	0.022	0.821	0.951	0.750	3.805	0.065
Wilbur 1r ²	Tmax	0.384	0.735	0.927	0.632	2.516	0.116
Willbur 2r ²	Tmax, WSmax	0.385	0.727	0.927	0.618	2.429	0.118
Willbur 3r ²	Tmax, WSmax, RHmax	0.411	0.795	0.829	0.776	3.707	0.220
Willbur 1x.1 ³	Tmax, AWDR	0.311	0.748	0.927	0.649	2.638	0.113
Willbur 1x.2 ³	Tmax, RHmean	0.242	0.795	0.902	0.737	3.429	0.132
Willbur 1x.3 ³	Tmax, RHmean, AWDR	0.231	0.791	0.927	0.716	3.266	0.102
Willbur 2x.1 ³	Tmax, WSmax, AWDR	0.348	0.748	0.927	0.649	2.638	0.113
Willbur 2x.2 ³	Tmax, WSmax, RHmean	0.060	0.803	1.000	0.697	3.304	0.000
Willbur 3x.1 ³	Tmax, WSmax, RHmax, AWDR	0.352	0.809	0.927	0.743	3.610	0.098
Willbur 3x.2 ³	Tmax, WSmax, RHmean, AWDR	0.091	0.809	0.976	0.716	3.438	0.034

¹Original Willbur et al. (2018) equations.

Abbreviations: LR+, Positive Likelihood Ratio; LR-, Negative Likelihood Ratio; Tmax, Maximum Temperature (°C); WSmax, Maximum Wind Speed (km/h); RHmax, Maximum Relative Humidity (%); RHmean, Mean Relative Humidity (%); AWDR, Abundant and Well-Distributed Rainfall (mm). All weather variables are 30-day moving averages.

²Revised Willbur et al. (2018) equations updated using 70% of the data collected in Québec from 2019 to 2021.

³Extended Willbur et al. (2018) equations updated using 70% of the data collected in Québec from 2019 to 2021.

4.3.6 Dominance analysis for modified apothecia formation models

A dominance analysis was performed to assess the importance of each predictor in relation to the others in the two 4-parameter models Willbur 3x.1 and Willbur 3x.2 (Figure 4. 6 and Figure 4. 7). The results of the analysis varied from 2019 to 2021, as well as between the models including either mean or maximum relative humidity. In the Willbur 3x.1 model based on AWDR, maximum temperature, maximum wind speed and maximum relative humidity, temperature explained most of the deviance in apothecia presence in 2019, while the humidity variables AWDR and maximum relative humidity were more important in 2020 and 2021 (Figure 4. 6A, B and C). In addition, in that model, temperature was the most important variable in for the three pooled years as shown by its larger McFadden index value (R²_M) in the general dominance analysis (Figure 4. 6D). In the Willbur 3x.2 model based on AWDR, maximum temperature, maximum wind speed and mean relative humidity, maximum temperature's contribution to explain apothecia presence also generally dominated the other variables in 2019 (Figure 4. 7A). However, mean relative humidity was the most important variable for 2020, 2021 and the three pooled years as shown by its larger R²_M in the general dominance analysis (Figure 4. 7 B, C and D).

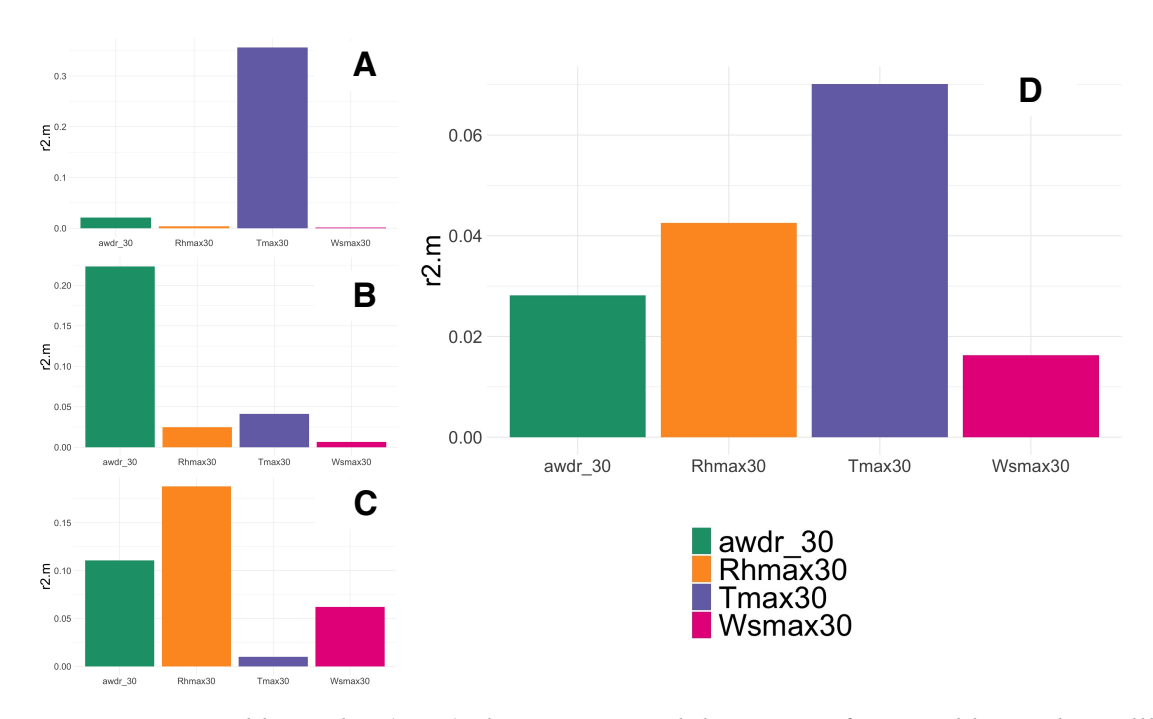


Figure 4. 6. McFadden index (r2.m) showing general dominance for variables in the Willbur 3x.1 model based on 30-day moving averages of maximum temperature (Tmax30), maximum wind speed (Wsmax30), AWDR (awdr_30) and maximum relative humidity (Rhmax30) in A) 2019, B) 2020, C) 2021 and D) 2019-2021.

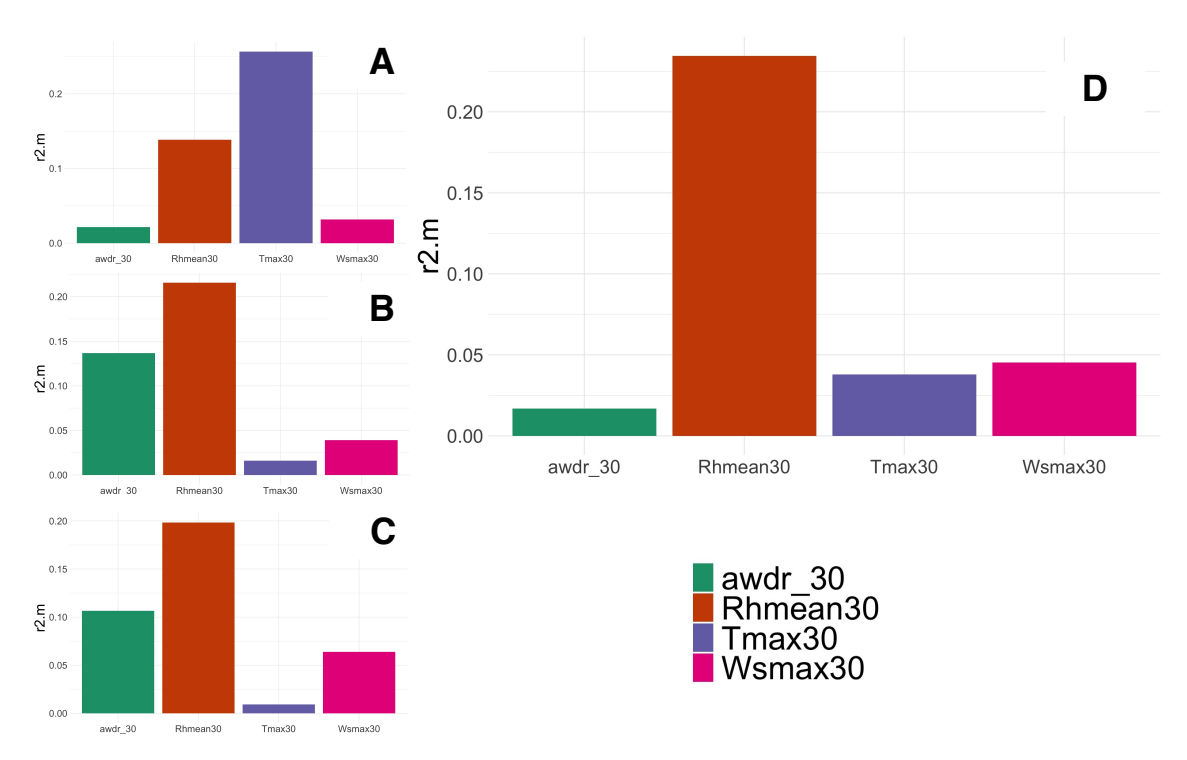


Figure 4. 7. McFadden index (r2.m) showing general dominance for variables in the Willbur 3x.2 model based on 30-day moving averages of maximum temperature (Tmax30), maximum wind speed (Wsmax30), AWDR (awdr_30) and mean relative humidity (Rhmean30) in A) 2019, B) 2020, C) 2021 and D) 2019-2021.

4.4 Discussion

In this report, three bioclimatic apothecia formation models developed in the North-Midwestern region of the United States were studied for their predictive ability in Québec. Model validation was performed through ROC curve analysis, a method frequently used in the medical field, that has gained popularity in other domains such as in botanical epidemiology. This method not only allowed us to validate whether models were better than chance at identifying apothecia presence in the field, but the AUC also served to compare the prediction ability amongst models and to identify possible action thresholds with the Youden index.

The validation of the original Willbur model equations showed that all three models had acceptable performance in identifying apothecia presence in Québec soybean fields during the flowering period, and throughout the growing season from 2019 to 2021. Some differences in model performance over the three years of data collection indicated that the model using 30-day moving averages of maximum temperature, wind speed and relative humidity (Willbur 3) had the most

consistent capacity to identify apothecia presence. In comparison, the performance of the model using only maximum temperature (Willbur 1) varied considerably from one year to another, mainly because of the variations in prevailing weather conditions between the growing seasons. In 2019, the Willbur 1 model had excellent discrimination and Québec environmental conditions were characterized by spring floods, and light and frequent precipitations. However, in 2020 and 2021, seasons where record heat and drought conditions predominated in Québec (MELCC, 2020, MELCC, 2021a), Willbur 1's performance was much lower. This suggests that when moisture is not a limiting factor, temperature alone is sufficient to distinguish situations promoting apothecia formation from those preventing carpogenic germination. It further shows that relying on both temperature and moisture factors is overall preferable to using only one of those parameters while assessing the risk of apothecia presence in fields.

On some aspects, the results obtained in Québec differ from those obtained in the development and validation phases of the models. For example, Willbur et al. (2018b) had identified the model based on maximum temperature and wind speed as amongst the most promising for apothecia prediction. However, from 2019 to 2021 in Québec, that model was never more accurate than the two other models evaluated. Wind speed had been suggested as a measure of dryness that could prove useful in predicting apothecial germination (Willbur et al., 2018b); however, except for the development of these Willbur models, its link to apothecia presence had not been extensively studied before. Furthermore, the findings from the model validation and dominance analyses in Québec fail to strongly support such a relationship. The fact that weather stations from which environmental data were sourced in Québec were not directly on-site might have affected the usefulness of the wind speed predictor. However, the influence of air temperature on the life cycle of *S. sclerotiorum* has been previously described by many and agreed with the results shown here (Clarkson et al., 2007, Clarkson et al., 2003, Young et al., 2004, Abawi and Grogan, 1975).

The calibration and the probability threshold analyses revealed adjustment issues that needed to be addressed prior to these models being used reliably as disease management tools in Québec. As it is often reported, a model's performance in new settings tends to diminish since there are often discrepancies between the outcome incidence in the development setting and in the new environment (Van Calster et al., 2019). In Québec, for models including dryness or moisture-

related parameters such as maximum wind speed and relative humidity, poor calibration resulted in very low predicted probabilities and low Youden indices (J<0.05). Such low thresholds would potentially lead to incorrect decisions to apply fungicides since all predicted probabilities above 0.05, even if they are actual situations of apothecia absence, would be mistaken for instances of apothecial presence. This would go against the purpose of prediction models to reduce the use of fungicides in low-risk situations. Youden index values changed from very small to moderate values after model modifications. This showed that the predicted probabilities of modified models were no longer concentrated in very low ranges, highlighting their increased capacity to discriminate between apothecia presence and absence. However, a drawback of the Youden index as a possible action threshold is that it equally values specificity and sensitivity. Yet, the cost of false positives and false negatives may not be equal, especially not to the producers at risk of financial loss (Madden, 2006). These considerations stressed the need for models to be properly calibrated for the Québec context.

Several methods were used to modify the Willbur models and address both underlying miscalibration and poor discrimination. The more complex modifications, obtained using revision and extension methods, were not only associated with some calibration improvement, especially for models extended with mean relative humidity, but they also led to the most gain in model discrimination capacity. In comparison, simpler recalibration methods were not sufficient to significantly change model AUCs. In the past, model revision has been shown to be required to improve model discrimination (Janssen et al., 2008, Steyerberg, 2019).

The fit of the modified models was evaluated in the training set. Following those analyses, we identified differences in model fit based on two main factors: the predictors included in model equations, and whether the values of the variables were 30-day moving averages of daily means or daily maximums. The models with the strongest fit, based on a combination of statistical measures, included maximum temperature and some moisture-related parameter. Out of all of the moisture predictors, which included the AWDR parameter, mean and maximum daily values of wind speed and relative humidity, the preferred one was mean relative humidity. It was included in four of the best fitted models. In addition, the modified models including maximum temperature and mean relative humidity successfully discriminated between apothecia presence and absence in

two additional datasets: one containing 30% of the data collected between 2019 and 2021 and another including apothecia observations during the soybean flowering period in Québec between 2017 and 2018. Ideally, models should aim to fit the data and be parsimonious (Landau et al., 2000). As such, the addition of variables should increase the accuracy of the model, which was not always the case in our validation experiments. Some 3-parameter models had lower AUCs and accuracy than the model based only on maximum temperature and mean relative humidity. This exact combination of variables was not included in the reported models of interest in the United States, but many of these models include mean relative humidity in combination with other predictors (Willbur et al., 2018b). In addition, there are multiple reports of an association between relative humidity and ascospore germination, disease incidence, and the rapidity of disease development in *Sclerotinia* spp. (Hannusch and Boland, 1996, Clarkson et al., 2014, Abawi, 1979, Torés and Moreno, 1991).

Currently, model validations are limited by the low proportion of apothecial presence and disease incidence cases in the datasets used for model validations in Québec. As more data become available, model modifications and validations are expected to improve. In addition, environmental conditions are only part of the factors influencing the risk of apothecia presence and disease incidence. Other factors related to the crop and the inoculum should also be assessed to adequately manage the risk of disease. An assessment of cultivar branching pattern and growth characteristics, and row spacing effect on carpogenic germination of *S. sclerotiorum* and end-of-season disease incidence will further inform the development of a risk assessment tool for soybean producers and agronomists in Québec. During this study, apothecial germination was monitored using sclerotia deposits artificially buried at each experimental sites for data collection purposes. However, disparities in natural inoculum densities at the field level likely exist based on the prior history of SSR at each of the locations. Thus, differences in previous disease management practices such as tillage and the length of the crop rotation without a host crop should also be considered.

4.5 Conclusion

To conclude, the Willbur apothecial formation models were validated in Québec using apothecia observations from 2019 to 2021. Despite showing acceptable discrimination capacity, the original models were further improved by revision of the regression coefficients. In addition, the best-fitting and most parsimonious model used a combination of 30-day moving average of maximum temperature and mean relative humidity to predict apothecia presence. Used in an integrated disease management strategy, these models could help Québec producers make informed decisions regarding the need for fungicides to reduce the risk of Sclerotinia stem rot development in soybean.

Chapter 5: General discussion

The first objective of this project was to evaluate environmental and agronomic conditions that affect *Sclerotinia sclerotiorum* (Lib.) de Bary apothecia formation and SSR disease development in Québec soybean-producing regions. The second objective was to test, compare, and improve SSR risk and apothecia formation forecast models, initially developed outside of Québec, under the province's growing conditions. This section revisits the results obtained, discusses their implication for soybean SSR management in Québec and suggests future areas of research.

Among the weather variables evaluated, temperature and relative humidity were originally thought to be most strongly associated with *S. sclerotiorum* carpogenic germination and SSR development. This hypothesis was confirmed through the work described in this thesis. In Québec, from 2019 to 2021, apothecia presence and DSI were negatively correlated with temperature and positively correlated with relative humidity. Moving-average durations from 10- to 30-days of relative humidity and temperature were most strongly associated with carpogenic germination. The *S. sclerotiorum* pathogen is present worldwide and associations with temperature and moisture have been repeatedly observed throughout geographical areas (Fall et al., 2018a, Foster et al., 2011, Twengström et al., 1998, Clarkson et al., 2014, Koch et al., 2007). In comparison, correlations between SSR disease indicators and other weather variables, such as wind speed and rainfall distribution patterns, varied based on the period considered and were overall weaker for fields surveyed in Québec from 2019 to 2021.

The row spacing at planting was studied as an agronomic factor influencing apothecia presence. The hypothesis that a narrower row spacing would promote early and abundant carpogenic germination and result in higher end-of-season disease severity was not confirmed. There was limited apothecia formation and disease development in most of the plots at the research centres, and thus no significant effect of row spacing was observed in the three years of data collection. The results at IRDA in 2021, the site-year where the most apothecia and disease development were observed, suggested that when environmental conditions are favourable to carpogenic germination, the 38.1-cm plots could exacerbate inoculum dispersal resulting in higher DSIs (T. Copley, personal communication, October 2021). Yearly differences in environmental conditions

contribute to the variation in SSR development in a field from one year to the next. Additionally, agronomic practices, such as crop rotations and plant population density, as well as tillage practices, likely explain variability in carpogenic germination among fields exposed to similar environmental conditions, but managed differently (Rousseau et al., 2007, Lee et al., 2005).

From 2019 to 2021, DSI ranged from 0.0 to 94.4%. Disease severity index was most strongly associated with apothecia observed during the R2, R3, and R4 soybean growth stages. There was inoculum in most sites scouted in Québec; however, carpogenic germination rates were low in some fields surveyed from 2019 to 2021. Variability in carpogenic germination following artificial soil inoculation with sclerotia produced under laboratory conditions was previously observed in Québec (Rousseau et al., 2004). Also, apothecia presence was rarely detected at the start or during the beginning and full bloom periods (R1-R2). Instead, most apothecia formation occurred when the pods and seeds were developing (R3 and beyond). S. sclerotiorum sclerotia produced and preconditioned in laboratory conditions prior to field burial have been associated with delayed and reduced carpogenic germination rates when burial was done in late spring and early summer as opposed to during winter or early spring in the United Kingdom (Clarkson et al., 2007). Winters in the temperate oceanic climate of the United Kingdom are generally warmer than those occurring in the continental humid climate where soybean is produced in Québec (Beck et al., 2018). Conditioning requirements of S. sclerotiorum vary based on multiple factors including isolate adaptation to local conditions (Huang et al., 1998, Dillard, 1995). Due to the extended period from November to March where soil temperatures are generally below 0°C in Québec, sclerotia naturally occurring in the province's fields would be assumed to be fully conditioned at the start of the soybean growing season (MELCC, 2021b). In comparison, sclerotia used in the deposits were produced from one S. sclerotiorum strain, isolate NB-5, exposed to a laboratory conditioning protocol of 12 weeks at 4°C, with carpogenic germination rates between 85 and 90% in pre-burial tests from 2019 to 2021 (T. Copley, personal communication, 2021). Comparing the timing and rate of carpogenic germination of naturally occurring and artificially buried pre-conditioned S. sclerotiorum sclerotia isolates in Québec would improve our understanding of the role of temperature on apothecia formation in local conditions.

Given the strong influence of environmental conditions on carpogenic germination and SSR development, weather-based prediction modelling is an opportunity to support decision-making and strategically reduce unjustified pesticide use (Willbur et al., 2018c). Developing new models is resource-intensive, and multiple *Sclerotinia*-related forecasters are already available (Foster et al., 2011, Twengström et al., 1998, Turkington, 1993, Mila et al., 2004). The performance of a selection of these models was evaluated over three growing seasons to identify models with the most potential to be used by Québec soybean producers (Willbur et al., 2018b). Following ROC curve analyses, two model attributes were identified as most appropriate for the Québec agroenvironmental context. First, to predict end-of-season disease development, using models based on weather conditions suitable for the presence of apothecia during the soybean flowering period, such as those developed by Willbur et al. (2018b), performed better than disease prediction models that did not focus on forecasting in-season inoculum such as those developed by Fall et al. (2018a) and Harikrishnan et al. (2008), confirming our hypothesis. Second, among apothecia formation models, those using a combination of temperature and moisture-related predictors were more reliable over the three years of data collection than the model using only temperature.

The miscalibration of models is a challenge limiting the use of existing forecasters in new settings (Van Calster et al., 2019). Model revision and extension addressed some of these issues when the Willbur models were modified using data collected in Québec during the soybean growing season. The adjusted models identified conditions favourable to the development of apothecia better than the original models. The modifications responsible for the most gain in model performance were the adjustment of coefficients associated with the model input, and the use of mean relative humidity instead of maximum relative humidity as a predictor. The most parsimonious model used 30-day moving averages of maximum temperature and mean relative humidity and was among the best models following modifications (Formula 5.1).

Formula 5.1 Willbur 1x.2.

 $Logit(\mu) = -0.172(TMax_{30MA}) + 0.310 (RHMean_{30MA}) - 19.812$

Where TMax_{30MA} is the 30-day moving average of the maximum value of air temperature (°C), and RHMean_{30MA} is the 30-day moving average of the mean relative humidity (%).

Model improvement is a dynamic process, and further modifications for the Québec setting could be made as additional data becomes available (Fall and Carisse, 2022). Integrating additional scouting observations from multiple locations during the soybean flowering stages in particular, would customize models to the period most relevant to SSR development.

Results from of the evaluation of the original and modified apothecia formation models in Chapter 4 are directly related to the findings from Chapter 3. With regards to the original Willbur models, the fluctuations in model performance over the years reflected the variations observed in the correlation analyses. In 2019, temperature was strongly correlated to the presence of apothecia and the model containing only that variable had the highest discrimination ability. However, in 2021 the correlation between moisture-related variables and carpogenic germination was stronger than in the previous years at the benefit of the accuracy of the models using such predictors. In addition, the association observed between weather variables and apothecia presence allowed for an informed choice of the model modifications. For example, mean relative humidity was strongly and consistently correlated with apothecia presence in all three years of data collection; however, it was not originally included in the Willbur models (Willbur et al., 2018b). Following model extension using mean values of relative humidity, the modified equations incorporating this predictor had high classification ability and accuracy in both internal and external validations.

While model validation is the first step towards successful integrated disease management, another essential aspect is the adoption of the model by producers (Gent et al., 2013). SSR is one of the most critical yield-reducing diseases affecting soybeans in Québec. Producers are concerned because the disease impacts their current harvest and because epidemics increase the sclerotia load in the field, threatening future crops. Their past experiences with the disease coupled with their desire to prevent long-term consequences inform their decision-making behaviour. For example, in 2021, three surveyed sites were removed from the analyses since the producers had applied fungicides in the experimental plots. These anecdotes show the risk-averse behaviour of farmers and suggest that decision theory should be integrated into projects aimed at changing disease management practices (McRoberts et al., 2011, Gent et al., 2011).

This work's emphasis was largely on characterizing environmental conditions promoting *S. sclerotiorum* carpogenic germination in Québec soybean-producing regions. Describing disease development is not limited to inoculum production, but also involves multiple intricately linked crop and pathogen aspects. Additional research with a greater focus on the impact of agronomic factors and cultural practices such as row spacing, plant population, cultivar choice, fertilization at planting, and cover cropping on SSR is needed to provide further guidelines to producers.

Chapter 6: General conclusion

Conditions favourable to carpogenic germination occurring past the soybean susceptibility window limited SSR development in fields surveyed in Québec from 2019 to 2021. Observations like these highlight the importance of the disease triangle for infections to occur and stress the need for integrated risk-based, rather than calendar-based, SSR management programs. SSR is a sporadic disease, yet it is common for producers to use fungicides preventatively once or twice during the soybean flowering period to limit SSR, regardless of the risk of disease development (Faucher et al., 2017). Environmental and health concerns are driving governments to address sustainability challenges in agriculture. For example, in its 2020-2030 "Plan d'agriculture durable" the Québec Ministry of Agriculture, Fisheries and Food (MAPAQ) directly targets reducing pesticide use on Québec farms (MAPAQ, 2020). Cutting down on unnecessary use of fungicide applications can contribute to diminishing the negative environmental impacts of food production. To achieve these outcomes without compromising yield, Québec soybean producers need reliable tools such as adapted disease prediction models to manage the risks associated with irregular SSR development.

References

- AAFC 2006. Crop profile for soybean in Canada. *Agriréseau*. Ottawa: Agriculture and AgriFood Canada.
- Abawi, G. S. 1979. Epidemiology of diseases caused by *Sclerotinia* species. *Phytopathology*, 69 (8), 899-904.
- Abawi, G. S. & Grogan, R. G. 1975. Source of primary inoculum and effects of temperature and moisture on infection of beans by *Whetzelinia sclerotiorum*. *Phytopathology*, 65 (3), 300-309.
- Adams, P. B. 1979. Ecology of Sclerotinia species. Phytopathology, 69 (8), 896-899.
- Allen, T. W., Bradley, C. A., Sisson, A. J., Byamukama, E., Chilvers, M. I., Coker, C. M., Collins, A. A., Damicone, J. P., Dorrance, A. E., Dufault, N. S., Esker, P. D., Faske, T. R., Giesler, L. J., Grybauskas, A. P., Hershman, D. E., Hollier, C. A., Isakeit, T., Jardine, D. J., Kelly, H. M., Kemerait, R. C., Kleczewski, N. M., Koenning, S. R., Kurle, J. E., Malvick, D. K., Markell, S. G., Mehl, H. L., Mueller, D. S., Mueller, J. D., Mulrooney, R. P., Nelson, B. D., Newman, M. A., Osborne, L., Overstreet, C., Padgett, G. B., Phipps, P. M., Price, P. P., Sikora, E. J., Smith, D. L., Spurlock, T. N., Tande, C. A., Tenuta, A. U., Wise, K. A. & Wrather, J. A. 2017. Soybean yield loss estimates due to diseases in the United States and Ontario, Canada, from 2010 to 2014. *Plant Health Progress*, 18 (1), 19-27.
- Alves, K. S. & Del Ponte, E. M. 2021. Analysis and simulation of plant disease progress curves in R: introducing the epifitter package. *Phytopathology Research*, 3 (1), 1-3.
- Arahana, V. S., Graef, G. L., Specht, J. E., Steadman, J. R. & Eskridge, K. M. 2001. Identification of QTLs for resistance to *Sclerotinia sclerotiorum* in soybean. *Crop Science*, 41 (1), 180-188.
- Azen, R. & Traxel, N. 2009. Using dominance analysis to determine predictor importance in logistic regression. *Journal of Educational and Behavioral Statistics*, 34 (3), 319-347.
- Baazeem, A., Almanea, A., Manikandan, P., Alorabi, M., Vijayaraghavan, P. & Abdel-Hadi, A. 2021. In Vitro Antibacterial, Antifungal, Nematocidal and Growth Promoting Activities of Trichoderma hamatum FB10 and Its Secondary Metabolites. *Journal of Fungi*, 7 (5), 331.
- Bailey, K. L., Couture, L., Gossen, B. D., Gugel, R. K. & Morral, R. R. A. 2004. *Maladies des grandes cultures au Canada*, Saskatoon, SK, Canada, La Société Canadienne de phytopathologie, 171-185.
- Bamber, D. 1975. The area above the ordinal dominance graph and the area below the receiver operating characteristic graph. *Journal of Mathematical Psychology*, 12 (4), 387-415.
- Beck, H. E., Zimmermann, N. E., McVicar, T. R., Vergopolan, N., Berg, A. & Wood, E. F. 2018. Present and future Köppen-Geiger climate classification maps at 1-km resolution. *Scientific Data*, 5 (1), 180214.
- Bedi, K. Light, air and moisture in relation to the formation of apothecia of *Sclerotinia sclerotiorum* (Lib.) de Bary. *In:* SCIENCES, I. A. O., ed. Proceedings Section B, 1962. 213-223.
- Biggerstaff, B. J. 2000. Comparing diagnostic tests: a simple graphic using likelihood ratios. *Statistics in Medicine*, 19 (5), 649-663.
- Bipfubusa, M., Rioux, S., Copley, T., Olishevska, S., Tremblay, G. & Belzile, L. 2020. Évaluation de l'efficacité de quatre biofongicides dans la répression de la Sclérotinose (pourriture à sclérotes) dans la culture de soya. CÉROM.

- Boland, G. J. & Hall, R. 1994. Index of plant hosts of *Sclerotinia sclerotiorum*. Canadian Journal of Plant Pathology, 16 (2), 93-108.
- Bom, M. & Boland, G. J. 2000. Evaluation of disease forecasting variables for Sclerotinia stem rot (*Sclerotinia sclerotiorum*) of canola. *Canadian Journal of Plant Science*, 80 (4), 889-898.
- Bouchard, J. 2008. Épidémiologie et évaluation de systèmes prévisionnels comme outil de lutte raisonnée contre le blanc (Sphaerotheca macularis) chez le fraisier à jour neutre et conventionnel. Master Thesis, Université Laval, 36-60.
- Bourgeois, G., Beaudry, N., Plouffe, D., Chouinard, G., Audet, R. & Deaudelin, G. 2005. Forecasting pests in field crops using real-time weather information: The Cipra Network in Quebec. *Acta Horticulturae*, 674 303-304.
- Bradley, C. A., Allen, T. W., Sisson, A. J., Bergstrom, G. C., Bissonnette, K. M., Bond, J., Byamukama, E., Chilvers, M. I., Collins, A. A., Damicone, J. P. & Dorrance, A. E. 2021a. Soybean yield loss estimates due to diseases in the United States and Ontario, Canada, from 2015 to 2019. . *Plant Health Progress*, PHP-01.
- Bradley, C. A., Allen, T. W., Tenuta, A. U., Mehl, K. & Sisson, A. J. 2021b. *Soybean disease loss estimates from the United States and Ontario, Canada 2020* [Online]. Available: https://cropprotectionnetwork.org/resources/publications/soybean-disease-loss-estimates-from-the-united-states-and-ontario-canada-2020 [Accessed December 2 2021].
- Breault, J., Rioux, S. & Duval, B. 2017. *La pourriture à sclérote chez le soya* [Online]. Available: https://www.agrireseau.net/documents/Document_92969.pdf [Accessed October 17 2021].
- Bustos Navarrete, C. & Coutinho Soares, F. 2020. *Dominance Analysis* [Online]. Available: https://cran.r-project.org/web/packages/dominanceanalysis/dominanceanalysis.pdf [Accessed August 11 2021].
- Caesar, A. J. & Pearson, M. 1983. Environmental factors affecting survival of ascospores of *Sclerotinia sclerotiorum*. *Phytopathology*, 73 (7), 1024-1030.
- Carisse, O. & Fall, M. L. 2021. Decision trees to forecast risks of strawberry powdery mildew caused by *Podosphaera aphanis*. *Agriculture*, 11 (1), 29.
- Carisse, O., Tremblay, D. M. & Lefebvre, A. 2014. Comparison of *Botrytis cinerea* airborne inoculum progress curves from raspberry, strawberry and grape plantings. *Plant Pathology*, 63 (5), 983-993.
- Chun, D. 1987. Laboratory and field assessment of resistance in soybean to stem rot caused by *Sclerotinia sclerotiorum*. *Plant Disease*, 71 (9), 811-815.
- Clarkson, J. P., Fawcett, L., Anthony, S. G. & Young, C. 2014. A model for *Sclerotinia* sclerotiorum infection and disease development in lettuce, based on the effects of temperature, relative humidity and ascospore density. *PLoS ONE*, 9 (4), e94049.
- Clarkson, J. P., Phelps, K., Whipps, J. M., Young, C. S., Smith, J. A. & Watling, M. 2007. Forecasting *Sclerotinia* disease on lettuce: A predictive model for carpogenic germination of *Sclerotinia sclerotiorum* sclerotia. *Phytopathology*, 97 (5), 621-31.
- Clarkson, J. P., Staveley, J., Phelps, K., Young, C. S. & Whipps, J. M. 2003. Ascospore release and survival in *Sclerotinia sclerotiorum*. *Mycological Research*, 107 (2), 213-22.
- Cline, M. N. 1983. Methods for evaluating soybean cultivars for resistance to *Sclerotinia sclerotiorum*. *Plant Disease*, 67 (7), 784-786.
- Coley-Smith, J. & Cooke, R. 1971. Survival and germination of fungal sclerotia. *Annual Review of Phytopathology*, 9 (1), 65-92.

- Cook, G. E. 1975. Survival of *Whetzelinia sclerotiorum* and initial infection of dry edible beans in western Nebraska. *Phytopathology*, 65 (3), 250-255.
- Curtin, D., Dahly, D. L., Smeden, M., O'Donnell, D. P., Doyle, D., Gallagher, P. & O'Mahony, D. 2019. Predicting 1-year mortality in older hospitalized patients: external validation of the HOMR model. *Journal of the American Geriatrics Society*, 67 (7), 1478-1483.
- Davar, R., Darvishzadeh, R. & Jahanbakhsh-Godehkahriz, S. 2012. AWERProcedia information technology analysis of aggressiveness among isolates of *Sclerotinia sclerotiorum* from sunflower. *Global Journal on Technology*, 1 543-546.
- Del Rio, L. E., Martinson, C. A. & Yang, X. B. 2002. Biological control of Sclerotinia stem rot of soybean with *Sporidesmium sclerotivorum*. *Plant Disease*, 86 (9), 999-1004.
- DeLong, E. R., DeLong, D. M. & Clarke-Pearson, D. L. 1988. Comparing the areas under two or more correlated receiver operating characteristic curves: a nonparametric approach. *Biometrics*, 44 (3), 837-45.
- Dillard, H. R. 1995. Conditioning sclerotia of *Sclerotinia sclerotiorum* for carpogenic germination. *Plant Disease*, 79 411-415.
- Duan, Y.-B., Ge, C.-Y. & Zhou, M.-G. 2013. Molecular and biochemical characterization of *Sclerotinia sclerotiorum* laboratory mutants resistant to dicarboximide and phenylpyrrole fungicides. *Journal of Pest Science*, 87 (1), 221-230.
- Duncan, R. W., Dilantha Fernando, W. G. & Rashid, K. Y. 2006. Time and burial depth influencing the viability and bacterial colonization of sclerotia of Sclerotinia sclerotiorum. *Soil Biology and Biochemistry*, 38 (2), 275-284.
- Fall, M. L., Boyse, J. F., Wang, D., Willbur, J. F., Smith, D. L. & Chilvers, M. I. 2018a. Case study of an epidemiological approach dissecting historical soybean Sclerotinia stem rot observations and identifying environmental predictors of epidemics and yield loss. *Phytopathology*, 108 (4), 469-478.
- Fall, M. L. & Carisse, O. 2022. Dynamic simulation for predicting warning and action thresholds: A novelty for strawberry powdery mildew management. *Agricultural and Forest Meteorology*, 312 108711.
- Fall, M. L., Willbur, J. F., Smith, D. L., Byrne, A. M. & Chilvers, M. I. 2018b. Spatiotemporal distribution pattern of *Sclerotinia sclerotiorum* apothecia is modulated by canopy closure and soil temperature in an irrigated soybean field. *Plant Disease*, 102 (9), 1794-1802.
- Faucher, Y., Mathieu, S., Frechette, L., G & Samson, V. 2017. Avons-nous besoin de fongicides pour le soya au Quebec? *Reseau d'Avertissements Phytosanitaires* [Online]. Available: https://www.agrireseau.net/documents/Document_95753.pdf [Accessed February 8 2020].
- Fehr, W. & Caviness, C. 1977. Stages of soybean development. Special Report.
- Foley, M., Dogramaci, M., West, M. & Underwood, W. 2016. Environmental factors for germination of *Sclerotinia sclerotiorum* sclerotia. *Journal of Plant Pathology and Microbiology*, 7 2157-7471.
- Foster, A. J., Kora, C., McDonald, M. R. & Boland, G. J. 2011. Development and validation of a disease forecast model for Sclerotinia rot of carrot. *Canadian Journal of Plant Pathology*, 33 (2), 187-201.
- Garza, J. A. G., Neumann, S., Vyn, T. J. & Boland, G. J. 2002. Influence of crop rotation and tillage on production of apothecia by *Sclerotinia sclerotiorum*. *Canadian Journal of Plant Pathology*, 24 (2), 137-143.

- Gbur, E. E., Stroup, W. W., McCarter, K. S., Durham, S., Young, L. J., Christman, M., West, M. & Kramer, M. 2012. *Analysis of Generalized Linear Mixed Models in the agricultural and natural resources sciences*, Madison WI, 109-184., American Society of Agronomy, Crop Science Society of America, and Soil Science Society of America, 109-184.
- Gent, D. H., De Wolf, E. & Pethybridge, S. J. 2011. Perceptions of risk, risk aversion, and barriers to adoption of decision support systems and integrated pest management: an introduction. *Phytopathology*, 101 (6), 640-3.
- Gent, D. H., Mahaffee, W. F., McRoberts, N. & Pfender, W. 2013. The use and role of predictive systems in disease management. *Annual Review of Phytopathology*, 51 267-289.
- Giroux, M. E., Bourgeois, G., Dion, Y., Rioux, S., Pageau, D., Zoghlami, S., Parent, C., Vachon, E. & Vanasse, A. 2016. Evaluation of forecasting models for Fusarium head blight of wheat under growing conditions of Quebec, Canada. *Plant Disease*, 100 (6), 1192-1201.
- Grau, C. R. 1984. Effects of cultivars and cultural practices on Sclerotinia stem rot of soybean. *Plant Disease*, 68 (1), 56-58.
- Grau, C. R., Radke, V. L. & Gillespie, F. L. 1982. Resistance of soybean cultivars to *Sclerotinia* sclerotiorum. Plant Disease, 66 (1), 506-508.
- Guimaraes, R. L. & Stotz, H. U. 2004. Oxalate production by *Sclerotinia sclerotiorum* deregulates guard cells during infection. *Plant Physiology*, 136 (3), 3703-11.
- Guo, X., Wang, D., Gordon, S. G., Helliwell, E., Smith, T., Berry, S. A., St. Martin, S. K. & Dorrance, A. E. 2008. Genetic mapping of QTLs underlying partial resistance to in soybean PI 391589A and PI 391589B. *Crop Science*, 48 (3), 1129-1139.
- Hanley, J. A. & McNeil, B. J. 1982. The meaning and use of the area under a receiver operating characteristic (ROC) curve. *Radiology*, 143 (1), 29-36.
- Hannusch, D. J. & Boland, G. 1996. Influence of air temperature and relative humidity on biological control of white mold of bean (*Sclerotinia sclerotiorum*). *Phytopathology*, 86 156-162.
- Harikrishnan, R. & del Río, L. E. 2008. A logistic regression model for predicting risk of white mold incidence on dry bean in North Dakota. *Plant Disease*, 92 (1), 42-46.
- Hartman, G., Rupe, L., Sikora, C., Domier, L., Davis, J. & Steffey, K. 2015. *Compendium of soybean diseases and pests*, St-Paul MN, 167-173, American Phytopathological Society, 167-173.
- Harvey, I. 1999. *In:* PASTURES., L. H. O. S. S. I. R. T. I. U. A. A. M. T. C. C. A. I. (ed.). Lincoln, New Zealand.
- Henson, J. M., Butler, M. J. & Day, A. W. 1999. The dark side of the mycelium: melanins of phytopathogenic fungi. *Annual Review of Phytopathology*, 37 (1), 447-471.
- Hjelkrem, A.-G. R., Eikemo, H., Le, V. H., Hermansen, A. & Nærstad, R. 2021. A process-based model to forecast risk of potato late blight in Norway (The Nærstad model): model development, sensitivity analysis and Bayesian calibration. *Ecological Modelling*, 450 1-10.
- Huang, H. C., Chang, C. & Kozub, G. C. 1998. Effect of temperature during sclerotial formation, sclerotial dryness, and relative humidity on myceliogenic germination of sclerotia of *Sclerotinia sclerotiorum*. *Canadian Journal of Botany*, 76 (3), 494-499.
- Hughes, G., McRoberts, N. & Burnett, F. J. 1999. Decision making and diagnosis in disease management. *Plant Pathology*, 48 (2), 147-153.

- Humpherson-Jones, F. & Cooke, R. 1977. Morphogenesis in sclerotium-forming fungi. II Rhytmic production of sclerotia by *Sclerotinia sclerotiorum* (Lib.) de Bary. *New Phytologist*, 78 (1), 181-187.
- Huzar-Novakowiski, J. & Dorrance, A. E. 2018. Ascospore inoculum density and characterization of components of partial resistance to *Sclerotinia sclerotiorum* in soybean. *Plant Disease*, 102 (7), 1326-1333.
- Imolehin, E. D. 1980. Effect of temperature and moisture tension on growth, sclerotial production, germination, and infection by *Sclerotinia minor*. *Phytopathology*, 70 (12), 1153-1157.
- Janssen, K. J., Moons, K. G., Kalkman, C. J., Grobbee, D. E. & Vergouwe, Y. 2008. Updating methods improved the performance of a clinical prediction model in new patients. *Journal of Clinical Epidemiology*, 61 (1), 76-86.
- Kim, H. S. & Diers, B. W. 2000. Inheritance of partial resistance to Sclerotinia stem rot in soybean. *Crop Science*, 40 (1), 55-61.
- Koch, S., Dunker, S., Kleinhenz, B., Rohrig, M. & Tiedemann, A. 2007. A crop loss-related forecasting model for Sclerotinia stem rot in winter oilseed rape. *Phytopathology*, 97 (9), 1186-1194.
- Kuhn, M. 2011. *The caret package* [Online]. Available: http://cran.r-project.org/web/packages/caret/vignettes/caretTrain.pdf [Accessed October 15 2021].
- Kurle, J. E., Grau, C. R., Oplinger, E. S. & Mengistu, A. 2001. Tillage, crop sequence, and cultivar effects on Sclerotinia stem rot incidence and yield in soybean. *Agronomy Journal*, 93 (5), 973-982.
- Landau, S., Mitchell, R. A. C., Barnett, V., Colls, J. J., Craigon, J. & Payne, R. W. 2000. A parsimonious, multiple-regression model of wheat yield response to environment. *Agricultural and Forest Meteorology*, 101 (2-3), 151-166.
- Lane, D., Denton-Giles, M., Derbyshire, M. & Kamphuis, L. G. 2019. Abiotic conditions governing the myceliogenic germination of *Sclerotinia sclerotiorum* allowing the basal infection of *Brassica napus*. *Australasian Plant Pathology*, 48 (2), 85-91.
- Le Tourneau, D. 1979. Morphology, cytology, and physiology of *Sclerotinia* species in culture. *Phytopathology*, 69 (8), 887-890.
- Lee, C. D., Renner, K. A., Penner, D., Hammerschmidt, R. & Kelly, J. D. 2005. Glyphosate-resistant soybean management system effect on Sclerotinia stem rot. *Weed Technology*, 19 (3), 580-588.
- Li, D.-W. & Kendrick, B. 1994. Functional relationships between airborne fungal spores and environmental factors in Kitchener-Waterloo, Ontario, as detected by Canonical correspondence analysis. *Grana*, 33 (3), 166-176.
- Li, M. & Rollins, J. A. 2009. The development-specific protein (Ssp1) from *Sclerotinia* sclerotiorum is encoded by a novel gene expressed exclusively in sclerotium tissues. *Mycologia*, 101 (1), 34-43.
- Madden, L. V. 2006. Botanical epidemiology: some key advances and its continuing role in disease management. *European Journal of Plant Pathology*, 115 (1), 3-23.
- Manubens, N., Caron, L.-P., Hunter, A., Bellprat, O., Exarchou, E., Fučkar, N. S., Garcia-Serrano, J., Massonnet, F., Ménégoz, M., Sicardi, V., Batté, L., Prodhomme, C., Torralba, V., Cortesi, N., Mula-Valls, O., Serradell, K., Guemas, V. & Doblas-Reyes, F. J. 2018. An R package for climate forecast verification. *Environmental Modelling & Software*, 103 29-42.

- MAPAQ. 2020. Plan d'agriculture durable 2020-2030. Available:

 https://www.quebec.ca/gouv/politiques-orientations/politique-bioalimentaire/agriculture-durable [Accessed October 15 2021].
- Marukawa, S., Funakawa, S. & Satomura, Y. 2014. Some physical and chemical factors on formation of sclerotia in *Sclerotinia libertiana* Fuckel. *Agricultural and Biological Chemistry*, 39 (2), 463-468.
- Matheron, M. E. & Porchas, M. 2005. Influence of soil temperature and moisture on eruptive germination and viability of sclerotia of *Sclerotinia minor* and *S. sclerotiorum*. *Plant Disease*, 89 (1), 50-54.
- McCaghey, M., Willbur, J., Ranjan, A., Grau, C. R., Chapman, S., Diers, B., Groves, C., Kabbage, M. & Smith, D. L. 2017. Development and evaluation of *Glycine max* germplasm lines with quantitative resistance to *Sclerotinia sclerotiorum*. *Frontiers in Plant Science*, 8 1-13.
- McRoberts, N., Hall, C., Madden, L. V. & Hughes, G. 2011. Perceptions of disease risk: from social construction of subjective judgments to rational decision making. *Phytopathology*, 101 (6), 654-665.
- MELCC. 2020. Juillet 2020: le mois le plus chaud en au moins 100 ans au Québec, la sécheresse se poursuit [Online]. Available:

 https://www.environnement.gouv.qc.ca/climat/Faits-saillants/2020/juillet.htm [Accessed December 10 2020].
- MELCC. 2021a. Changements Climatiques: Faits saillants [Online]. Gouvernement du Québec Available: https://www.environnement.gouv.qc.ca/climat/Faits-saillants/index.htm [Accessed October 29 2021].
- MELCC. 2021b. *Normales climatiques 1981-2010* [Online]. Gouvernement du Québec. Available: https://www.environnement.gouv.qc.ca/climat/normales/climat-qc.htm [Accessed November 25 2021].
- Meno, L., Escuredo, O., Rodríguez-Flores, M. S. & Seijo, M. C. 2020. Modification of the TOMCAST model with aerobiological data for management of potato early blight. *Agronomy*, 10 (12), 1872.
- Metz, C. E. 1978. Basic principles of ROC analysis. Seminars in Nuclear Medicine, 8 (4), 283-98.
- Mila, A. L., Carriquiry, A. L. & Yang, X. B. 2004. Logistic regression modeling of prevalence of soybean Sclerotinia stem rot in the north-central region of the United States. *Phytopathology*, 94 (1), 102-110.
- Moons, K. G., Kengne, A. P., Grobbee, D. E., Royston, P., Vergouwe, Y., Altman, D. G. & Woodward, M. 2012. Risk prediction models: II. External validation, model updating, and impact assessment. *Heart*, 98 (9), 691-698.
- Moore, W. D. 1949. Flooding as a means of destroying the sclerotia of *Sclerotinia sclerotiorum*. *Phytopathology*, 39 (11), 920-927.
- Mueller, D. S., Bradley, C. A., Grau, C. R., Gaska, J. M., Kurle, J. E. & Pedersen, W. L. 2004. Application of thiophanate-methyl at different host growth stages for management of Sclerotinia stem rot in soybean. *Crop Protection*, 23 (10), 983-988.
- Mueller, D. S., Dorrance, A. E., Derksen, R. C., Ozkan, E., Kurle, J. E., Grau, C. R., Gaska, J. M., Hartman, G. L., Bradley, C. A. & Pedersen, W. L. 2002. Efficacy of fungicides on *Sclerotinia sclerotiorum* and their potential for control of Sclerotinia stem rot on soybean. *Plant Disease*, 86 (1), 26-31.

- Nelson, K. A., Renner, K. A. & Hammerschmidt, R. A. Y. 2002. Effects of protoporphyrinogen oxidase inhibitors on soybean (*Glycine max* L.) response, *Sclerotinia sclerotiorum* disease development, and phytoalexin production by soybean. *Weed Technology*, 16 (2), 353-359.
- Newton, H. & Sequeira, L. 1972. Ascospores as the primary infective propagule of *Sclerotinia* sclerotiorum in Wisconsin. *Plant Disease Reporter*, 56 (9), 798-802.
- Oleo Quebec 2019. Comparaison des cultivars. Oleo Quebec.
- OMAFRA. 2017. Agronomy guide for field crops. *Ministry of Agriculture Food and Rural Affairs* [Online]. Available: http://www.omafra.gov.on.ca/english/crops/pub811/pub811.pdf [Accessed June 6 2021].
- Onofri, A., Piepho, H.-P. & Kozak, M. 2019. Analysing censored data in agricultural research: A review with examples and software tips. *Annals of Applied Biology*, 174 (1), 3-13.
- Peltier, A. J., Bradley, C. A., Chilvers, M. I., Malvick, D. K., Mueller, D. S., Wise, K. A. & Esker, P. D. 2012. Biology, yield loss and control of Sclerotinia stem rot of soybean. *Journal of Integrated Pest Management*, 3 (2), 1-7.
- Pethybridge, S. J., Brown, B. J., Kikkert, J. R. & Ryan, M. R. 2020. Rolled–crimped cereal rye residue suppresses white mold in no-till soybean and dry bean. *Renewable Agriculture and Food Systems*, 35 (6), 599-607.
- Phillips, A. J. L. 1986. Carpogenic germination of sclerotia of *Sclerotinia sclerotiorum* after periods of conditioning in soil. *Journal of Phytopathology*, 116 (3), 247-258.
- Ping, J., Liu, Y., Sun, L., Zhao, M., Li, Y., She, M., Sui, Y., Lin, F., Liu, X., Tang, Z., Nguyen, H., Tian, Z., Qiu, L., Nelson, R. L., Clemente, T. E., Specht, J. E. & Ma, J. 2014. Dt2 is a gain-of-function MADS-domain factor gene that specifies semideterminacy in soybean. *Plant Cell*, 26 (7), 2831-2842.
- R Core Team 2021. R: A language and environment for statistical computing.: R Foundation for Statistical Computing.
- Raynal, G. 1990. Kinetics of the ascospore production of *Sclerotinia trifoliorum* (Eriks) in growth chamber and under natural climatic conditions practical and epidemiologic incidence. *Agronomie*, 10 (7), 561-572.
- Ritz, C., Baty, F., Streibig, J. C. & Gerhard, D. 2015. Dose-Response analysis using R. *PLoS One*, 10 (12), e0146021.
- Robin, X., Turck, N., Hainard, A., Tiberti, N., Lisacek, F., Sanchez, J. C. & Muller, M. 2011. pROC: an open-source package for R and S+ to analyze and compare ROC curves. *BMC Bioinformatics*, 12 77.
- Rothman, L. & McLaren, N. 2018. *Sclerotinia sclerotiorum* disease prediction: A review and potential applications in South Africa. *South African Journal of Science*, 114 (3-4), 1-9.
- Rousseau, G., Huynh Thanh, T., Dostaler, D. & Rioux, S. 2004. Greenhouse and field assessments of resistance in soybean inoculated with sclerotia, mycelium, and ascospores of *Sclerotinia sclerotiorum*. *Canadian Journal of Plant Science*, 84 (2), 615-623.
- Rousseau, G., Rioux, S. & Dostaler, D. 2007. Effect of crop rotation and soil amendments on Sclerotinia stem rot on soybean in two soils. *Canadian Journal of Plant Science*, 87 (3), 605-614.
- SAgE Pesticides. 2020. *Traitements phytosanitaires et risques associes* [Online]. Available: https://www.sagepesticides.qc.ca/Recherche/Resultats?clang=fr&cu=Soya&cid=51&elang=fr&tt=5&e1=1525%3F2&ta=1&pc=6&p=1 [Accessed April 5 2021].

- Saharan, G. & Mehta, N. 2008. Sclerotinia diseases of crop plants: Biology, ecology and disease management, Springer Science & Business Media, 1-485.
- Scherm, H. & Ojiambo, P. S. 2004. Applications of Survival Analysis in Botanical Epidemiology. *Phytopathology*, 94 (9), 1022-1026.
- Singh, G. 2010. The soybean: botany, production and uses, CABI, 276-299.
- Small, I. M., Joseph, L. & Fry, W. E. 2015. Development and implementation of the BlightPro decision support system for potato and tomato late blight management. *Computers and Electronics in Agriculture*, 115 57-65.
- Solutions Mesonet 2021. Agrométéo Québec 2.0. 2021 ed. Québec.
- Statistics Canada 2021. Estimated areas, yield, production, average farm price and total farm value of principal field crops, in metric and imperial units. *In:* CANADA, S. (ed.). Ottawa, Ontario.
- Steyerberg, E. W. 2019. Updating for a New Setting. *Clinical Prediction Models*. Springer, Cham, 399-429.
- Steyerberg, E. W., Borsboom, G. J., van Houwelingen, H. C., Eijkemans, M. J. & Habbema, J. D. 2004. Validation and updating of predictive logistic regression models: a study on sample size and shrinkage. *Statistics in Medicine*, 23 (16), 2567-2586.
- Steyerberg, E. W. & Vergouwe, Y. 2014. Towards better clinical prediction models: seven steps for development and an ABCD for validation. *European Heart Journal*, 35 (29), 1925-1931.
- Sun, P. & Yang, X. B. 2000. Light, temperature, and moisture effects on apothecium production of *Sclerotinia sclerotiorum*. *Plant Disease*, 84 (12), 1287-1293.
- Swets, J. A. 1979. ROC analysis applied to the evaluation of medical imaging techniques. *Investigative Radiology*, 14 (2), 109-121.
- Torés, J. A. & Moreno, R. 1991. *Sclerotinia sclerotiorum*: epidemiological factors affecting infection of greenhouse aubergine crops. *Journal of Phytopathology*, 132 (1), 65-74.
- Tremblay, G., Maisonhaute, J. E., Rioux, S. & Faucher, Y. 2016. Utilisation des fongicides foliaires en grandes cultures. Saint-Mathieu-de-Beloeil: CÉROM.
- Tremblay, N., Bouroubi, Y. M., Bélec, C., Mullen, R. W., Kitchen, N. R., Thomason, W. E., Ebelhar, S., Mengel, D. B., Raun, W. R., Francis, D. D., Vories, E. D. & Ortiz-Monasterio, I. 2012. Corn response to nitrogen is influenced by soil texture and weather. *Agronomy Journal*, 104 (6), 1658-1671.
- Turkington, T. K. 1993. Use of petal infestation to forecast Sclerotinia stem rot of canola: the influence of inoculum variation over the flowering period and canopy density. *Phytopathology*, 83 (6), 682-689.
- Twengström, E., Sigvald, R., Svensson, C. & Yuen, J. 1998. Forecasting Sclerotinia stem rot in spring sown oilseed rape. *Crop Protection*, 17 (5), 405-411.
- Van Calster, B., McLernon, D. J., van Smeden, M., Wynants, L. & Steyerberg, E. W. 2019. Calibration: the Achilles heel of predictive analytics. *BMC Medicine*, 17 (1), 1-7.
- Vega, R. R. & Le Tourneau, D. 1974. The effect of Zinc on growth and sclerotial formation in *Whetzelinia sclerotiorum Mycologia*, 66 (2), 256-264.
- Vuong, T. D., Diers, B. W. & Hartman, G. L. 2008. Identification of QTL for resistance to Sclerotinia stem rot in soybean plant introduction 194639. *Crop Science*, 48 (6), 2209-2214.

- Wang, H., Sanchez-Molina, J. A., Li, M. & Berenguel, M. 2020. Development of an empirical tomato crop disease model: a case study on gray leaf spot. *European Journal of Plant Pathology*, 156 (2), 477-490.
- Wang, S. Y. & Le Tourneau, D. 1972. Trehalase from *Sclerotinia sclerotiorum*. *Archives of Microbiology*, 87 (3), 235-241.
- Wegulo, S. N., Sun, P., Martinson, C. A. & Yang, X. B. 2000. Spread of Sclerotinia stem rot of soybean from area and point sources of apothecial inoculum. *Canadian Journal of Plant Science*, 80 (2), 389-402.
- Willbur, J., McCaghey, M., Kabbage, M. & Smith, D. L. 2018a. An overview of the *Sclerotinia sclerotiorum* pathosystem in soybean: impact, fungal biology, and current management strategies. *Tropical Plant Pathology*, 44 (1), 3-11.
- Willbur, J. F., Fall, M. L., Bloomingdale, C., Byrne, A. M., Chapman, S. A., Isard, S. A., Magarey, R. D., McCaghey, M. M., Mueller, B. D., Russo, J. M., Schlegel, J., Chilvers, M. I., Mueller, D. S., Kabbage, M. & Smith, D. L. 2018b. Weather-based models for assessing the risk of *Sclerotinia sclerotiorum* apothecial presence in soybean (*Glycine max*) fields. *Plant Disease*, 102 (1), 73-84.
- Willbur, J. F., Fall, M. L., Byrne, A. M., Chapman, S. A., McCaghey, M. M., Mueller, B. D., Schmidt, R., Chilvers, M. I., Mueller, D. S., Kabbage, M., Giesler, L. J., Conley, S. P. & Smith, D. L. 2018c. Validating *Sclerotinia sclerotiorum* apothecial models to predict Sclerotinia stem rot in soybean (*Glycine max*) fields. *Plant Disease*, 102 (12), 2592-2601.
- Willbur, J. F., Mitchell, P. D., Fall, M. L., Byrne, A. M., Chapman, S. A., Floyd, C. M., Bradley, C. A., Ames, K. A., Chilvers, M. I., Kleczewski, N. M., Malvick, D. K., Mueller, B. D., Mueller, D. S., Kabbage, M., Conley, S. P. & Smith, D. L. 2019. Meta-analytic and economic approaches for evaluation of pesticide impact on Sclerotinia stem rot control and soybean yield in the north central United States. *Phytopathology*, 109 (7), 1157-1170.
- Willetts, H. J. & Wong, J. A. L. 1980. The biology of *Sclerotinia sclerotiorum*, *S. trifoliorum*, and *S. minor* with emphasis on specific nomenclature. *The Botanical Review*, 46 (2), 101-165.
- Williams, G. & Western, J. 1965. The biology of *Sclerotinia trifoliorum* Erikss and other species of sclerotiorum-forming fungi. *Annals of Applied Biology*, 56 (2), 261-268.
- Workneh, F. & Yang, X. B. 2000. Prevalence of Sclerotinia stem rot of soybeans in the north-central United States in relation to tillage, climate, and latitudinal positions. *Phytopathology*, 90 (12), 1375-1382.
- Wu, B. M. & Subbarao, K. V. 2008. Effects of soil temperature, moisture, and burial depths on carpogenic germination of *Sclerotinia sclerotiorum* and *S. minor. Phytopathology*, 98 (10), 1144-1152.
- Youden, W. J. 1950. Index for rating diagnostic tests. Cancer, 3 (1), 32-35.
- Young, C. S., Clarkson, J. P., Smith, J. A., Watling, M., Phelps, K. & Whipps, J. M. 2004. Environmental conditions influencing *Sclerotinia sclerotiorum* infection and disease development in lettuce. *Plant Pathology*, 53 (4), 387-397.
- Yuen, J. E. & Hughes, G. 2002. Bayesian analysis of plant disease prediction. *Plant Pathology*, 51 (4), 407-412.
- Zeng, W., Kirk, W. & Hao, J. 2012. Field management of Sclerotinia stem rot of soybean using biological control agents. *Biological Control*, 60 (2), 141-147.
- Zimmer, R. C. 1978. Downy mildew, a new disease of buckwheat (*Fagopyrum Esculentum*) in Manitoba, Canada. *Plant Disease Reporter*, 62 (6), 471-473.

Appendix 1 - Tables

Table A. 1 Soybean development stages (adapted from Fehr and Caviness 1977).

Stage	Abbreviated stage	Description
	title	
VE	Emergence	Cotyledons above the soil surface.
VC	Cotyledon	Unifoliolate leaves unrolled sufficiently so the leaf edges are
		not touching.
V1	First-node	Fully developed leaves at unifoliolate nodes.
V2	Second-node	Fully developed trifoliolate leaf at node above the unifoliolate
		nodes.
V3	Third-node	Three nodes on the main steam with fully developed leaves
		beginning with the unifoliolate nodes.
V(n)	Nth-node	n number of nodes on the main stem with fully developed
		leaves beginning with the unifoliolate nodes. n can be any
		number beginning with 1 for V1, first-node stage.
R1	Beginning bloom	One open flower at any node on the main stem.
R2	Full bloom	Open flower at one of the two uppermost nodes on the main
		stem with a fully developed leaf.
R3	Beginning pod	Pod 5 mm (3/16 inch) long at one of the four uppermost nodes
		on the main stem with a fully developed leaf
R4	Full pod	Pod 2 cm (3/4 inch) long at one of the four uppermost nodes
		on the main stem with a fully developed leaf.
R5	Beginning seed	Seed 3 mm (1/8 inch) long in a pod at one of the four
		uppermost nodes on the main stem with a fully developed leaf.
R6	Full seed	Pod containing a green seed that fills the pod cavity at one of
		the four uppermost nodes on the main stem with a fully
		developed leaf.
R7	Beginning maturity	One normal pod on the main stem that has reached its mature
		pod color.
	I	

Table A.1 Soybean development stages (adapted from Fehr and Caviness 1977) (cont'd).

Stage	Abbreviated	stage	Description
	title		
R8	Full maturity		Ninety-five percent of the pods that have reached their mature
			pod color. Five to ten days of drying weather are required after
			R8 before the soybeans have less than 15 percent moisture.

Table A. 2 Active substance in pesticides used to control Sclerotinia stem rot of soybean commercially available in Québec (SAgE Pesticides, 2020).

Active Substance	Class	Commercial Products
Azoxystrobine	11	Miravis Neo, Quilt, Top Notch, Trivapro A
Bacillus amyloliquefaciens	N/A	Double Nickel 55 and LC, Stargus
strains D747 and F727		
Bacillus subtilis strain QSR	N/A	QST713 Liquid, Serenade Aso, CPb, Max and Opti
713		
Boscalid	7	Cotegra
Coniothyrium minitans strain	N/A	Contans WG
CON/M/91-08		
Fluazinam	29	Allegro 500F
Fluopyram	7	Luna Privilege
Fluxapyroxade	7	Xemium EC and SC, Acapela,
Picoxystrobine	11	Priaxor, Pyr Flu Form 1, Cerefit A
Propiconazole	3	Miravis Neo, Quilt, Top Nutch, Trivapro A
Prothioconazole	3	Stratego Pro, USF0728 325 SC, Cotegra
Pydiflumetofene	7	A19649, Miravis Neo
Pyraclostrobine	11	Priaxor, Pyr Flu Form 1
Reynoutria sachalinensis	P	Regalia Rx
Trifloxystrobine	11	Stratego Pro, USF0728 325 SC

N/A: classification non applicable (biological control). The class numbers 3, 7, 11, 29 and letter P are modes of action associated with the pesticide active substances (Table A. 3).

Table A. 3 Modes of action of fungicide active substances by FRAC group number (SAgE Pesticides, 2020)

Class	Mode of Action
3	Inhibition of demethylation at the sterol biosynthesis stage
	Inhibition of cell respiration and energy production and inhibition of
7	succinate dehydrogenase (SDH, complex II) in the mitochondrial electron
	transport chain.
	Inhibition of the mitochondrial respiratory chain at the complexe III
11	(ubiquinol-cytochrome c reductase) and inhibition of Qol (ubiquinol
	oxidation site) of bc1 cytochrome.
20	Decoupling of oxidative phosphorylation (disturbance of the establishment
29	of the H + gradient).
P	Plant defense simulator

Table A. 4 Soybean sowing date and cultivar for experimental sites in Québec from 2019 to 2021.

Code_site	Sowing date	Cultivar	SSR	Agrometeo	Distance
			Rating ¹	Station	(km)
CÉROM_2019	2019-05-29	P09A53X	NA	Saint-Hilaire ²	9.14
CÉROM_2020	NA	P09A53X	NA	Saint-Hilaire ²	9.14
CÉROM_2021	2021-06-01	P09A53X	NA	Saint-Hilaire ²	9.14
CHA1_2019	2019-06-06	P00A75X	NA	Saint-Bernard	12.23
CHA1_2020	2020-05-17	P06A13R	NA	Saint-Bernard	11.52
CHA1_2021	2021-05-10	A13	NA	Saint-Bernard	11.54
CHA2_2019	2019-05-22	Corus IP	NA	Saint-Bernard	16.13
CHA2_2020	2020-05-21	Podaga R2	NA	Saint-Bernard	17.10
CN1_2019	2019-05-16	NA	NA	Saint-Léonard-	4.19
				de-Portneuf	
CN1_2020	2020-05-09	Bravent B0	NA	Deschambault	0.49
		39Y1		SM	

Table A. 4 Soybean sowing date and cultivar for experimental sites in Québec from 2019 to 2021 (cont'd).

Code_site	Sowing date	Cultivar	SSR	Agrometeo Station	Distance
			Rating ¹		(km)
CN1_2021	NA	Salto	2.3	Deschambault SM	0.25
CN2_2020	2020-05-17	Hydra R2	3	Saint-Léonard-de-	17.59
				Portneuf	
CN2_2021	2021-05-05	Hydra R2	3	Saint-Léonard-de-	16.54
				Portneuf	
CQ1_2019	2019-05-22	Marula	1.5	Nicolet	11.05
CQ1_2020	2020-05-13	Altitude R2	1.2	Princeville	0.20
CQ1_2021	2021-05-09	Marula	1.5	Nicolet	11.18
CQ2_2020	2020-05-07	Marula	1.5	Nicolet	6.85
CQ2_2021	2021-05-16	Altitude R2	1.2	Inverness	8.13
ES1_2019	2019-05-27	На	1.4	Stanstead	7.15
ES1_2020	2020-05-08	Salto	2.3	Saint-Georges-de-	11.71
				Windsor	
ES1_2021	NA	S04-D3	3.1	Melbourne	12.08
ES2_2020	2020-05-14	Elite Chiba	NA	Melbourne	8.33
ES2_2021	NA	Fresco 2RX	NA	Saint-Georges-de-	7.15
				Windsor	
IRDA_2019	2019-06-17	Kendo R2	4.2	Saint-Bernard ²	4.49
IRDA_2020	NA	Kendo R2	4.2	Saint-Bernard ²	4.49
IRDA_2021	NA	Kendo R2	4.2	Saint-Bernard ²	4.49
LAN1_2019	2019-05-26	Pro seed	NA	L'Assomption	2.00
		H503RT33			
LAN1_2020	2020-04-29	Calypso	NA	Saint-Jacques	2.71
LAN1_2021	2021-05-14	AAC Corylis	NA	Saint-Jacques	1.56
LAN2_2019	2019-05-08	Calypso	NA	Saint-Jacques	2.77
LAN2_2020	2020-05-05	S04-D3	3.1	Lanoraie	14.34
LAN2_2021	2021-05-24	P2712	NA	Saint-Jacques	9.97

Table A. 4 Soybean sowing date and cultivar for experimental sites in Québec from 2019 to 2021 (cont'd).

(cont'd). Code_site	Sowing date	Cultivar	SSR	Agrometeo Station	Distance
			Rating ¹		(km)
LAU1_2019	2019-05-22	Dekalb 2510	NA	Mont-Laurier F ²	14.16
LAU1_2020	2020-05-13	Podaga R2	NA	Mont-Laurier F ²	12.17
LAU1_2021	2021-05-31	Akras R2	NA	Mont-Laurier F ²	11.90
LAVAL_2019	NA	Kendo R2	4.2	Saint-Antoine-de-	2.56
				Tilly ²	
LAVAL_2020	NA	Kendo R2	4.2	Saint-Antoine-de-	2.56
				Tilly ²	
LAVAL_2021	NA	Kendo R2	4.2	Saint-Antoine-de-	2.56
				Tilly ²	
MAU1_2019	NA	Marula	1.5	Saint-Barnabé	8.62
MAU1_2020	NA	NA	NA	Saint-Barnabé	8.55
MAU1_2021	2021-05-10	Myco Progres	NA	Saint-Barnabé ²	2.05
MCGILL_201	2019-05-23	P09A53X	NA	Sainte-Anne-de-	0.73
9				Bellevue	
MCGILL_202	2020-05-27	P09A53X	NA	Sainte-Anne-de-	0.73
0				Bellevue	
MCGILL_202	2021-05-18	P09A53X	NA	Sainte-Anne-de-	0.73
1				Bellevue	
ME1_2019	2019-05-19	NA	NA	Calixa-Lavallée	9.39
ME1_2020	2020-05-13	PS1162	2.3	Saint-Paul-	10.03
				d'Abbotsford	
ME1_2021	2021-05-16	P05A35X	NA	Saint-Hilaire	12.16
ME2_2019	2019-05-30	Zana	1.2	Saint-Paul-	10.32
				d'Abbotsford	
ME2_2020	2020-05-11	P05T80	NA	Saint-Hilaire	12.77
ME3_2019	2019-06-05	Dekalb 2815	NA	Saint-Grégoire	10.39
ME3_2020	2020-05-05	NK 07M8	NA	Calixa-Lavallée	13.34

Table A. 4 Soybean sowing date and cultivar for experimental sites in Québec from 2019 to 2021 (cont'd).

Sowing date	Cultivar	SSR	Agrometeo Station	Distance
		Rating ¹		(km)
2021-05-11	NA	NA	Rougemont	3.40
2019-05-25	Cara	NA	Rougemont	10.82
2020-05-11	Dekalb 2815	NA	Saint-Grégoire	9.77
2019-05-19	Acora	1.7	Saint-Hilaire	10.94
2020-05-13	NK S09R8X	NA	Saint-Hilaire	11.13
2021-05-08	Ezra	NA	Rougemont	10.07
2019-05-19	Natto	NA	Saint-Hilaire	11.67
2019-06-13	Calypso	NA	Hemmingford	10.83
2020-05-25	AAC Corylis	NA	Hemmingford	10.91
NA	NA	NA	Hemmingford	10.83
NA	Katonda	1.5	Hemmingford	10.83
2020-06-04	09A62	NA	Hemmingford	10.83
NA	NA	NA	Hemmingford	10.83
2020-06-05	Ajico	0.9	Hemmingford	10.83
NA	NA	NA	Hemmingford	10.83
2019-06-10	Katonda	1.5	Masson	3.28
	2021-05-11 2019-05-25 2020-05-11 2019-05-19 2020-05-13 2021-05-08 2019-06-13 2020-05-25 NA NA 2020-06-04 NA 2020-06-05 NA	2021-05-11 NA 2019-05-25 Cara 2020-05-11 Dekalb 2815 2019-05-19 Acora 2020-05-13 NK S09R8X 2021-05-08 Ezra 2019-05-19 Natto 2019-06-13 Calypso 2020-05-25 AAC Corylis NA NA Katonda 2020-06-04 09A62 NA NA 2020-06-05 Ajico NA NA	Rating¹ 2021-05-11 NA NA 2019-05-25 Cara NA 2020-05-11 Dekalb 2815 NA 2019-05-19 Acora 1.7 2020-05-13 NK S09R8X NA 2021-05-08 Ezra NA 2019-05-19 Natto NA 2019-06-13 Calypso NA NA NA NA </td <td>Rating¹ 2021-05-11 NA NA Rougemont 2019-05-25 Cara NA Rougemont 2020-05-11 Dekalb 2815 NA Saint-Grégoire 2019-05-19 Acora 1.7 Saint-Hilaire 2020-05-13 NK S09R8X NA Saint-Hilaire 2021-05-08 Ezra NA Rougemont 2019-05-19 Natto NA Saint-Hilaire 2019-06-13 Calypso NA Hemmingford 2020-05-25 AAC Corylis NA Hemmingford NA NA NA Hemmingford NA Katonda 1.5 Hemmingford NA Katonda 1.5 Hemmingford NA NA NA Hemmingford</td>	Rating¹ 2021-05-11 NA NA Rougemont 2019-05-25 Cara NA Rougemont 2020-05-11 Dekalb 2815 NA Saint-Grégoire 2019-05-19 Acora 1.7 Saint-Hilaire 2020-05-13 NK S09R8X NA Saint-Hilaire 2021-05-08 Ezra NA Rougemont 2019-05-19 Natto NA Saint-Hilaire 2019-06-13 Calypso NA Hemmingford 2020-05-25 AAC Corylis NA Hemmingford NA NA NA Hemmingford NA Katonda 1.5 Hemmingford NA Katonda 1.5 Hemmingford NA NA NA Hemmingford

¹SSR Rating: Sclerotinia Stem Rot susceptibility rating, the susceptibility scale ranges from 0 to 10, with 10 being comparable to the extremely susceptible cultivar Nattosan (Oleo Quebec, 2019). ²Data from on-site weather stations was collected to assess the validity of remote weather stations. NA, Information Not Available.

Table A. 5 Number of significant environmental variables for each moving average duration correlated with the apothecia binary variable of 0.25 apothecia/deposit (n = 9 total).

Criteria	Number of correlated variables				
	10-day	20-day	30-day	40-day ¹	
P < 0.05	9	9	9	7	
Coefficient $> 0.2 $ and $P < 0.05$	4	5	4	2	

¹8 weather variables (AWDR was excluded) were tested for the 40-day moving average durations.

Table A. 6 Number of significant 20-day moving average environmental variables (n = 9 total) correlated with apothecia binary response variables established at four thresholds.

Moving average	Criteria	Number of correlated variables				
duration	Cincia	0.25	0.50	0.75	1.00	
20-day	P < 0.05	9	9	9	9	
	Coefficient $> 0.2 $ and $P < 0.05$	6	6	6	6	
30-day	P < 0.05	9	9	9	9	
	Coefficient $> 0.2 $ and $P < 0.05$	5	5	5	5	

Table A. 7 Number of significant weather variables (n = 12 total) correlated with the DSI in Québec from 2019 to 2021.

		Number of correlated variables					
Criteria	June	July	August	September	July- September		
P < 0.05	12	1	0	9	0		
Coefficient $> 0.2 $	6	3	0	2	2		
Coefficient $> 0.2 $ and $P < 0.05$	6	1	0	2	0		

Table A. 8 Estimated values for the time to 50% carpogenic germination at IRDA, CÉROM, Laval University and McGill University from 2019 to 2021.

Research Centre	Year	Row Spacing (cm)	T50 (days) ¹	Standard error
IRDA		17.8	56.41	3.94
	2019	38.1	60.31	4.20
		76.2	64.66	4.51
		17.8	43.41	4.01
	2020	38.1	44.56	4.14
		76.2	45.95	4.31
		17.8	33.47	2.79
	2021	38.1	31.13	2.57
		76.2	28.77	2.38
CÉROM		17.8	NA	NA
	2019	38.1	NA	NA
		76.2	NA	NA
		17.8	NA	NA
	2020	38.1	NA	NA
		76.2	NA	NA
		17.8	33.94	4.94
	2021	38.1	43.42	6.50
		76.2	41.11	5.97
LAVAL		17.8	77.18	4.89
	2019	38.1	77.18	5.20
		76.2	78.70	5.36
		17.8	46.45	2.35
	2020	38.1	48.02	2.44
		76.2	43.32	2.23
		17.8	68.37	23.68
	2021	38.1	67.32	21.99
		76.2	118.92	43.67

Table A. 8 Estimated values for the time to 50% carpogenic germination at IRDA, CÉROM,

Laval University and McGill University from 2019 to 2021 (cont'd).

Research Centre	Year	Row Spacing (cm)	T50 (days) ¹	Standard error
		17.8	76.23	3.62
	2019	38.1	72.11	3.46
		76.2	74.19	3.49
		17.8	NA	NA
MCGILL	2020	38.1	NA	NA
		76.2	NA	NA
		17.8	NA	NA
	2021	38.1	NA	NA
		76.2	NA	NA

¹T50, the estimated values for the number of days until the presence of the one apothecium was observed in half of the sclerotia deposits representing the time to 50% germination.

Table A. 9 Least square means for the area under the inoculum progress curve at research centres in Québec from 2019 to 2021.

Year	Research Centre	LS Mean ¹	Standard error
2021	IRDA	616.04 a	40.78
2019	IRDA	340.46 b	40.78
2019	MCGILL	113.71 с	40.78
2020	IRDA	97.29 с	40.78
2021	LAVAL	42.50 c	40.78
2020	LAVAL	41.50 c	40.78
2021	MCGILL	22.75 с	40.78
2021	CÉROM	19.58 с	40.78
2019	LAVAL	17.38 с	40.78
2020	CÉROM	15.46 с	40.78
2019	CÉROM	1.46 c	40.78
2020	MCGILL	0.33 с	40.78
	I I		

Least square means followed by the same letter are not statistically different (α =0.05).

Table A. 10 Statistical model fit parameters for the effect of row spacing on apothecia formation at IRDA from 2019 to 2021.

Distribution, covariance structure	AIC	Pearson Chi-square/DF
Poisson, cs	1541.40	0.37
Poisson, ar1	195.65	0.40
Negative binomial, cs	1532.68	2.67
Negative binomial, ar1	1497.67	0.40

Abbreviations: Cs: Compound Symmetry Covariance Structure, ar1: 1st order Auto-Regressive Covariance Structure; AIC, Akaike's Information Criterion; DF, Degrees of Freedom.

Table A. 11 Least square means for disease severity index at R8 for 17.8-, 38.1-, and 76.2-cm spaced experimental plots at IRDA in 2021.

Row Spacing (cm)	LS Mean ¹	Standard error		
17.8	7.5 a	5.4		
38.1	19.2 a	5.4		
76.2	5.0 a	5.4		

¹ LS, Least Square means followed by the same letter are not statistically different (α =0.05).

Table A. 12 Comparison between the area under the receiver of operating characteristic curve of Willbur models predicting DSI 10 based on the risk of apothecia presence from R1 to R3 and from R1 to R4 in Québec from 2019 to 2021.

Model	Year	AUC R1-R3	AUC R1-R4	Z-statistic	P-value
	2019	0.646	0.625	0.71	0.5
Willbur 1	2020	0.967	0.967	0.00	1.0
WIIIOUI I	2021	0.775	0.763	0.71	0.5
	2019-2021	0.754	0.750	1.00	0.3
	2019	0.583	0.500	1.20	0.2
Willbur 2	2020	0.833	0.817	0.71	0.5
Willouf Z	2021	0.663	0.681	-0.47	0.6
	2019-2021	0.654	0.633	0.75	0.5
	2019	0.479	0.458	0.31	0.8
Willbur 3	2020	0.833	0.817	0.71	0.5
Willouf 3	2021	0.688	0.744	-1.10	0.3
	2019-2021	0.675	0.667	0.31	0.8

Abbreviations: R1-R3: Area under the Receiver Operating Curve of Willbur models during the soybean growth stages from beginning bloom to beginning pod formation.

R1-R4: Area under the Receiver Operating Curve of Willbur models during the soybean growth stages from beginning bloom to full pod formation.

Table A. 13 Comparisons between the AUCs and the line of no-discrimination of SSR prediction models for different apothecia maturity levels in Québec from 2019 to 2021.

Apothecia Maturity	Model	AUC ¹	\mathbf{SE}^2	Z-Statistic	P-value ³
	Willbur 1	0.657 ab	0.0004	7.020	1.11E-12
Immature	Willbur 2	0.636 b	0.0004	6.090	5.49E-10
	Willbur 3	0.677 a	0.0004	7.910	1.38E-15
	Willbur 1	0.680 ab	0.0005	7.560	2.09E-14
Mature	Willbur 2	0.654 b	0.0005	6.460	5.26E-11
	Willbur 3	0.698 a	0.0005	141.420	5.11E-17
	Willbur 1	0.685 ab	0.0004	141.420	5.45E-18
Total	Willbur 2	0.675 b	0.0004	8.080	2.86E-16
	Willbur 3	0.718 a	0.0004	141.420	2.72E-24

¹AUC: Area under the Receiver Operator Curve was calculated using the Delong et. al. (1988) method. AUC followed by the same letter are not statistically different ($\alpha = 0.05$).

²SE: Standard Error.

³Significance between model AUC and the AUC of the line of no-discrimination was determined at $\alpha = 0.05$.

Table A. 14 Evaluation of the Willbur models' original and recalibrated versions on 70% of the 2019-2021 dataset.

Model	AUC	SE	Z-Statistic	P-value ⁴
Willbur 1 ¹	0.693	0.0005	7.430	5.26E-14
W1_recal1 ²	0.693	0.0005	7.430	5.26E-14
W1_recal2 ³	0.693	0.0005	7.430	5.26E-14
Willbur 2 ¹	0.695	0.0005	7.500	3.07E-14
W2_recal1 ²	0.695	0.0005	7.500	3.07E-14
W2_recal2 ³	0.695	0.0005	7.500	3.06E-14
Willbur 3 ¹	0.740	0.0005	141.420	1.71E-20
W3_recal1 ²	0.740	0.0005	141.420	1.71E-20
W3_recal2 ³	0.739	0.0005	141.420	1.73E-20

¹Original Willbur et al. (2018) equations.

Abbreviations: AUC, Area under the Receiver Operating Curve; SE, Standard Error.

²Recalibrated-in-the-large Willbur models using 70% of the data collected in Québec from 2019 to 2021.

³Logistic recalibrated Willbur models using 70% of the data collected in Québec from 2019 to 2021.

⁴Significance between model AUC and the AUC of the line of no-discrimination was determined at $\alpha = 0.05$.

Table A. 15 Evaluation of the Willbur models' original and recalibrated versions on 30% of the 2019-2021 dataset.

Model	AUC ²	SE ³	Z-Statistic	P-value ⁴
Willbur 1 ¹	0.664	0.001	4.200	1.35E-05
W1_recal1	0.664	0.001	4.200	1.35E-05
W1_recal2	0.664	0.001	4.200	1.36E-05
Willbur 2 ¹	0.632	0.001	3.380	3.57E-04
W2_recal1	0.632	0.001	3.380	3.57E-04
W2_recal2	0.632	0.001	3.380	3.57E-04
Willbur 3 ¹	0.673	0.001	4.450	4.39E-06
W3_recal1	0.673	0.001	4.450	4.39E-06
W3_recal2	0.673	0.001	4.450	4.39E-06

¹Original Willbur et al. (2018) equations.

Abbreviations: AUC, Area under the Receiver Operator Curve; SE, Standard Error.

²Recalibrated-in-the-large Willbur models using 70% of the data collected in Québec from 2019 to 2021.

³Logistic recalibrated Willbur models using 70% of the data collected in Québec from 2019 to 2021.

⁴Significance between model AUC and the AUC of the line of no-discrimination was determined at $\alpha = 0.05$.

Table A. 16 Model fit for various combinations of 20-day moving average durations of weather variables.

Variables	AIC	R2	Kappa	AUC	Threshold	Accuracy	Sensitivity	Specificity	Fpos	Fneg	LR+	LR-
Tmax20d	691.500	0.119	0.144	0.700	0.362	0.683	0.567	0.741	0.259	0.433	2.189	0.584
Tmax20d, WSmax20d	676.900	0.154	0.179	0.704	0.268	0.635	0.840	0.531	0.469	0.160	1.792	0.301
Tmax20d, WSmax20d, RHmax20d	650.200	0.214	0.295	0.730	0.255	0.641	0.876	0.523	0.477	0.124	1.838	0.236
Tmax20d, AWDR20	670.100	0.169	0.165	0.703	0.249	0.643	0.928	0.500	0.500	0.072	1.856	0.144
Tmax20d, RHmean20d	598.900	0.310	0.328	0.791	0.352	0.738	0.737	0.738	0.262	0.263	2.817	0.356
Tmax20d, WSmax20d, AWDR20	656.900	0.200	0.209	0.704	0.264	0.676	0.897	0.565	0.435	0.103	2.061	0.183
Tmax20d, RHmean20d, AWDR20	593.900	0.323	0.319	0.780	0.249	0.697	0.887	0.601	0.399	0.113	2.222	0.189
Tmax20d, WSmax20d, RHmean20d	548.100	0.403	0.442	0.818	0.356	0.760	0.758	0.762	0.238	0.242	3.179	0.318
Tmax20d, WSmax20d, RHmax20d, AWDR20	632.400	0.253	0.302	0.734	0.265	0.707	0.887	0.617	0.383	0.113	2.312	0.184
Tmax20d, WSmax20d, RHmean20d, AWDR20	547.400	0.408	0.422	0.808	0.376	0.766	0.727	0.785	0.215	0.273	3.380	0.348

Abbreviations: AIC, Akaike's Information Criterion; R2, Pearson Coefficient of Determination; AUC, Area under the Receiver Operator Curve; Fpos, False Positive Rate; Fneg, False Negative Rate; LR+, Positive Likelihood Ratio; LR-, Negative Likelihood Ratio.

Table A. 17 Modified model coefficients for the best performing models in Québec from 2019 to 2021.

Model	Parameter	Coefficient	\mathbf{SE}^1	Pr(> Z)
Willbur 1r	Tmax	-0.345	0.0538	<0.0001
willour ir	Intercept	8.417	1.4151	< 0.0001
	Tmax	-0.374	0.0549	<0.0001
Willbur 2r	Wsmax	-0.171	0.0449	0.0001
	Intercept	10.657	1.5541	< 0.0001
	Tmax	-0.413	0.0577	< 0.0001
Willbur 3r	Wsmax	-0.235	0.0566	< 0.0001
willour 3r	Rhmax	0.130	0.0271	< 0.0001
	Intercept	-0.310	3.0193	0.9183
	Tmax	-0.351	0.0539	< 0.0001
Willbur 1x.1	AWDR	0.011	0.0025	< 0.0001
	Intercept	7.843	1.4123	< 0.0001
	Tmax	-0.172	0.0629	0.0062
Willbur 1x.2	Rhmean	0.310	0.0316	< 0.0001
	Intercept	-19.812	3.1607	< 0.0001
	Tmax	-0.191	0.0631	0.0024
Willbur 1x.3	Rhmean	0.299	0.0317	< 0.0001
Willour 1x.3	AWDR	0.006	0.0028	0.0329
	Intercept	-18.925	3.1424	< 0.0001
	Tmax	-0.380	0.0552	< 0.0001
Willbur 2x.1	Wsmax	-0.168	0.0464	0.0003
w iiibur 2x. i	AWDR	0.011	0.0025	< 0.0001
	Intercept	10.07	1.5614	<0.0001

Table A. 17 Modified model coefficients for the best performing models in Québec from 2019 to

2021 (cont'd).

Model	Parameter	Coefficient	\mathbf{SE}^1	Pr(> Z)
	Tmax	-0.188	0.0659	0.0044
Willbur 2x.2	Wsmax	-0.383	0.0593	< 0.0001
Willbur 2x.2	Rhmean	0.363	0.0351	< 0.0001
	Intercept	-20.286	3.2717	< 0.0001
	Tmax	-0.419	0.0579	< 0.0001
	Wsmax	-0.239	0.0580	< 0.0001
Willbur 3x.1	Rhmax	0.130	0.0269	< 0.0001
	AWDR	0.011	0.0026	< 0.0001
	Intercept	-0.815	2.9588	0.7829
	Tmax	-0.205	0.0661	0.0020
	Wsmax	-0.374	0.0593	< 0.0001
Willbur 3x.2	Rhmean	0.354	0.0353	< 0.0001
	AWDR	0.005	0.0030	0.0748
	Intercept	-19.617	3.2698	< 0.0001

¹SE: Standard Error.

Abbreviations: Tmax, Maximum Temperature (°C); WSmax, Maximum Wind Speed/1.609 (km/h); RHmax, Maximum Relative Humidity (%); RHmean, Mean Relative Humidity (%); AWDR, Abundant and Well-Distributed Rainfall (mm). All weather variables are 30-day moving averages.

Appendix 2 - Figures

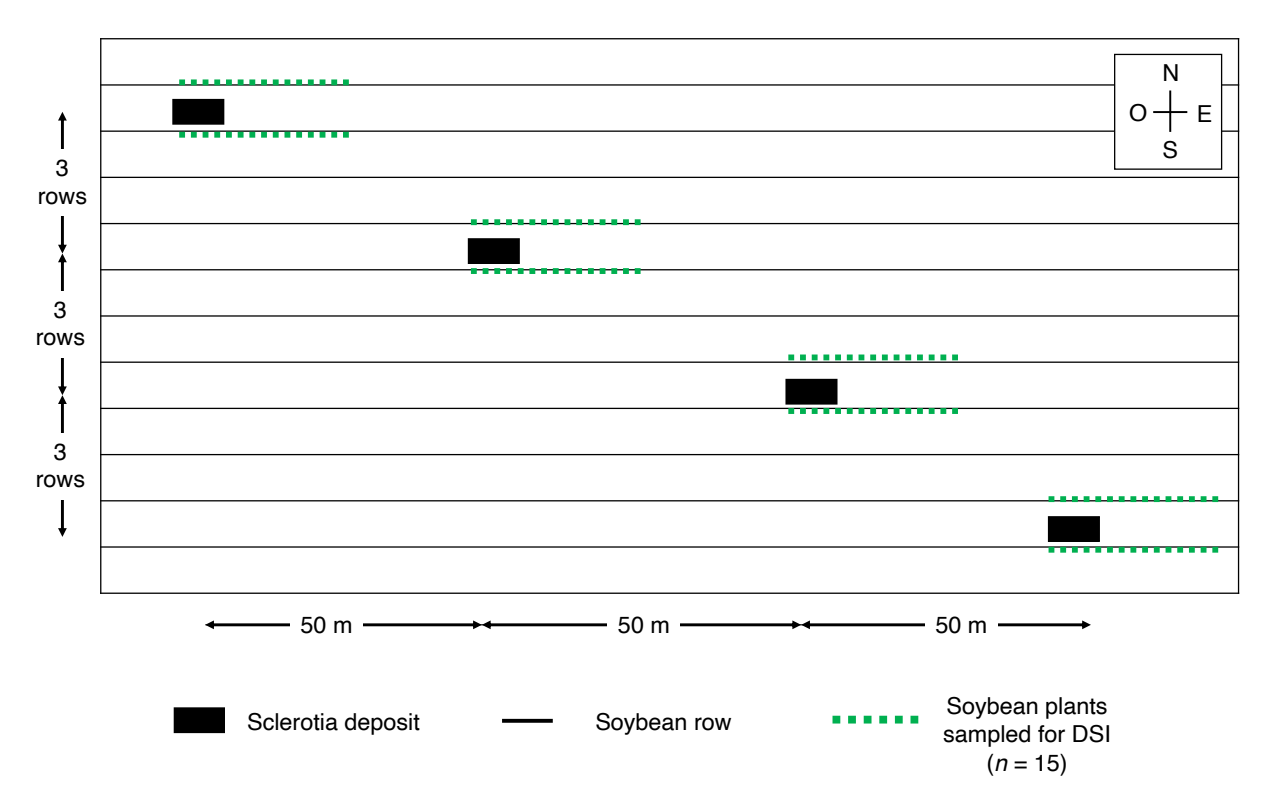


Figure A. 1 Experimental design at the commercial sites in Québec from 2019 to 2021. Figure not to scale.

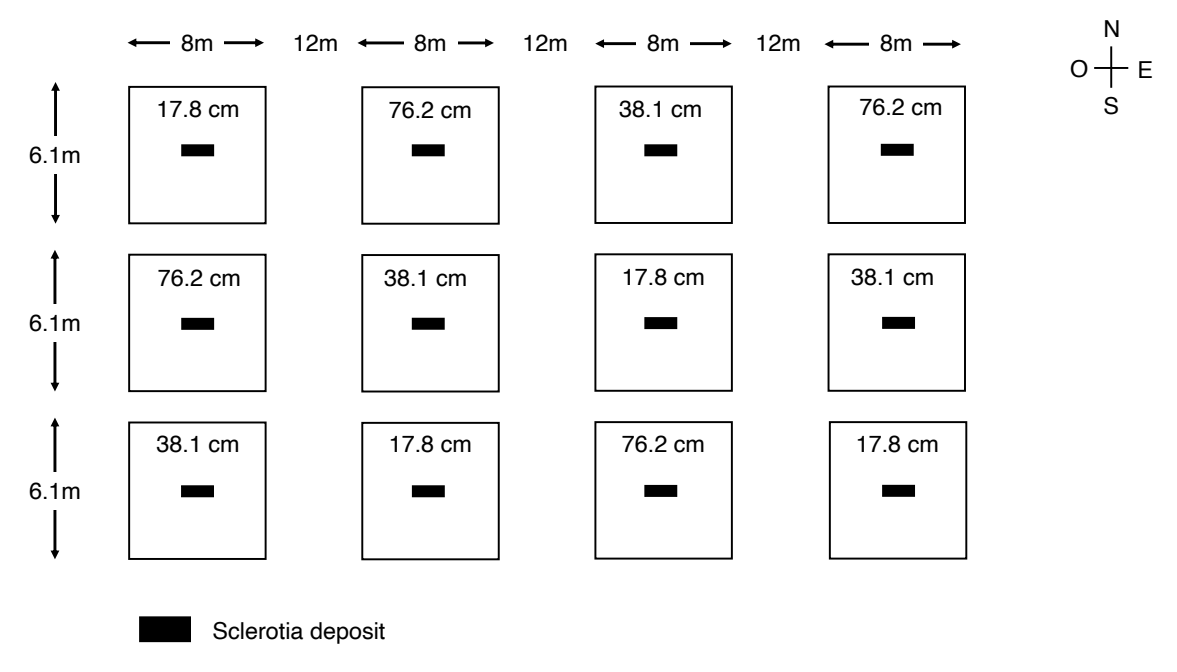


Figure A. 2 Experimental design at the CÉROM, IRDA, Laval University and McGill University research sites in Québec from 2019 to 2021. Figure not to scale.

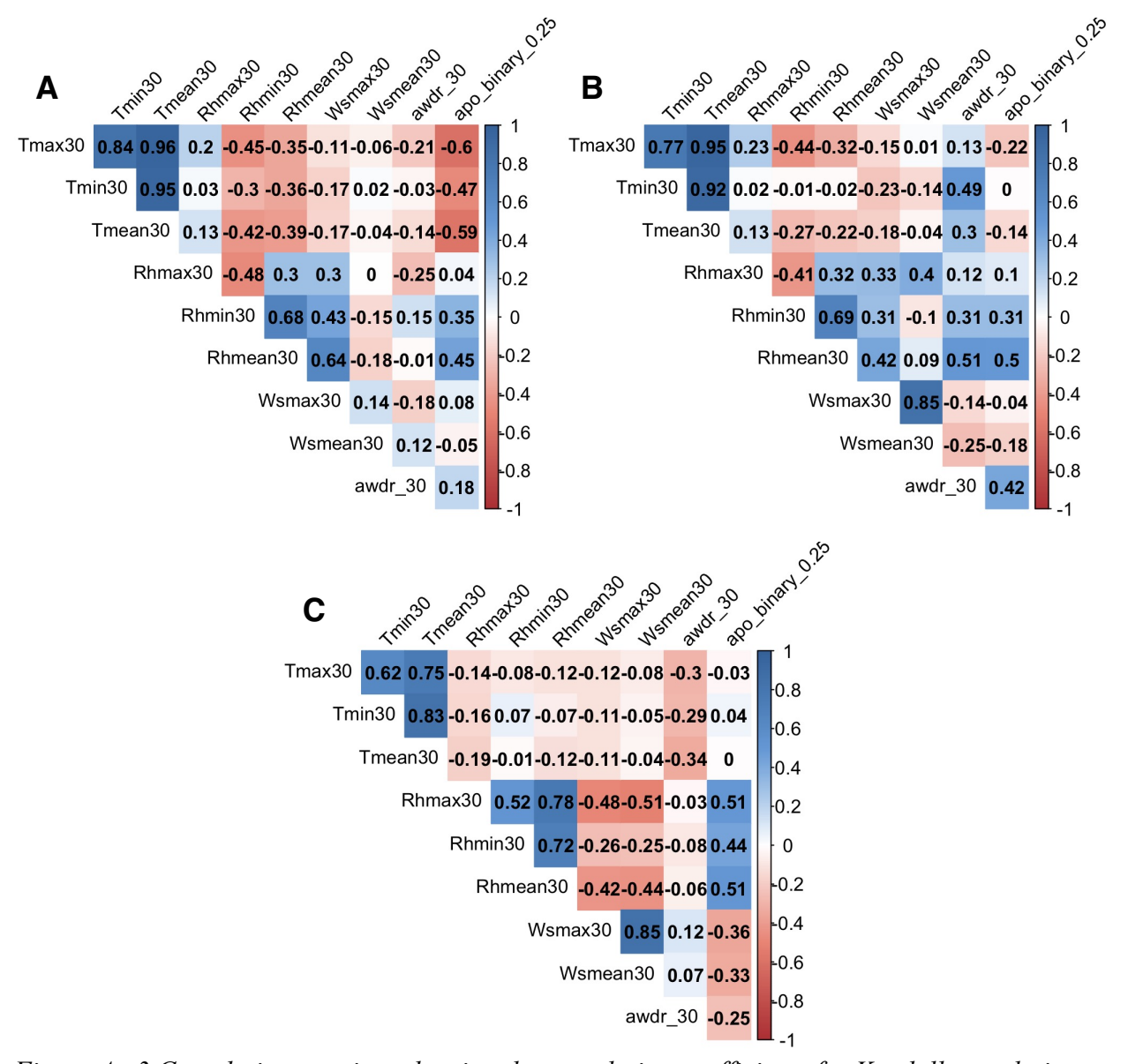


Figure A. 3 Correlation matrices showing the correlation coefficients for Kendall correlations between 30-day moving averages of weather variables and the apothecia binary variable created based on a threshold of 0.25 mean apothecia/deposit in Québec in A) 2019, B) 2020 and C)2021.

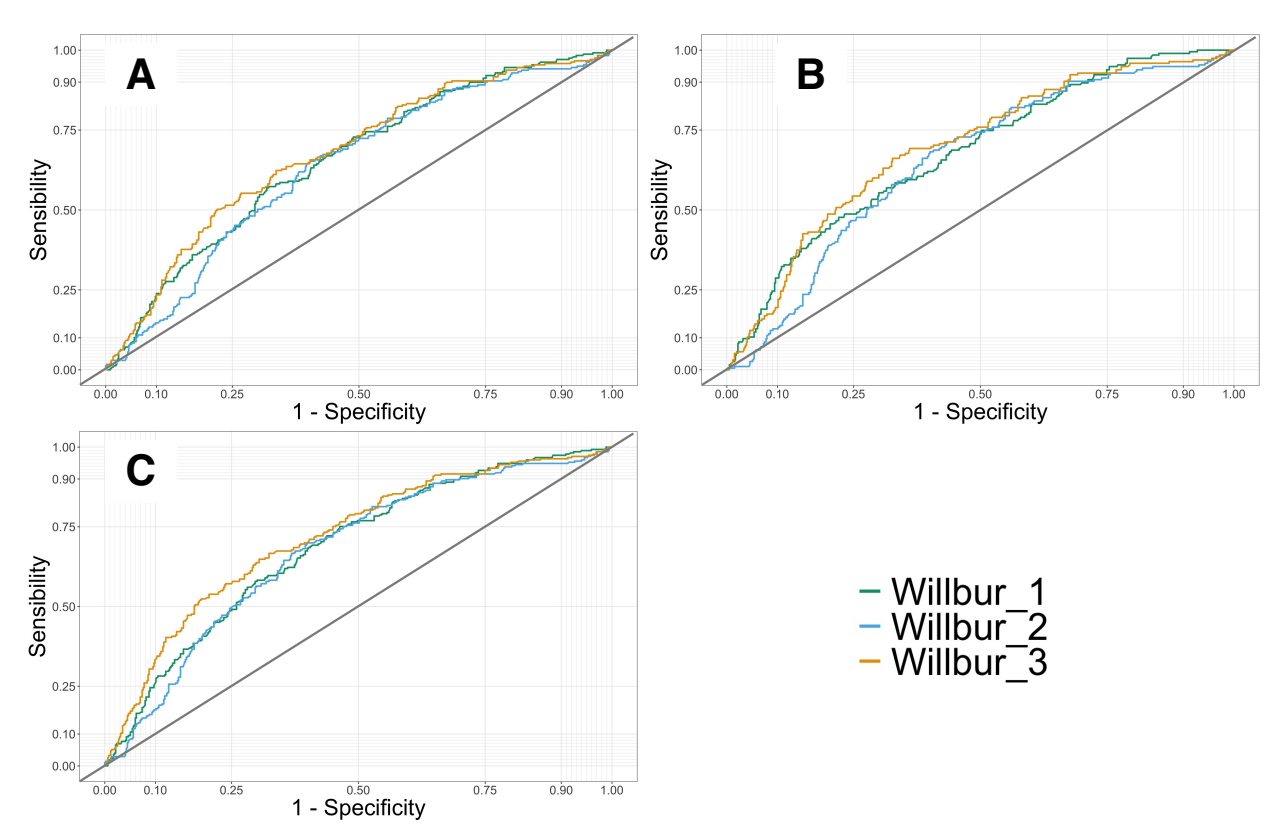


Figure A. 4 Receiver operating characteristic curve for Sclerotinia stem rot apothecia formation models in Québec for A) immature apothecia, B) mature apothecia, and C) total apothecia from 2019-2021.